BBA - Biomembranes 1862 (2020) 183405

Contents lists available at ScienceDirect

BBA - Biomembranes

journal homepage: www.elsevier.com/locate/bbamem

Bacillus subtilis cardiolipin protects its own membrane against surfactin-induced permeabilization

Dominik Pinkas[a], Radovan Fišer[a,*], Petr Kozlík[b], Tereza Dolejšová[a], Klára Hryzáková[a], Ivo Konopásek[a], Gabriela Mikušová[a,*]

[a] Department of Genetics and Microbiology, Faculty of Science, Charles University, Viničná 5, 128 00 Prague, Czech Republic
[b] Department of Analytical Chemistry, Faculty of Science, Charles University, Hlavova 8, 128 00 Prague, Czech Republic

ARTICLE INFO

Keywords:
Bacillus subtilis
Membrane
Surfactin
Cardiolipin
Liposome

ABSTRACT

Surfactin, a cyclic lipoheptapeptide produced by *Bacillus subtilis*, is a surface-active antimicrobial that targets the barrier function of lipid membranes. It inserts itself into the membrane, where it forms conductive pores. Depending on its concentration, it eventually disintegrates the membrane in a detergent-like manner. The molecular details of this activity are not yet sufficiently understood, nor are the mechanisms that the surfactin producer employs to resist its own toxic product. We have previously shown that *B. subtilis* modifies its membrane lipid composition upon the onset of surfactin production, mainly increasing the cardiolipin content. Here we show that the increased cardiolipin content leads to a decreased surfactin-induced leakage of liposomes reconstituted from lipids isolated from the surfactin producer. This stabilizing effect of cardiolipin is concentration-dependent. Using a propidium iodide-based cell permeabilization assay, we further confirmed that the cytoplasmic membrane of the mutant *B. subtilis* strain lacking cardiolipin was substantially more susceptible to the action of surfactin, even though the amount of bound surfactin was the same as in the wild-type strain. We propose that membrane remodelling; due to the increase in cardiolipin content, contributes to the surfactin tolerance of *B. subtilis*.

1. Introduction

The need for new effective antimicrobial compounds is a current global issue. One of the strategies for tackling this is to target the bacterial cytoplasmic membrane [1], which plays a fundamental role in cell function and survival. Traditionally, the cytoplasmic membrane has been compromised via antibiotics interfering with lipid metabolism enzymes, namely fatty acid synthesis [2]. Recently, the discovery of the functional membrane microdomains (FMMs) together with an increasing number of FMM-associated membrane proteins with domain-bound functions [3] have uncovered new opportunities for combating pathogens. Agents that disassemble FMMs, and thus affect the enzymatic functions allocated to them, cause an inhibition of bacterial growth [4]. Lastly, membrane-targeting antimicrobial peptides (AMPs) acting via pore formation are still a focus of antimicrobial research. These agents include not only the host-defense AMPs or their artificially modified variants, but also other complex compounds of microbial origin.

Surfactin is a pore-forming antimicrobial produced by *Bacillus subtilis*. This cyclic lipoheptapeptide consists of a hydrophobic fatty acid and a peptide moiety with a negatively charged hydrophilic "claw" formed of Glu1 and Asp5. The amphiphilic nature of the molecule results in very strong surface activity, allowing the surfactin to lower water surface tension from 72 to approximately 30 mN/m at concentrations as low as 10–20 μM [5,6], making it one of the strongest biosurfactants. The surfactin molecule can also adopt at least two different conformations [7], and forms various micelles and aggregates depending on the conditions in the solution [8,9]. Surfactin is produced via non-ribosomal proteosynthesis by large modular protein complexes and contains both L- and D-amino acids, ensuring difficult degradation by proteases.

Most importantly, surfactin is able to enter lipid membranes and interfere with their barrier function, which is the basis of its broad-spectrum antimicrobial effect which include *Enterococcus faecalis*, *Staphylococcus aureus*, *Pseudomonas aeruginosa*, *Escherichia coli* [10], *Listeria monocytogenes* [11] or *Legionella pneumophila* [12]. Once inside a membrane, surfactin affects membrane organization by forming conductive pores [13,14] and local bilayer failures, resulting in cell death. A sufficient concentration can even disintegrate the membrane in a detergent-like manner [15–17]. The conical shape of the surfactin

* Corresponding authors.
E-mail addresses: fiserr@natur.cuni.cz (R. Fišer), seydlova@natur.cuni.cz (G. Mikušová).

https://doi.org/10.1016/j.bbamem.2020.183405
Received 3 March 2020; Received in revised form 15 May 2020; Accepted 19 June 2020
Available online 25 June 2020
0005-2736/

molecule introduces curvature stress, makes the membrane thinner and disorganizes it [17]. Surfactin molecules added from the external milieu can traverse to the inner leaflet either as single monomers via a spontaneous flip-flop mechanism or through local bilayer failures, which releases surfactin-induced tension while leaking cellular contents. Due to its poor miscibility with lipids, surfactin then forms segregated domains with a high local surfactin/lipid ratio, which probably leads to more bilayer discontinuities [18] and possibly even to stable pore formation. This multimodal effect causes a rapid eradication of bacterial cells, regardless of their physiological state. This feature is especially important in medical applications due to the increasing prevalence of antibiotic-resistant pathogens or pathogens that are able to survive antibiotic therapy in metabolically-inactive states.

The cytoplasmic membrane is still considered an underexploited antibiotic target [19]. In the last 15 years, the few new antibiotics that were launched to clinical praxis such as daptomycin or telavancin act directly in the cytoplasmic membrane. More compounds sharing this mode of action are at different stages of clinical development (such as brilacidin, LTX-109). The cytoplasmic membrane as a target site has several advantages compared to an enzyme and/or compounds inhibiting a metabolic pathway. Unlike other antibiotics, a membrane-targeting compound does not have to pass through the semipermeable lipid barrier, because the membrane itself is the target. Even if the exposure to the membrane-active antibiotic is not lethal, it may enhance the effectivity of other simultaneously administered drugs by facilitating their internalization by the cell [20]. Disrupting the membrane harms not only fast-growing cells, but also slow-growing and dormant ones. Another beneficial factor is the lower risk of resistance development, as the membrane plays an essential role in many cellular pathways. Even though cells have mechanisms for membrane remodelling, they mostly aim to keep the membrane microenvironment stable. If not, it is highly likely that the degree of changes in chemicophysical parameters necessary for the development of resistance would interfere with membrane-bound cell functions, which would interfere with proper cell physiology.

A resistance mechanism against surfactin must exist by which the producer prevents killing itself with its own toxic product. In *B. subtilis*, a surfactin-connected increase in the expression of the RND (resistance-nodulation-division) transporter-coding gene yerP has been described [21]. Another study showed that the overexpression of YerP together with YcxA and KrsA, members of the major facilitator superfamily, led to an increased production of surfactin by enhancing its transport from the cell [22]. On the other hand, the deletion of yerP had no impact on the sensitivity of the producing strain of *B. subtilis* towards surfactin [21]. We can presume that this efflux system has more to do with the export of surfactin produced in the cytoplasm than with clearing membrane-bound surfactin molecules. Previously, we focused on a possible modification of the membrane as the target site in response to surfactin exposure. We reported that a non-producing *B. subtilis* strain was able to efficiently adapt the proportions of its membrane phospholipids after the surfactin challenge [23]. We further showed that the surfactin-producing *B. subtilis* strain significantly alters its membrane lipid composition during surfactin production [24,25], mainly by increasing the cardiolipin content and by rigidifying the membrane. In this study, we directly tested a hypothesis that the increased cardiolipin content in the membrane can explain the tolerance of *B. subtilis* to surfactin. Using both a model liposome membrane and living *B. subtilis* cells, we show here that cardiolipin stabilizes the target membrane against surfactin-induced permeabilization.

2. Materials and methods

2.1. Bacterial strains

Four strains of *Bacillus subtilis* were used (Table 1): the laboratory strain *B. subtilis* 168 (trpC2, Bacillus Genetic Stock Center) which is designated below as "CL+"; *B. subtilis* SDB206 (clsA::pMutin4, ywjE1::spc, ywiE2::neo) – a strain based on *B. subtilis* 168 with disrupted genes clsA, ywjE1 and ywiE2 [26], which are essential for cardiolipin synthesis, designated below as "CL−"; wild-type strain *B. subtilis* ATCC 21332 (American Type Culture Collection), a natural surfactin producer designated below as "SF+" and its derivative *Bacillus subtilis* 0164 (sfp0) – a mutant with disrupted gene sfp which is essential for surfactin production [24], designated below as "SF−".

2.2. Cell cultivation

B. subtilis cultures were grown aerobically in nutrient broth (Oxoid) at 30 °C. The growth was monitored by measuring the optical density at 420 nm. Exponential cultures for lipid isolation (CL+ and CL− strains) were harvested by filtration through a Synpor No. 5 filter after reaching OD_{420} = 0.5, and biomass was immediately used for lipid isolation. Cultures of SF+ and SF− strains were cultivated at 30 °C for 24 h to be well past the onset of surfactin production, biomass was harvested via centrifugation (4500*g*, 4 °C, 15 min) and immediately used for membrane isolation.

2.3. Membrane isolation

Cell pellets were resuspended in 50 mM phosphate buffer (pH 8) with lysozyme (10 mg/ml), DNase (25 µg/ml), RNase (25 µg/ml), and 10 mM $MgSO_4$, and incubated at 30 °C for 1 h. After the incubation, K^+EDTA was added to a final concentration of 15 mM and after 1 min, $MgSO_4$ was added to a total concentration of 20 mM. Unlysed spores were removed by centrifugation (3000*g*, 4 °C, 10 min) [27]. The supernatant containing lysed vegetative cells was further centrifuged (25,000*g*, 4 °C, 25 min) to sediment the membrane vesicles, which were immediately used for lipid isolation.

2.4. Lipid isolation

Harvested biomass from exponential cultures of CL+ and CL− strains or membranes from SF+ and SF− cultures were resuspended by intensive mixing in hexane:isopropanol 3:2 (v/v) and then extracted at 4 °C overnight. Non-lipidic non-soluble material was removed by centrifugation (5000*g*, 4 °C, 10 min), and the extract was evaporated using a rotary vacuum evaporator (38 °C). The lipid fraction was dissolved in chloroform and filtered through a Whatman GF/C filter to remove the remaining non-soluble compounds. The lipid extract was immediately used for liposome preparation.

2.5. Preparation of carboxyfluorescein-loaded liposomes

The lipids used in this study were either natural lipids directly isolated from *B. subtilis* cultures, commercially available isolates - phosphatidylcholine from egg yolk (PC; Avanti Polar Lipids) or synthetic phospholipids (Avanti Polar Lipids): dioleylphosphatidylglycerol (DOPG), dimyristoylphosphatidylglycerol (DMPG), dioleylphosphatidylethanolamine (DOPE), dimyristoylphosphatidylethanolamine (DMPE), dimyristoylphosphatidic acid (DMPA), tetraoleylcardiolipin (TOCL), and tetramyristoylcardiolipin (TMCL).

Liposomes were prepared from natural isolated lipids (total lipid extract) or combinations of synthetic phospholipids (as indicated in the figure legends) mixed in chloroform. The total amount of 1 mg of lipid (s) in chloroform was dried using a rotary vacuum evaporator (38 °C) to form a thin transparent film on the inside walls of a glass tube. The hydration was performed by the addition of 1 ml of 50 mM carboxyfluorescein (CF) solution in 5 mM HEPES (pH 7.4) and vigorous shaking for 90 min with intervals of heating in a water bath at 38 °C. The resulting suspension of multilamellar liposomes of various sizes was then extruded through a polycarbonate filter with a pore size of 100 nm using a mini-extruder (Avanti Polar Lipids) to form uniform large

Table 1
Bacterial strains used in this study.

	Strain	Based on	Mutations	Source
SF +	*B. subtilis* ATCC 21332			American Type Culture Collection
SF −	*B. subtilis* 0164	ATCC 21332	sfp0	[24]
CL +	*B. subtilis* 168		trpC2	Bacillus Genetic Stock Center
CL −	*B. subtilis* SDB206	168	clsA::pMutin4, ywjE1::spc, ywiE2::neo	[26]

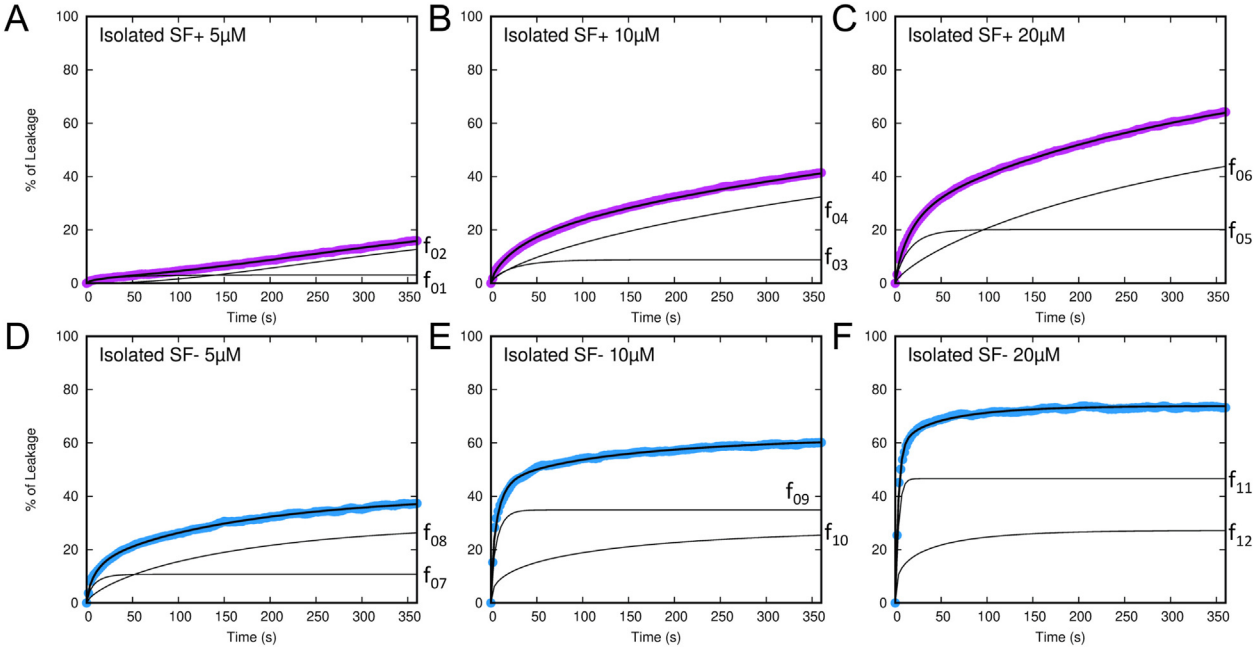

Fig. 1. Leakage of carboxyfluorescein from liposomes prepared from total phospholipid extract from SF + (A–C) and SF − (D–F) B. subtilis strains. The phospholipid composition of the isolates was assessed previously [24]. Surfactin was added at time 0 to a final concentration of 5, 10 or 20 μM (indicated in the graph legend). 100% leakage was achieved using 0.1% Triton X-100. The parameters for fitting the curves to the convolution of functions f_{01}-f_{12} presented in (A)–(F) are listed in Supplementary Table 1. The rates of CF release (v) were 2.7 ± 0.3 and 66.6 ± 16.8%/min (p = 0.03) for kinetics presented in A and D, respectively, 54.1 ± 10.0 and 247.1 ± 44.6%/min (p = 0.02) for the kinetics in B and E, respectively, and 122.6 ± 21.0%/min and 561.3 ± 32.1%/min (p = 0.01) for the kinetics presented in C and F, respectively.

unilamellar vesicles (LUVs) filled with CF. Free probe was removed by gel filtration in a column (20 ml) filled with sephadex G50 (GE Healthcare) with 100 mM NaCl, 5 mM HEPES and 0.5 mM Na_2EDTA as the elution buffer. Flowthrough was collected in fractions of 0.5 ml, and their phospholipid concentration was determined via inorganic phosphate content measurement [28]. Fractions with the highest phosphate concentration were collected and diluted accordingly to form the appropriate stock solution (10 times the intended final concentration). Unless otherwise stated in the figure legends, the phospholipid concentration in liposome suspensions was 10 μM.

2.6. Liposome leakage assay

The liposome leakage assay [29] was performed in quartz cuvettes with a minimal volume of 100 μl. Fluorescence was measured at 515 nm using a Fluoromax-3 spectrofluorometer (Jobin Yvon, Horiba) with an excitation wavelength of 480 nm. The liposome suspension was diluted to the appropriate concentration using the elution buffer (see the Section 2.5 Preparation of carboxyfluorescein-loaded liposomes) and the background fluorescence intensity FI_0 was measured. The amount of added surfactin (Sigma-Aldrich) is indicated in the figure legends. For liposomes composed of dioleylphospholipids, we had to use a relatively high surfactin-lipid ratio (5:1), as lower surfactin concentrations only resulted in a weak long-lasting leakage (Supplementary Fig. 1). After the addition of surfactin, the suspension was mixed thoroughly and fluorescence intensity FI was collected every 2 s. The order of additions (i.e. surfactin solution to liposome suspension or vice versa) had essentially no effect on the observed kinetics (data not shown). While CMC of surfactin was found to be 10 μM [15, 30, our unpublished data] and the concentrations used in our experiments were 5, 10, 20 and 50 μM, the effects of the surfactin in our systems were not affected by micelle formation. Triton X-100 (final concentration of 0.1%, v/v) was added at the end of the measurement to obtain the maximal fluorescence FI_{max} achievable after the disintegration of all liposomes. Leakage kinetics was then plotted as the percentage of leakage against time (Eq. (1)); representative curves from at least three experiments are shown.

$$\%\text{of leakage} = \frac{FI - FI_0}{FI_{max} - FI_0} \times 100 \quad (1)$$

The Value $T_{1/2}$, meaning "leakage half-time" is used to compare the rate of CF leakage - it expresses the time required after the addition of surfactin necessary to reach 50% of the maximal fluorescence intensity. A mean value ± standard deviation from all the measured kinetics is shown. Using Fityk software [31], the time courses of liposome lysis were fitted to the function:

$$f(t) = \alpha(1 - \exp(-t/\tau))^n, \quad (2)$$

where t is the time, α is the amplitude of the effect, τ is the time constant of the effect, and n is the coefficient that expresses positive ($n > 1$) or negative ($n < 1$) cooperativity of the leakage, respectively [32]. For simplicity, we call the parameter n the Hill coefficient here. For better readability, the functions with $n < 1$ are further designated

as “non-cooperative” and functions with n > 1 as “cooperative”. A single function or combination of several functions can be used to describe the kinetics, suggesting a multi-modal action. Where appropriate, before reaching the plateau phase, the rate of lysis was determined by fitting the curves to the linear function y = v·t, where t is the time and v is the rate of lysis expressed as the percentage of maximum lysis per minute. The statistical significance of differences in v and $T_{1/2}$ values was tested by Student's *t*-test.

In the experiments presented in Figs. 1 and 5, where the total lipid cell isolates were used for liposome preparation, some spontaneous liposome leakage occurred, which increased the background fluorescence accordingly (< 15%) over the 3 h. The experiments were done within this interval, which ensured reproducible kinetics (Supplementary Fig. 2).

2.7. Cell permeabilization assay

For the propidium iodide-based cell permeabilization assay [33], exponential cultures of *B. subtilis* (CL+ and CL− strains) were harvested via centrifugation (5000*g*, 25 °C, 10 min) and resuspended in 0.5% glucose, 10 mM HEPES (pH 7.4), and 10 μM propidium iodide to a final concentration of ~2×10^7 cells/ml. Fluorescence was measured in quartz cuvettes at 620 nm using a Fluoromax-3 spectrofluorometer (Jobin Yvon, Horiba) with an excitation wavelength of 515 nm. Optical filters were used to suppress light scattered by the cells (Omega Optical filters 3RD500-530 and 3RD570LP in the excitation and emission paths, respectively). At the time point 0 s, cells were added to a final concentration of 2×10^7/ml in the cuvette with the buffer and desired concentration of surfactin and dye. The final volume in the quartz cuvette was 2 ml. Fluorescence intensity was recorded every 2 s. Permeabilization kinetics were plotted as a percentage of fluorescence intensity against time (Eq. (1)) relative to the maximum fluorescence reached after using 2.5 μM melittin (Fl_{max}) as a positive control. Representative curves from three experiments are shown.

2.8. Conductivity measurements on planar lipid bilayers

A Teflon chamber separated by a diaphragm with an aperture of about 0.5 mm in diameter was filled with a buffered salt solution containing 1 M KCl, and 10 mM Tris at pH 7.4. A planar lipid bilayer was painted across the aperture using 3% (w/v) dioleylphosphatidylglycerol (DOPG, Avanti Polar Lipids) in decane-butanol (9:1, v/v). Surfactin at a concentration of 4 μM was added to the positive *cis* side of the membrane. The membrane current was measured using Ag/AgCl electrodes with an applied voltage of 50 mV, amplified with an LCA-200-10G amplifier (Femto), digitized with a KPCI-3108 card (Keithley), and processed with QuB software [34]. Data are presented as a single-pore conductance (G, pS) histogram with logarithmic binning.

3. Results

3.1. Surfactin-adapted lipid membranes are less prone to surfactin-induced lysis

As we have shown previously [24], the SF+ strain of *Bacillus subtilis* alters its membrane composition when exposed to self-produced surfactin, specifically the proportion of cardiolipin (CL) is enhanced in the SF+ membrane. To determine whether the observed changes lead to a higher tolerance of the membrane to the action of surfactin, we isolated total membrane lipids from the adapted SF+ and the non-adapted SF− cultures. Further, we used those lipids to form carboxyfluorescein-loaded liposomes. In the liposome leakage assay, the liposome suspensions were diluted to the same phosphate concentration (see the Section 2.5). Upon the addition of surfactin to either liposome suspension (Fig. 1), we observed an immediate rise in fluorescence intensity, indicating membrane permeabilization. In SF+ kinetics, the leakage process was somewhat gradual; in contrast, the SF− leakage curves exhibited a steep rise which stopped sharply and maintained an almost constant value of fluorescence intensity.

At all of the surfactin concentrations tested, the rate of dye leakage was faster and reached higher maximum levels in non-adapted (SF−) lipid membranes. The difference was most pronounced in the SF+ and SF− liposomes exposed to 5 μM surfactin, where the rate of CF release was just 2.7%/min in SF+ liposomes compared to 66.6%/min in SF− liposomes. At higher concentrations of 10 and 20 μM surfactin, the difference in the rate of dye leakage between the SF+ and SF− liposomes was still more than fourfold (Fig. 1, Supplementary Table 1). In isolated SF+ liposomes, double the surfactin concentration was required to induce the same permeabilizing effect as in SF− liposomes. The exposure of SF− liposomes to 5 and 10 μM surfactin led to a comparable effect to 10 and 20 μM surfactin in SF+ liposomes, respectively.

In general, the kinetics could not be fitted to a simple exponential function (Supplementary Fig. 3); instead, Eq. (2) was used. All the leakage curves in Fig. 1 could be fitted to a combination of two kinetic functions. In SF+ liposomes, the data can be always described by one “rapid” function with a short τ and smaller amplitude (f_{01}, f_{03}, f_{05}) and another one with a long τ and higher amplitude (f_{02}, f_{04}, f_{06}). In comparison, in SF− liposomes this postponed action was faster (functions f_{08}, f_{10}, f_{12}) than in SF+ liposomes, and had a comparable amplitude to the initial rapid onset (functions f_{07}, f_{09}, f_{11}). In all SF+ and SF− kinetics, the parameter n exhibited a rather non-cooperative behavior of surfactin molecules in the membrane (Supplementary Table 1).

We next prepared mixtures of synthetic lipids that resembled the simplified composition of the lipid isolates previously used in Fig. 1. We decided to use a ternary system composed of those phospholipids present in the *B. subtilis* membrane that exhibited the most substantial changes in response to surfactin production [24]. These were phosphatidylglycerol (PG), phosphatidylethanolamine (PE) and cardiolipin (CL) in DOPG/DOPE/TOCL ratios of 0.35:0.20:0.45 (w/w/w) for the SF+ membrane and 0.55:0.30:0.15 (w/w/w) for the SF− membrane. Fig. 2 shows that both the synthetic SF+ and SF− leakage curves exhibited a rather unusual S-shape, which indicates a multi-response behavior of surfactin in the membrane. The leakage curves might be described by a combination of three functions – a non-cooperative one with a small amplitude (functions f_{13} and f_{16}), followed by the other two functions with rising n and comparable amplitudes (f_{14} - f_{15} and f_{17} - f_{18} in the synthetic SF+ and SF− curves, respectively). The liposomes formed from the lipid mixture that resembled the SF+ membrane proved to be more resilient to surfactin-induced lysis; in synthetic SF+ kinetics, the τ values of the cooperative functions were three times as long as in synthetic SF− ones, meaning an overall slower leakage. The rate of lysis was v = 1.7%/min, compared to 5.0%/min for synthetic SF+ and SF−, respectively. Thus, differences in the susceptibility to surfactin action were observed in both liposomal systems composed of either isolated lipids or of the corresponding synthetic lipids. In liposomes composed of isolated lipids, this difference was demonstrated both by the rate and overall time-course of lysis. In liposomes composed of membrane-mimicking lipids, we only observed changes in overall τ.

3.2. Effect of different phospholipid classes on membrane stability against surfactin action

To test the influence of individual phospholipid classes on membrane resistance against surfactin, we used liposomes consisting of the carrier lipid phosphatidylcholine (PC, not present in the *B. subtilis* membrane), with 2:1 (w/w) additions of major *B. subtilis* phospholipids - PG, PE, CL, and phosphatidic acid (PA). Fig. 3A demonstrates that liposomes composed solely from PC were quite sensitive to surfactin-induced leakage. After the addition of surfactin, the fluorescence intensity rose steeply, after 110 s the lysis was almost complete (90%), and at the end it reached 99%. Liposomes composed of binary

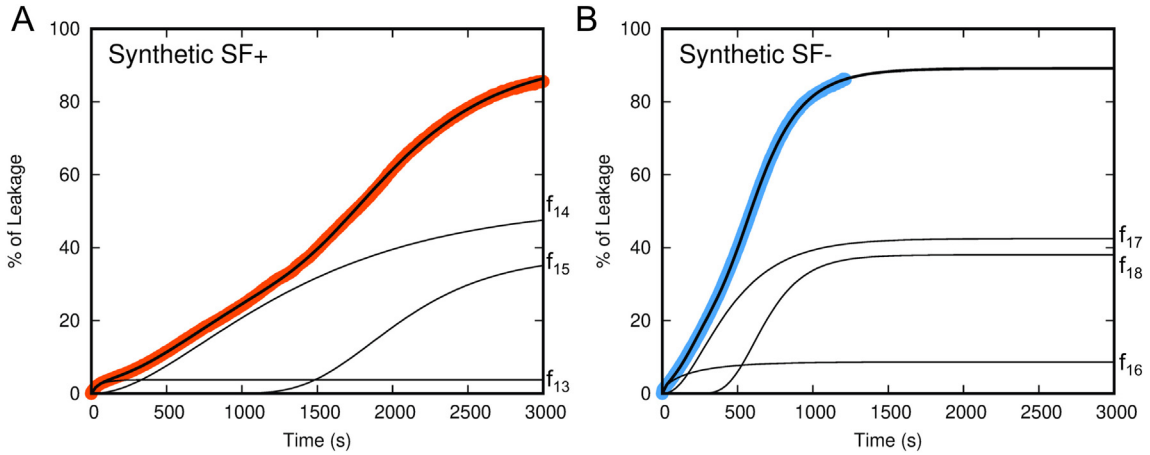

Fig. 2. Leakage of carboxyfluorescein from liposomes prepared from a mixture of synthetic phospholipids mimicking the composition of the lipid isolates presented in Fig. 1 - DOPG:DOPE:TOCL 0.35:0.20:0.45 (w/w/w) and 0.55: 0.30: 0.15 (w/w/w) for SF + (A) and SF − respectively (B). Surfactin was added at time 0 to a final concentration of 50 μM. 100% leakage was achieved using 0.1% Triton X-100. The parameters for fitting the curves to the convolution of functions f_{13}-f_{18} presented in (A) and (B) are listed in Supplementary Table 1. The rates of CF release were 1.7 ± 0.0%/min and 5.0 ± 0.0%/min (p = 0.0002) for the kinetics presented in A and B, respectively.

phospholipid mixtures (PC with the tested phospholipid in a 2:1, w/w ratio) were less susceptible to surfactin-induced lysis compared to the ones with PC alone (Fig. 3B–E). The stabilizing effect of the tested phospholipids increased in the order PE < PA < PG < CL, and is demonstrated by the decreased rate of leakage and decreased maximal surfactin-induced leakage over the same period. For PC/PE, the value of v (%/min) dropped slightly in comparison to liposomes solely composed of PC, v = 51.4 and 44.6%/min for PC and PC/PE, respectively. With PC/PA, the rate was 28.9%/min, and with PC/PG the rate of lysis decreased to 22.9%/min. The maximal surfactin-induced leakage decreased from 99% (in PC) to approximately 90% in all three of these (PC/PE, PC/PA and PC/PG) liposomal systems. The presence of CL in the liposomal membrane exhibited the strongest stabilizing effect on liposome integrity (Fig. 3B). The rate of lysis dropped more than threefold to v = 14.1%/min in comparison to liposomes composed solely from PC, and the maximum lysis was reduced to 80%. Quite obviously, in PC/CL liposomes (Fig. 3B), the character of the leakage kinetics differed the most from the other systems.

To further investigate the concentration dependency of the CL stabilization effect in the membrane, we used liposomes consisting of PG/CL mixtures containing 0%, 15% and 30% cardiolipin (w/w) and exposed them to surfactin (Fig. 4). All the curves might be described by

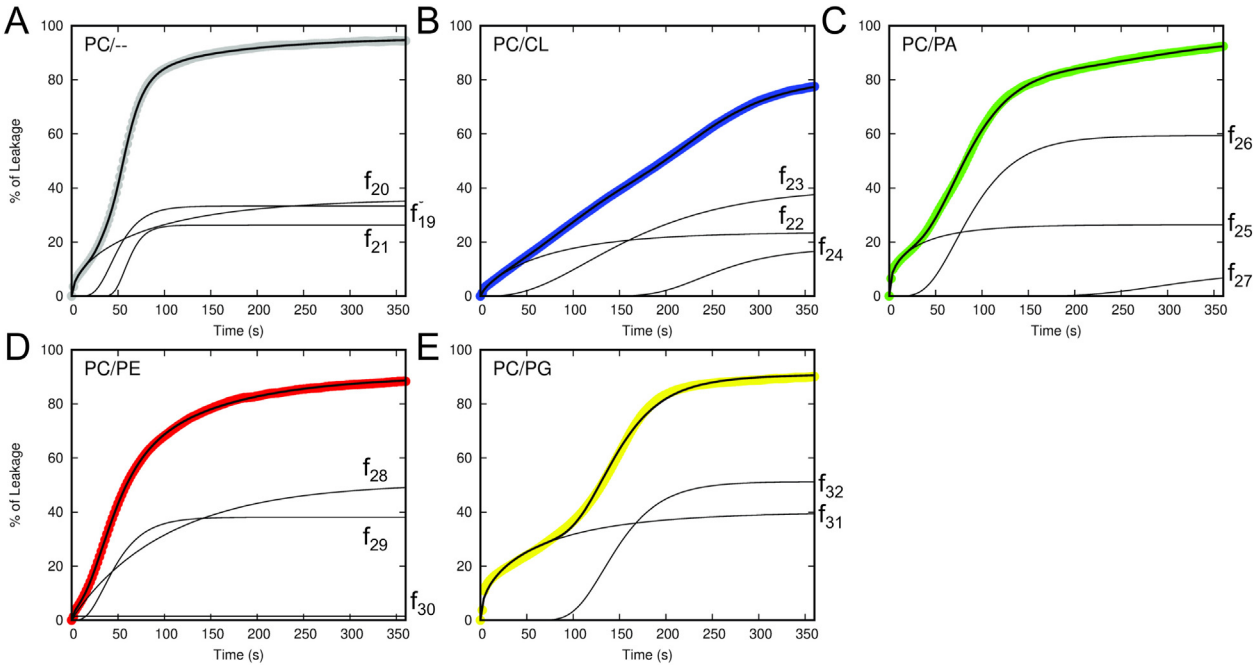

Fig. 3. Leakage of carboxyfluorescein from liposomes prepared from phosphatidylcholine (PC) and PC with the main phospholipid representatives of B. subtilis membrane. (A) Pure PC, (B) mixture of PC and cardiolipin (TMCL), (C) mixture of PC and phosphatidic acid (DMPA), (D) mixture of PC and phosphatidylethanolamine (DMPE), (E) mixture of PC and phosphatidylglycerol (DMPG). In (B)–(E) the ratio of PC to the given phospholipid in the liposome membrane was 2:1 (w/w). The phospholipid concentration in the liposome suspension was 25 μM, and surfactin was added at time 0 to a final concentration of 10 μM. 100% leakage was achieved using 0.1% Triton X-100. The parameters for fitting the curves to functions f_{19}-f_{31} presented in (A)–(E) are listed in Supplementary Table 1. The rates of CF release were as follows – PC/– (i.e. PC only) 51.4 ± 0.4, PC/PE 44.6 ± 1.9 (p = 0.16), PC/PA 28.9 ± 1.5 (p = 0.03), PC/PG 22.9 ± 0.9 (p = 0.01) and PC/CL 14.1 ± 0.2%/min (p = 0.0004).

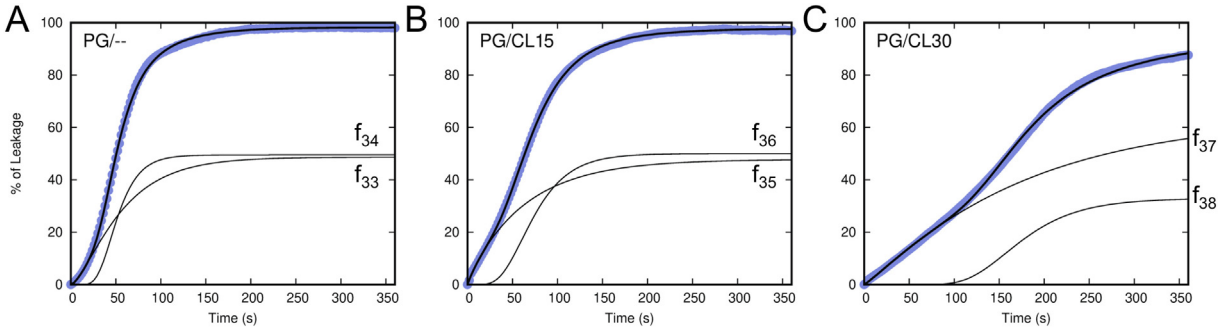

Fig. 4. Leakage of carboxyfluorescein from liposomes as a function of cardiolipin concentration. Pure DOPG (A) and DOPG with 15 (B) and 30% (C) additions (w/w) of TOCL were used. The phospholipid concentration in the liposome suspension was 10 μM. Surfactin was added at time 0 to a final concentration of 50 μM. 100% leakage was achieved using 0.1% Triton X-100. The parameters for fitting the curves to functions f_{33}-f_{38} presented in (A)–(C) are listed in Supplementary Table 1. The rates of CF release were 57.4 ± 4.8, 41.7 ± 6.7 (p = 0.06) and 17.2 ± 2.1%/min (p = 0.003) for the kinetics presented in A, B and C, respectively.

the combination of two functions (Eq. (2)) – one with longer τ (f_{33}, f_{35} and f_{37}) followed by a delayed cooperative one (f_{34}, f_{36} and f_{38}). Raising the proportion of CL in the membrane gradually prolonged the τ of both functions (Supplementary Table 1) and in PG/CL30 also lowered the amplitude of the postponed cooperative function (f_{38} compared to f_{34} and f_{36}). The susceptibility of the liposomes to surfactin-induced leakage decreased with increasing content of cardiolipin, with pure PG reaching a rate of lysis v = 57.4%/min, while the presence of 15% CL resulted in v = 41.7%/min, and the highest proportion of CL (30%) gave v = 17.2%/min. Thus, the presence of cardiolipin in the liposomal membrane decreases the rate of lysis in a concentration-dependent manner.

3.3. Cardiolipin-deficient *B. subtilis* is more prone to surfactin-induced membrane permeabilization

All the above experiments pointed to the essential role of CL in membrane stabilization against the action of surfactin. We further decided to validate the role of CL in the complex environment of a *B. subtilis* membrane that has never been exposed to surfactin. We used a pair of *B. subtilis* strains - a wild-type CL+ strain and its CL− derivative (Table 1), whose membrane lacks cardiolipin, and accordingly the membrane lipids have a higher proportion of PG [35]. We isolated total cell lipids from each of the strains and reconstituted CF-loaded liposomes. These liposomes were exposed to surfactin to final surfactin concentrations of 5, 10 and 20 μM. The data in Fig. 5 clearly demonstrate a higher stability of CL-containing membranes (isolated CL+) in comparison to CL− ones (isolated CL−). With 10 and 20 μM surfactin, the rates of dye leakage were twice as high in the CL− liposomes than the CL+ ones (Fig. 5, Supplementary Table 1). The functions fitted to the kinetic data show that the cooperative phase of leakage is faster in the CL− liposomes (τ is lowered in f_{48} and f_{50}) than in the CL+ ones (f_{42} and f_{44}). It is noteworthy that in the CL− liposomes treated with 20 μM surfactin, the proportion (amplitude) of the initial non-cooperative function (f_{49}) also increases sixfold compared to CL+ liposomes (f_{43}).

Thus, these experiments with liposomes composed of total lipids isolated from CL+ and CL− *B. subtilis* strains confirmed that membranes containing CL are less prone to surfactin-induced leakage. Next, we directly tested the stabilizing effect of cardiolipin against surfactin in living *B. subtilis* CL+ and CL− strains. We employed a membrane permeabilization assay with propidium iodide (Fig. 6). In this experiment with the suspension of living cells, the surfactin concentration needed to be increased up to 200 μM, as *B. subtilis* cells are capable of resisting high surfactin concentrations [21]. When we exposed the cells of *B. subtilis* CL− to surfactin concentrations of 50, 100 and 200 μM, the fluorescence intensity reached 50% after 7, 4.3 and 3.9 min, respectively. With the CL+ strain, almost doubled values of 13.5, 7.8 and 7.1 min were observed. While increasing the surfactin dose from 50 to 100 μM resulted in a substantially faster permeabilization of both strains, a further increase in the concentration to 200 μM led to only a minor difference in the rate of lysis. This suggests some sort of saturation effect, which we also observed in the CL− strain - using 100 and 200 μM surfactin also induced equal permeabilization. The data clearly show that the rate of permeabilization of CL− cells was faster and more effective. At an equal surfactin concentration, CL+ strain took approximately twice as long to reach 50% permeabilization as CL− cells. Or, in other words, a surfactin concentration of 100 and 200 μM had roughly the same effect on the CL+ strain as 50 μM of surfactin on the CL− strain, indicating a substantially higher susceptibility to surfactin of the CL− strain.

3.4. Surfactin forms diverse pores in DOPG membrane

In our wide range of liposomal systems, we always observed multimodal modes of membrane permeabilization induced by surfactin. This behavior was demonstrated in the non-trivial shape of the leakage curves that could not be fitted to a simple exponential function. The kinetics were only described with a set of functions given by Eq. (2). The parameters of these functions suggested that surfactin permeabilized the membranes via several mechanisms, even within a single experiment. This prompted us to check the distribution of surfactin pore conductances in the planar DOPG membrane. The histogram in Fig. 7 shows that surfactin forms pores with broad values of conductance (G, pS) ranging from a few pS up to 12 nS in 1 M KCl. The most frequent single-pore conductance unit was ~120 pS. The different conductance states might correspond to the heterogeneous pores in the liposomal membrane, which could be characterized by a varying number of surfactin monomers in the oligomeric pore explaining the multimodal leakage kinetics.

4. Discussion

We proved surfactin to be a pore-forming antimicrobial that forms a broad distribution of pores (Fig. 7), which may explain the multimodal leakage kinetics. Surfactin exerts antimicrobial potential against a wide range of microorganisms including bacterial and fungal pathogens [36], which might be of high importance in medicine [37], plant protection [38] or food safety [39]. Although surfactin's potential use in human medicine might be hindered by its relatively high hemolytic activity [40], surfactin could be employed in related areas: its anti-*Legionella* activity might be used to control natural *Legionella pneumophila* reservoirs in the environment [12]. Also, in basic research, surfactin can serve as a valuable model for other compounds with a similar mode of action, together with possible resistance or tolerance mechanisms in bacteria.

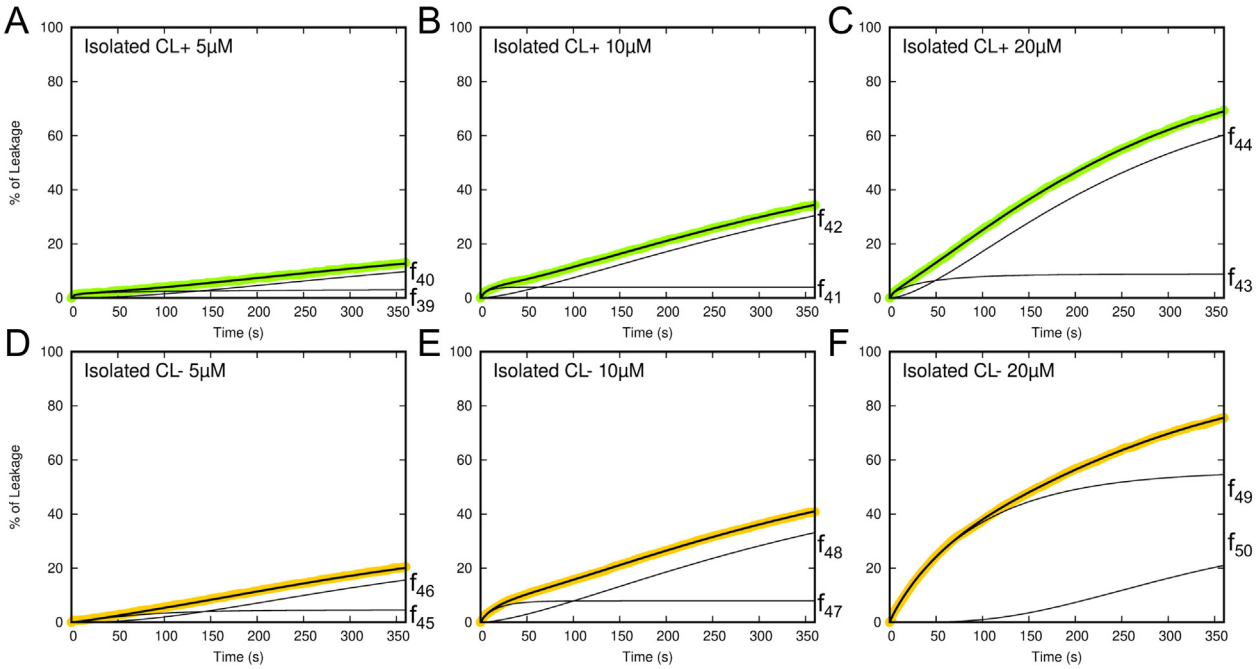

Fig. 5. Leakage of carboxyfluorescein from liposomes prepared from lipids isolated from CL+ (A–C) and CL− (D–F) B. subtilis strains. Surfactin was added at time 0 to a final concentration of 5, 10 and 20 μM (indicated in the graph legend). 100% leakage was achieved using 0.1% Triton X-100. C Parameters for fitting the curves to functions f_{39}-f_{50} presented in (A)–(F) are listed in Supplementary Table 1. The rates of CF release were 2.0 ± 0.8 and 2.2 ± 0.2%/min (p = 0.85) for the kinetics presented in A and D, respectively, 7.9 ± 0.4 and 15.5 ± 2.4%/min (p = 0.04) for B and E, respectively, and 13.7 ± 1.0%/min and 32.0 ± 0.8%/min (p = 0.0001) for the kinetics presented in C and F, respectively.

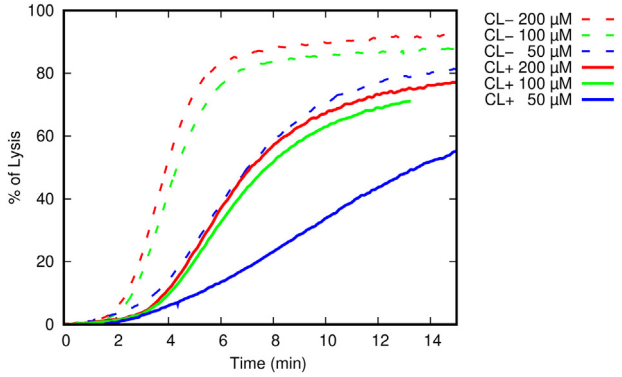

Fig. 6. Propidium iodide assay with living cells of B. subtilis CL+ and CL− strains. Cell concentration was 2×10^7/ml. Surfactin at a concentration of 50, 100 and 200 μM was added at time point 0 min. 100% permeabilization was achieved with 2.5 μM of melittin.

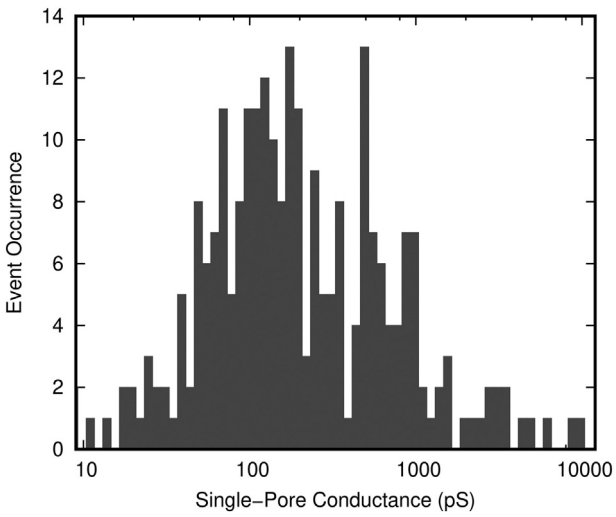

Fig. 7. Histogram of surfactin single-pore conductance. The pore-forming activity of surfactin (4 μM) was tested in 1 M KCl and 10 mM Tris, pH 7.4 with a constant voltage of 50 mV applied to the DOPG membrane. The histogram was created from pore openings (n = 252) using logarithmic bins (20 bins per decade). See Materials and methods (Section 2.8) for details.

Generally, the activity of membrane-active antimicrobials depends on target membrane characteristics such as membrane lipid composition and membrane potential. Unlike daptomycin, which is also a pore-forming lipopeptide antibiotic [41], the pore forming activity of surfactin is not affected by low membrane voltage [14,42]. This is a highly desirable feature of any antimicrobial compound, as it also enables its activity against dormant persistent cells with a low level of membrane potential. As for the lipid composition of the target membrane, the mode of action of some AMPs includes targeting specific lipids of the bacterial membrane – e.g. PG for daptomycin [43], CL for telomycin [44] or PE for cinnamycin [45]. Hand in hand with this principle, the mechanism of resistance also involves target site modification. In daptomycin-resistant strains of *B. subtilis*, *S. aureus*, *E. faecalis* or *E. faecium*, the resistance mechanism is realized by changes in teichoic or lipoteichoic acids of the cell wall, by altering membrane fluidity (either increasing or decreasing), by decreasing the content of PG, and the presence of CL or redistribution of CL microdomains leading to the diversion or repulsion of daptomycin from the membrane [46]. Even though it was thought that it is probably more difficult for bacteria to evolve a resistance mechanism towards membrane-targeting agents, it is becoming apparent that this is plausible. Thus, we need to improve our understanding about the AMP mechanism of action and the resistance and/or tolerance employed by bacteria.

We have previously shown that the surfactin-producing strain *B. subtilis* ATCC 21332 (SF+) progressively accumulated cardiolipin up to 22% of the total phospholipids during surfactin production. CL thus became the second major phospholipid of the membrane [24] and

brought about membrane rigidization that opposed the fluidizing effect of surfactin. In this paper, we isolated membrane lipids from the SF+ *B. subtilis* culture (20 h in the stationary phase, production of surfactin of up to 87 mg/l, which corresponds to 84 μM surfactin) and from the mutant surfactin-non-producing strain *B. subtilis* SF− (20 h in the stationary phase, surfactin 0 mg/ml). Although surfactin-producing strains can resist extremely high surfactin concentrations [47], a concentration in the range of tens of mg/l is harmful for a number of bacterial pathogens [48]. In our carboxyfluorescein-loaded SF+ and SF− liposomes (Fig. 1), the obvious difference in the shape of the leakage kinetics implied that the mechanism of lysis is different in isolated SF+ and SF− liposomes. In SF− liposomes exposed to 10 and 20 μM surfactin, we observed an abrupt steep rise in leakage, which took only a few seconds and stopped sharply upon reaching the plateau phase. We hypothesize that in SF− liposomes the initial fast phase of leakage depletes free surfactin from the solution, surfactin forms mixed micelles [30] with phospholipids from the disrupted membranes, and then there is a lack of monomers to form oligomeric pores in the later stages. In contrast, the time-course of the SF+ leakage curve was a more gradual one and would continue ad infinitum.

To obtain a deeper insight into the comparison of the leakage curves with each other, we performed a comparative analysis of the shapes of the curves. To clarify the principle, let's have curves *A* and *B* fitted to functions *a* and *b*, respectively (each could actually be a convolution of several functions). We fitted curve *A* to function *b* and tested (i) whether prolonging or shortening function *b* on the horizontal axis (changes in "global τ") and/or (ii) whether increasing or decreasing the amplitude of function *b* (changes in "global α") could describe the data in curve *A*. The same test was performed for curve *B* and function *a*. The quality of this global fit was evaluated by χ^2 values (Supplementary Fig. 3). This analysis confirmed that the leakage kinetics of isolated SF + liposomes with increasing surfactin concentration are very similar, and at the same time all the kinetics of isolated SF− liposomes are very much alike. In contrast, isolated SF+ and SF− kinetics differ greatly – we cannot overlap the SF− kinetics with any SF+ function (with the single trivial exception of slow kinetics at 5 μM surfactin, which can be described by a function corresponding to the SF+ function at 20 μM surfactin). This overall trend might point to a different mechanism of leakage of the SF+ and SF− membrane lipid composition and also a higher efficiency of the action of surfactin on SF− membranes.

With liposomes composed from the mixtures of synthetic phospholipids (Fig. 2), both the synthetic SF+ and SF− kinetics exhibited the same multi-phasic behavior demonstrated by the sigmoidal leakage kinetics. Such a shape of leakage curve is relatively uncommon, nevertheless it has also been described for certain membrane-active peptides [49–51]. The membrane composed of lipids resembling the SF− membrane was more prone to surfactin-induced lysis. The main difference between the SF+ and SF− membranes was the higher content of CL in the SF+ membrane at the expense of PG and PE which lead to a decreased rate of liposome lysis.

It is noteworthy that with these mixtures of synthetic phospholipids, the kinetics of surfactin-induced lysis were much slower than with the liposomes composed of isolated PLs (Fig. 1). We had to use a higher surfactin concentration (50 μM in Figs. 2 and 4 vs. a maximum of 20 μM in Fig. 1), while the phospholipid concentration in the liposome suspension was kept at 10 μM. We used such a relatively high surfactin-to-lipid ratio before in our previous study, working with liposomes composed of these types of synthetic lipid mixtures [23] to reach complete lysis within a reasonable timeframe (Supplementary Fig. 1). A surfactin-to-lipid ratio of up to 2.4 was also used in a study of the mechanism of membrane permeabilization by surfactin on liposomes composed of palmitoyl-oleoyl-phospholipids [17]. We propose that there might be two main reasons for such a relatively high surfactin concentration being required. Firstly, the liposomes from the total lipid extracts have an intrinsic property to be more vulnerable to spontaneous lysis [52,53]. Secondly, surfactin activity is higher in membranes containing PLs with shorter fatty acids [54,55]. Thus, membranes containing PLs with the fatty acid chain length of 18 carbon atoms found in dioleyl-PLs are less prone to surfactin-induced lysis.

We next tested the contribution of individual PL classes present in the *B. subtilis* membrane to the bilayer's stability towards the action of surfactin (Fig. 3). We chose PC as a neutral zwitterionic carrier lipid which is not present in the *B. subtilis* membrane. As was already shown, PC is highly miscible with surfactin [55] and such PC-based systems are suitable for studying any kind of stabilization effect of the PC/PL mixture. The lowered rate of lysis, at least with PC/PE liposomes, might be partially attributed to the difference between a binary PL mixture and a single-lipid bilayer. The binary lipid system composed of lipids with different molecule geometry (cone-shaped PE, cylindrical shape of PC) may better resist the strain induced by surfactin insertion into the membrane and by the subsequent membrane defects. We hypothesize that also the stabilizing effect of PA might be attributed, as with PE, to its conical shape and/or negative charge repulsing negatively charged surfactin. As we already showed in our previous work, PE and PA have a stabilizing effect against surfactin in liposomes composed of PG/PE 1:1 and PG/PE/PA 1:1:1 [23]. Also other studies showed that surfactin leakage from liposomes was inhibited by PE, however PE was always present in high proportion in the liposome membrane - PC/PE 1:1 [17] and PE/PG 3:2 [56].

The stabilizing effect of CL against surfactin permeabilization was the most pronounced. Compared to pure PC liposomes, in PC/CL liposomes the rate of lysis decreased more than threefold and the cooperative components of the kinetics (functions f_{23} and f_{24}) were delayed and with lower amplitudes (Fig. 3, Supplementary Table 1). Using PG liposomes with a different proportion of CL we corroborated the stabilizing effect of CL on membrane integrity against surfactin (Fig. 4). With respect to increasing CL concentration, the rate of liposome leakage decreased and with the 30% content of CL, also the second highly cooperative function (f_{38}) formed a smaller proportion of the whole kinetics compared to the pure PG liposomes. A decreased contribution of the cooperative component might suggest that mechanisms involving the formation of larger complexes/pores are suppressed with an increasing concentration of cardiolipin.

In parallel, we employed a *B. subtilis* mutant strain defective in cardiolipin synthesis and tested the role of cardiolipin in membrane protection against surfactin-induced permeabilization. Both carboxyfluorescein leakage from liposomes prepared from the total lipid extract and the membrane permeabilization assay with living cells (Figs. 5 and 6) confirmed that the absence of CL leads to a higher vulnerability to surfactin's action. Analysis of the global fit (Supplementary Fig. 4) of liposome leakage curves from Fig. 5 showed that we cannot fit the data of CL− kinetics to the CL+ ones and vice versa, which suggests that a different mechanism of lysis is occurring. On the other hand, we observed a similarity between the CL+ data and the fit describing the PC/CL and PG/CL15 kinetics, indicating that the presence of CL modifies the time-course of the leakage curves, suggesting a specific mode of action. Using living CL+ *B. subtilis* cells (Fig. 6), the kinetics of lysis induced by surfactin were slower and reached lower maximal values than with the CL− strain. In both CL+ and CL− cell suspensions, the increase in PI fluorescence begins after a lag time, which implies that the leakage requires the formation of some complexes in the membrane through which PI enters the cells. In CL+ cells, it took about 2 min before the onset of permeabilization, while this lag was shorter in the CL− strain – about 1 min. This phenomenon was not dependent on the surfactin concentration used.

Both the experiments with living cells and with liposomes from total lipid extract (both CL+/CL− and SF+/SF− systems) showed the increased effectiveness of surfactin-induced leakage in the absence of cardiolipin in the membrane. If we plot the rate of lysis as a function of surfactin concentration (Fig. 8), we obtain a linear dependence within the surfactin concentration range used. The slope of the linear function is more than four times steeper in SF− liposomes, which contain a

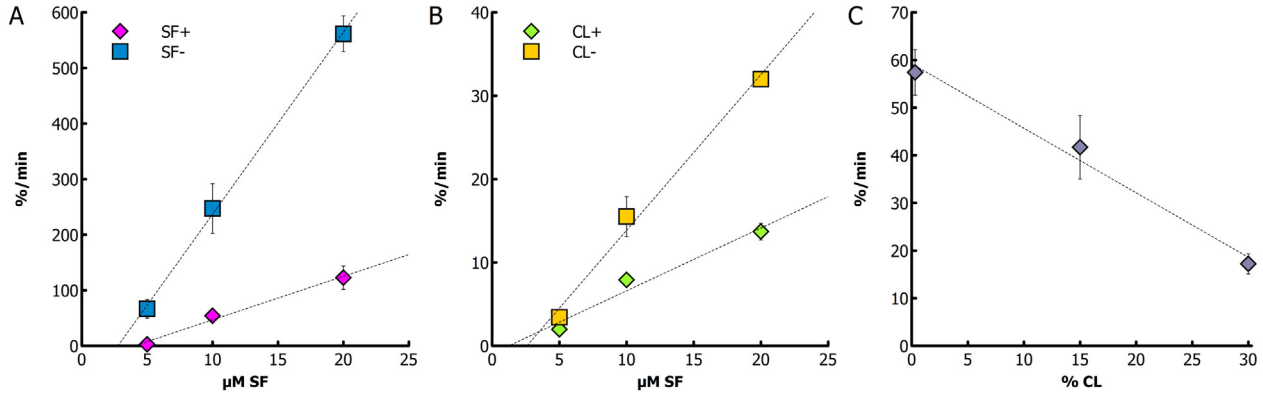

Fig. 8. Dependence of the rate of surfactin-induced leakage on surfactin concentration (A, B) and cardiolipin concentration (C). (A) and (B) show the dependence of the rate of lysis on the surfactin concentration used (data acquired from Fig. 1 and Fig. 5, respectively). The parameters of the linear fit are as follows: SF+ $y = 7.8x - 31.6$, SF− $y = 32.8x - 90.5$, CL+ $y = 0.8x - 0.9$, CL− $y = 1.9x - 4.8$. (C) shows the dependence of the rate of lysis as a function of the concentration of cardiolipin in the membrane (data acquired from Fig. 4). The parameters of the linear fit are as follows: $y = -1.4x + 59.2$.

lower amount of cardiolipin than SF+ ones (Fig. 8A). The absence of cardiolipin in CL− liposomes results in more than double the slope (Fig. 8B) compared to CL+ liposomes. Thus the higher propensity to surfactin-induced leakage is more pronounced in the SF+/SF− system than in the CL+/CL− one. This might be ascribed to the fact that the SF+/SF− liposomes consisted of lipids that differed more in their phospholipid composition [24] than the CL+/CL− ones [35]. Fig. 8C shows that increasing the proportion of cardiolipin in the liposomal membrane linearly decreases the rate of leakage. Thus, all the data point to an important role of cardiolipin in protecting the *B. subtilis* membrane against surfactin-induced leakage.

Nowadays, it is becoming increasingly apparent that antibiotic susceptibility may be associated with the lipid composition of a bacterial membrane. As for cardiolipin, surfactin is not the only antibiotic whose activity is affected by the content of this phospholipid. Enhanced levels of cardiolipin are associated with daptomycin resistance in *Enterococcus faecalis* and *E. faecium* [57] or in *Staphylococcus aureus* [58]. It was shown that CL does not affect daptomycin binding [58], but instead it inhibits pore formation by preventing daptomycin oligomerization [59] and by inhibiting the lipid-extraction effect [58]. Cardiolipin, which promotes negative membrane curvature, may also protect membranes against the positive curvature stress induced by pore-forming antimicrobial peptides such as magainin [60] or aurein [61]. On the other hand, in *Pseudomonas aeruginosa*, CL might also promote the action of a positively charged antibiotic - the aminoglycoside antibiotic 3′,6-dinonyl neamine. This antibiotic targets cardiolipin microdomains in the bacterial membrane, which leads to the disassembly of microdomains into cardiolipin clusters and the relocation of CL in the lateral organization of the membrane. This results in an impairment of the function of domain-bound proteins such as MreB and proteins of the respiratory chain [4]. It was also demonstrated that CL enhances membrane permeability and the efficiency of action of 3′,6-dinonyl neamine against *P. aeruginosa* [62].

We hypothesized about a plausible explanation for the stabilizing effect of the membrane CL against surfactin. As we have previously suggested [24], cardiolipin may increase the net negative charge of the membrane and thus prevent the electrostatic interaction of negatively-charged surfactin with the membrane. To explore this, we assessed the amount of bound surfactin to *B. subtilis* CL+ and CL− cells after incubation with 50, 100 and 200 μM surfactin (Supplementary Fig. 5). At all the surfactin concentrations used, the CL− strain bound a marginally higher amount of surfactin (ca. 20%) than CL+; however, it was only when using 50 μM surfactin that the difference was statistically significant (p value = 0.02). Interestingly, the total amount of bound surfactin did not change with increasing surfactin concentration. These results imply that the presence or absence of CL in the membrane does not affect the amount of tightly bound surfactin, and that both types of membranes reached some threshold concentration of membrane-bound surfactin. When the surfactin concentration is increased further, another mechanism of surfactin's mode of action probably takes over in the cell membrane. This may involve the formation of surfactin-rich clusters that disrupt the membrane locally [18]. In our opinion, the increased content of cardiolipin does not significantly limit this threshold. Nevertheless, due to its coulombic effect, CL may play a role in diverting surfactin monomers from the membrane surface, and thus slows down surfactin intake or reduces its effectivity once in the membrane. We can further speculate that CL+ membranes bind a comparable amount of surfactin to the CL− ones; however, similar to daptomycin [59], the formation of a functional pore or at least larger oligomeric pores is hindered. We should admit that the results of the amounts of bound surfactin could be affected by the fact that we assessed them in the plateau phase of the recorded PI kinetics (10 min exposure of cells to surfactin). The differences in CL+ and CL− kinetics are evident even from the lag-time before the onset of the PI fluorescence increase. We might speculate that this time interval of 1–2 min is crucial, and we suppose that it may indicate differences in surfactin binding capacity between the strains; however, this time interval is too short to analyze surfactin binding.

In conclusion, we demonstrate that a surfactin-adapted membrane obviously better resists surfactin-induced permeabilization. The phospholipid cardiolipin is naturally not the only factor in surfactin tolerance; however it is the key lipid component for stabilizing the *Bacillus subtilis* membrane. Its presence in the membrane slows down the surfactin-induced leakage and decreases the overall degree of lysis. We propose that the possible mechanism might involve a reduced primary interaction of surfactin with a membrane containing cardiolipin, blocking surfactin monomers from oligomerization, preventing the formation of large pores or counteracting the positive curvature stress introduced by surfactin insertion into the membrane. To resolve this, a separate study would need to be conducted using model membrane systems.

Declaration of competing interest

The authors declare that they have no known competing financial interests or personal relationships that could have appeared to influence the work reported in this paper.

Acknowledgements

This work was supported by grant GAUK 536217 from Charles University and SVV project 260568.

Appendix A. Supplementary data

Supplementary data to this article can be found online at https://doi.org/10.1016/j.bbamem.2020.183405.

References

[1] M.-P. Mingeot-Leclercq, J.-L. Décout, Bacterial lipid membranes as promising targets to fight antimicrobial resistance, molecular foundations and illustration through the renewal of aminoglycoside antibiotics and emergence of amphiphilic aminoglycosides, MedChemComm 7 (2016) 586–611, https://doi.org/10.1039/c5md00503e.

[2] J. Yao, C.O. Rock, Resistance mechanisms and the future of bacterial enoyl-acyl carrier protein reductase (FabI) antibiotics, Cold Spring Harbor Perspectives in Medicine 6 (2016), https://doi.org/10.1101/cshperspect.a027045.

[3] D. Lopez, G. Koch, Exploring functional membrane microdomains in bacteria: an overview, Curr. Opin. Microbiol. 36 (2017) 76–84, https://doi.org/10.1016/j.mib.2017.02.001.

[4] M. El Khoury, J. Swain, G. Sautrey, L. Zimmermann, P. Van Der Smissen, J.-L. Décout, M.-P. Mingeot-Leclercq, Targeting bacterial cardiolipin enriched microdomains: an antimicrobial strategy used by amphiphilic aminoglycoside antibiotics, Sci. Rep. 7 (2017) 10697, https://doi.org/10.1038/s41598-017-10543-3.

[5] F. Peypoux, J.M. Bonmatin, J. Wallach, Recent trends in the biochemistry of surfactin, Appl. Microbiol. Biotechnol. 51 (1999) 553–563, https://doi.org/10.1007/s002530051432.

[6] Y. Ishigami, M. Osman, H. Nakahara, Y. Sano, R. Ishiguro, M. Matsumoto, Significance of β-sheet formation for micellization and surface adsorption of surfactin, Colloids and Surfaces B-Biointerfaces 4 (1995) 341–348, https://doi.org/10.1016/0927-7765(94)01183-6.

[7] E. Vass, F. Besson, Z. Majer, L. Volpon, M. Hollosi, Ca^{2+}-induced changes of surfactin conformation: a FTIR and circular dichroism study, Biochem. Biophys. Res. Commun. 282 (2001) 361–367, https://doi.org/10.1006/bbrc.2001.4469.

[8] H.H. Shen, R.K. Thomas, C.Y. Chen, R.C. Darton, S.C. Baker, J. Penfold, Aggregation of the naturally occurring lipopeptide, surfactin, at interfaces and in solution: an unusual type of surfactant? Langmuir 25 (2009) 4211–4218, https://doi.org/10.1021/la802913x.

[9] A. Zou, J. Liu, V.M. Garamus, Y. Yang, R. Willumeit, B. Mu, Micellization activity of the natural lipopeptide [Glu1, Asp5] surfactin-C15 in aqueous solution, J. Phys. Chem. B 114 (2010) 2712–2718, https://doi.org/10.1021/jp908675s.

[10] P.A.V. Fernandes, I.R.d. Arruda, A.F.A.B.d. Santos, A.A.d. Araújo, A.M.S. Maior, E.A. Ximenes, Antimicrobial activity of surfactants produced by *Bacillus subtilis* R14 against multidrug-resistant bacteria, Braz. J. Microbiol. 38 (2007) 704–709, https://doi.org/10.1590/S1517-83822007000400022.

[11] D.C. Sabaté, M.C. Audisio, Inhibitory activity of surfactin, produced by different *Bacillus subtilis* subsp. subtilis strains, against *Listeria monocytogenes* sensitive and bacteriocin-resistant strains, Microbiol. Res. 168 (2013) 125–129, https://doi.org/10.1016/j.micres.2012.11.004.

[12] C. Loiseau, M. Schlusselhuber, R. Bigot, J. Bertaux, J.-M. Berjeaud, J. Verdon, Surfactin from *Bacillus subtilis* displays an unexpected anti-Legionella activity, Appl. Microbiol. Biotechnol. 99 (2015) 5083–5093, https://doi.org/10.1007/s00253-014-6317-z.

[13] H. Heerklotz, J. Seelig, Leakage and lysis of lipid membranes induced by the lipopeptide surfactin, Eur. Biophys. J. 36 (2007) 305–314, https://doi.org/10.1007/s00249-006-0091-5.

[14] J.D. Sheppard, C. Jumarie, D.G. Cooper, R. Laprade, Ionic channels induced by surfactin in planar lipid bilayer-membranes, Biochim. Biophys. Acta 1064 (1991) 13–23, https://doi.org/10.1016/0005-2736(91)90406-x.

[15] H. Heerklotz, J. Seelig, Detergent-like action of the antibiotic peptide surfactin on lipid membranes, Biophys. J. 81 (2001) 1547–1554, https://doi.org/10.1016/S0006-3495(01)75808-0.

[16] H.H. Shen, R.K. Thomas, J. Penfold, G. Fragneto, Destruction and solubilization of supported phospholipid bilayers on silica by the biosurfactant surfactin, Langmuir 26 (2010) 7334–7342, https://doi.org/10.1021/la904212x.

[17] C. Carrillo, J.A. Teruel, F.J. Aranda, A. Ortiz, Molecular mechanism of membrane permeabilization by the peptide antibiotic surfactin, Biochim. Biophys. Acta 1611 (2003) 91–97, https://doi.org/10.1016/s0005-2736(03)00029-4.

[18] M. Nazari, M. Kurdi, H. Heerklotz, Classifying surfactants with respect to their effect on lipid membrane order, Biophys. J. 102 (2012) 498–506, https://doi.org/10.1016/j.bpj.2011.12.029.

[19] J.G. Hurdle, A.J. O'Neill, I. Chopra, R.E. Lee, Targeting bacterial membrane function: an underexploited mechanism for treating persistent infections, Nat Rev Microbiol 9 (2011) 62–75, https://doi.org/10.1038/nrmicro2474.

[20] Y.-S. Wu, S.-C. Ngai, B.-H. Goh, K.-G. Chan, L.-H. Lee, L.-H. Chuah, Anticancer activities of surfactin and potential application of nanotechnology assisted surfactin delivery, Front. Pharmacol. 8 (2017) 761, https://doi.org/10.3389/fphar.2017.00761.

[21] K. Tsuge, Y. Ohata, M. Shoda, Gene yerP, involved in surfactin self-resistance in *Bacillus subtilis*, Antimicrob. Agents Chemother. 45 (2001) 3566–3573, https://doi.org/10.1128/aac.45.12.3566-3573.2001.

[22] X. Li, H. Yang, D. Zhang, H. Yu, Z. Shen, Overexpression of specific proton motive force-dependent transporters facilitate the export of surfactin in Bacillus subtilis, J. Ind. Microbiol. Biotechnol. 42 (2015) 93–103, https://doi.org/10.1007/s10295-014-1527-z.

[23] P. Uttlová, D. Pinkas, O. Bechyňková, R. Fišer, J. Svobodová, G. Seydlová, *Bacillus subtilis* alters the proportion of major membrane phospholipids in response to surfactin exposure, Biochimica et Biophysica Acta (BBA)-Biomembranes 1858 (2016) 2965–2971, https://doi.org/10.1016/j.bbamem.2016.09.006.

[24] G. Seydlova, R. Fiser, R. Cabala, P. Kozlik, J. Svobodova, M. Patek, Surfactin production enhances the level of cardiolipin in the cytoplasmic membrane of Bacillus subtilis, Biochimica Et Biophysica Acta-Biomembranes 1828 (2013) 2370–2378, https://doi.org/10.1016/j.bbamem.2013.06.032.

[25] G. Seydlová, J. Svobodová, Development of membrane lipids in the surfactin producer *Bacillus subtilis*, Folia Microbiol. 53 (2008) 303, https://doi.org/10.1007/s12223-008-0047-5.

[26] F. Kawai, M. Shoda, R. Harashima, Y. Sadaie, H. Hara, K. Matsumoto, Cardiolipin domains in *Bacillus subtilis* Marburg membranes, J. Bacteriol. 186 (2004) 1475–1483, https://doi.org/10.1128/jb.186.5.1475-1483.2004.

[27] G. Seydlová, J. Svobodová, Rapid and effective method for the separation of Bacillus subtilis vegetative cells and spores, Folia Microbiol. 57 (2012) 455–457, https://doi.org/10.1007/s12223-012-0157-y.

[28] G. Rouser, S. Fleische, A. Yamamoto, Two dimensional thin layer chromatographic separation of polar lipids and determination of phospholipids by phosphorus analysis of spots, Lipids 5 (1970) 494–496, https://doi.org/10.1007/BF02531316.

[29] J.N. Weinstein, R. Blumenthal, R.D. Klausner, Carboxyfluorescein leakage assay for lipoprotein-liposome interaction, Methods in Enzymology, vol. 128, Elsevier, 1986, pp. 657–668.

[30] M. Deleu, J. Lorent, L. Lins, R. Brasseur, N. Braun, K. El Kirat, T. Nylander, Y.F. Dufrene, M.P. Mingeot-Leclercq, Effects of surfactin on membrane models displaying lipid phase separation, Biochim. Biophys. Acta (2) (2013) 801–815, https://doi.org/10.1016/j.bbamem.2012.11.007.

[31] M. Wojdyr, Fityk: a general-purpose peak fitting program, J. Appl. Crystallogr. 43 (2010) 1126–1128, https://doi.org/10.1107/S0021889810030499.

[32] M. Gray, G. Szabo, A.S. Otero, L. Gray, E. Hewlett, Distinct mechanisms for K^+ efflux, intoxication, and hemolysis by *Bordetella pertussis* AC toxin, J. Biol. Chem. 273 (1998) 18260–18267, https://doi.org/10.1074/jbc.273.29.18260.

[33] I. Nicoletti, G. Migliorati, M. Pagliacci, F. Grignani, C. Riccardi, A rapid and simple method for measuring thymocyte apoptosis by propidium iodide staining and flow cytometry, J. Immunol. Methods 139 (1991) 271–279, https://doi.org/10.1016/0022-1759(91)90198-o.

[34] C. Nicolai, F. Sachs, Solving ion channel kinetics with the QuB software, Biophys. Rev. Lett. 08 (2013) 191–211, https://doi.org/10.1142/s1793048013300053.

[35] V.M. Bierhanzl, R. Cabala, M. Ston, P. Kotora, V. Ferenczy, J. Blasko, R. Kubinec, G. Seydlova, Direct injection mass spectrometry, thin layer chromatography, and gas chromatography of Bacillus subtilis phospholipids, Monatshefte Fur Chemie 147 (2016) 1385–1391, https://doi.org/10.1007/s00706-016-1734-6.

[36] H. Zhao, D. Shao, C. Jiang, J. Shi, Q. Li, Q. Huang, M.S.R. Rajoka, H. Yang, M. Jin, Biological activity of lipopeptides from *Bacillus*, Appl. Microbiol. Biotechnol. 101 (2017) 5951–5960, https://doi.org/10.1007/s00253-017-8396-0.

[37] S. Patel, S. Ahmed, J.S. Eswari, Therapeutic cyclic lipopeptides mining from microbes: latest strides and hurdles, World Journal of Microbiology & Biotechnology 31 (2015) 1177–1193, https://doi.org/10.1007/s11274-015-1880-8.

[38] J. Falardeau, C. Wise, L. Novitsky, T.J. Avis, Ecological and mechanistic insights into the direct and indirect antimicrobial properties of *Bacillus subtilis* lipopeptides on plant pathogens, J. Chem. Ecol. 39 (2013) 869–878, https://doi.org/10.1007/s10886-013-0319-7.

[39] K.R. Meena, S.S. Kanwar, Lipopeptides as the antifungal and antibacterial agents: applications in food safety and therapeutics, Biomed. Res. Int. 2015 (2015) 473050, https://doi.org/10.1155/2015/473050.

[40] S. Dufour, M. Deleu, K. Nott, B. Wathelet, P. Thonart, M. Paquot, Hemolytic activity of new linear surfactin analogs in relation to their physico-chemical properties, Biochim. Biophys. Acta Gen. Subj. 1726 (2005) 87–95, https://doi.org/10.1016/j.bbagen.2005.06.015.

[41] G. Seydlová, A. Sokol, P. Lišková, I. Konopásek, R. Fišer, Daptomycin pore formation and stoichiometry depend on membrane potential of target membrane, Antimicrob. Agents Chemother. 63 (2019), https://doi.org/10.1128/aac.01589-18 (e01589–01518).

[42] O.S. Ostroumova, V.V. Malev, M.G. Ilin, L.V. Schagina, Surfactin activity depends on the membrane dipole potential, Langmuir 26 (2010) 15092–15097, https://doi.org/10.1021/la102691y.

[43] A.B. Hachmann, E. Sevim, A. Gaballa, D.L. Popham, H. Antelmann, J.D. Helmann, Reduction in membrane phosphatidylglycerol content leads to daptomycin resistance in *Bacillus subtilis*, Antimicrob. Agents Chemother. 55 (2011) 4326–4337, https://doi.org/10.1128/AAC.01819-10.

[44] C.W. Johnston, M.A. Skinnider, C.A. Dejong, P.N. Rees, G.M. Chen, C.G. Walker, S. French, E.D. Brown, J. Bérdy, D.Y. Liu, N.A. Magarvey, Assembly and clustering of natural antibiotics guides target identification, Nat. Chem. Biol. 12 (2016) 233, https://doi.org/10.1038/nchembio.2018.

[45] G. Machaidze, J. Seelig, Specific binding of cinnamycin (Ro 09-0198) to phosphatidylethanolamine. Comparison between micellar and membrane environments, Biochemistry 42 (2003) 12570–12576, https://doi.org/10.1021/bi035225b.

[46] T.T. Tran, J.M. Munita, C.A. Arias, Mechanisms of drug resistance: daptomycin resistance, Ann. N. Y. Acad. Sci. 1354 (2015) 32–53, https://doi.org/10.1111/nyas.12948.

[47] F. Hu, Y. Liu, S. Li, Rational strain improvement for surfactin production: enhancing the yield and generating novel structures, Microb. Cell Factories 18 (2019) 42, https://doi.org/10.1186/s12934-019-1089-x.

[48] P. Das, S. Mukherjee, R. Sen, Antimicrobial potential of a lipopeptide biosurfactant derived from a marine *Bacillus circulans*, J. Appl. Microbiol. 104 (2008) 1675–1684, https://doi.org/10.1111/j.1365-2672.2007.03701.x.

[49] R. Ferre, M.N. Melo, A.D. Correia, L. Feliu, E. Bardají, M. Planas, M. Castanho,

Synergistic effects of the membrane actions of cecropin-melittin antimicrobial hybrid peptide BP100, Biophys. J. 96 (2009) 1815–1827, https://doi.org/10.1016/j.bpj.2008.11.053.

[50] R. Rathinakumar, W.C. Wimley, Biomolecular engineering by combinatorial design and high-throughput screening: small, soluble peptides that permeabilize membranes, J. Am. Chem. Soc. 130 (2008) 9849–9858, https://doi.org/10.1021/ja8017863.

[51] A. Pokorny, P.F.F. Almeida, Kinetics of dye efflux and lipid flip-flop induced by δ-lysin in phosphatidylcholine vesicles and the mechanism of graded release by amphipathic, α-helical peptides, Biochemistry 43 (2004) 8846–8857, https://doi.org/10.1021/bi0497087.

[52] J. Barbeau, S. Cammas-Marion, P. Auvray, T. Benvegnu, Preparation and characterization of stealth archaeosomes based on a synthetic PEGylated archaeal tetraether lipid, Journal of Drug Delivery 2011 (2011) 11, https://doi.org/10.1155/2011/396068.

[53] G.B. Patel, B.J. Agnew, H.C. Jarrell, G.D. Sprott, Stability of liposomes prepared from the total polar lipids of *Methanosarcina mazei* is affected by the specific salt form of the lipids, Journal of Liposome Research 9 (1999) 229–245, https://doi.org/10.3109/08982109909024787.

[54] A. Grau, J.C. Gómez Fernández, F. Peypoux, A. Ortiz, A study on the interactions of surfactin with phospholipid vesicles, Biochim. Biophys. Acta Biomembr. 1418 (1999) 307–319, https://doi.org/10.1016/S0005-2736(99)00039-5.

[55] O. Bouffioux, A. Berquand, M. Eeman, M. Paquot, Y.F. Dufrêne, R. Brasseur, M. Deleu, Molecular organization of surfactin–phospholipid monolayers: effect of phospholipid chain length and polar head, Biochim. Biophys. Acta Biomembr. 1768 (2007) 1758–1768, https://doi.org/10.1016/j.bbamem.2007.04.015.

[56] S. Fiedler, H. Heerklotz, Vesicle leakage reflects the target selectivity of antimicrobial lipopeptides from *Bacillus subtilis*, Biophys. J. 109 (2015) 2079–2089, https://doi.org/10.1016/j.bpj.2015.09.021.

[57] K.L. Palmer, A. Daniel, C. Hardy, J. Silverman, M.S. Gilmore, Genetic basis for daptomycin resistance in enterococci, Antimicrob. Agents Chemother. 55 (2011) 3345–3356, https://doi.org/10.1128/aac.00207-11.

[58] J.-H. Jiang, M.S. Bhuiyan, H.-H. Shen, D.R. Cameron, T.W.T. Rupasinghe, C.-M. Wu, A.P. Le Brun, X. Kostoulias, C. Domene, A.J. Fulcher, M.J. McConville, B.P. Howden, G.J. Lieschke, A.Y. Peleg, Antibiotic resistance and host immune evasion in *Staphylococcus aureus* mediated by a metabolic adaptation, Proc. Natl. Acad. Sci. 116 (2019) 3722–3727, https://doi.org/10.1073/pnas.1812066116.

[59] T. Zhang, J.K. Muraih, N. Tishbi, J. Herskowitz, R.L. Victor, J. Silverman, S. Uwumarenogie, S.D. Taylor, M. Palmer, E. Mintzer, Cardiolipin prevents membrane translocation and permeabilization by daptomycin, J. Biol. Chem. 289 (2014) 11584–11591, https://doi.org/10.1074/jbc.M114.554444.

[60] K. Matsuzaki, K.-i. Sugishita, N. Ishibe, M. Ueha, S. Nakata, K. Miyajima, R.M. Epand, Relationship of membrane curvature to the formation of pores by magainin 2, Biochemistry 37 (1998) 11856–11863, https://doi.org/10.1021/bi980539y.

[61] D. Poger, S. Pöyry, A.E. Mark, Could cardiolipin protect membranes against the action of certain antimicrobial peptides? Aurein 1.2, a case study, ACS Omega 3 (2018) 16453–16464, https://doi.org/10.1021/acsomega.8b02710.

[62] J. Swain, M. El Khoury, J. Kempf, F. Briée, P. Van Der Smissen, J.-L. Décout, M.-P. Mingeot-Leclercq, Effect of cardiolipin on the antimicrobial activity of a new amphiphilic aminoglycoside derivative on *Pseudomonas aeruginosa*, PLoS One 13 (2018) e0201752, , https://doi.org/10.1371/journal.pone.0201752.

Biochimica et Biophysica Acta 1858 (2016) 2965–2971

Contents lists available at ScienceDirect

Biochimica et Biophysica Acta

journal homepage: www.elsevier.com/locate/bbamem

Bacillus subtilis alters the proportion of major membrane phospholipids in response to surfactin exposure

Petra Uttlová, Dominik Pinkas, Olga Bechyňková, Radovan Fišer, Jaroslava Svobodová, Gabriela Seydlová *

Department of Genetics and Microbiology, Faculty of Science, Charles University in Prague, Viničná 5, 128 44, Prague 2, Czech Republic

ARTICLE INFO

Article history:
Received 1 July 2016
Received in revised form 6 September 2016
Accepted 8 September 2016
Available online 9 September 2016

Keywords:
surfactin
membrane
phospholipids
Bacillus subtilis

ABSTRACT

Surfactin, an anionic lipopeptide produced by *Bacillus subtilis*, is an antimicrobial that targets the cytoplasmic membrane. Nowadays it appears increasingly apparent that the mechanism of resistance against these types of antibiotics consists of target site modification. This prompted us to investigate whether the surfactin non-producing strain *B. subtilis* 168 changes its membrane composition in response to a sublethal surfactin concentration. Here we show that the exposure of *B. subtilis* to surfactin at concentrations of 350 and 650 μg/ml (designated as SF350 and SF650, respectively) leads to a concentration-dependent growth arrest followed by regrowth with an altered growth rate. Analysis of the membrane lipid composition revealed modifications both in the polar head group and the fatty acid region. The presence of either surfactin concentration resulted in a reduction in the content of the major membrane phospholipid phosphatidylglycerol (PG) and increase in phosphatidylethanolamine (PE), which was accompanied by elevated levels of phosphatidic acid (PA) in SF350 cultures. The fatty acid analysis of SF350 cells showed a marked increase in non-branched high-melting fatty acids, which lowered the fluidity of the membrane interior measured as the steady-state fluorescence anisotropy of DPH. The liposome leakage of carboxyfluorescein-loaded vesicles resembling the phospholipid composition of surfactin-adapted cells showed that the susceptibility to surfactin-induced leakage is strongly reduced when the PG/PE ratio decreases and/or PA is included in the target bilayer. We concluded that the modifications of the phospholipid content of *B. subtilis* cells might provide a self-tolerance of the membrane active surfactin.

1. Introduction

The cytoplasmic membrane is thought to be an underexploited antibiotic target. Nevertheless, antibiotics targeting the cytoplasmic membrane possess several advantages such as rapid action and also an activity against non-multiplying and multi-resistant bacteria. Also, possible obstacles with membrane permeability do not have to be considered, because the membrane itself is the primary target of such antibiotics. In addition, it is presumed that the development of a resistance mechanism against a membrane targeting antibiotic is more difficult for two main reasons. First, modifications of the cytoplasmic membrane may interfere with the proper functioning of the membrane and with cell physiology because it is a unique and essential cell structure. Second, the bactericidal action of membrane-targeting compounds is very rapid, thus decreasing the chance for resistance to occur. On the other hand a resistance mechanism against natural antimicrobial compounds must exist at least in the producing cells, which protect themselves in order to avoid suicide [1] and resistance could emerge in other bacterial species following clinical use. Membrane-active compounds such as daptomycin [2] produced by *Streptomyces roseosporus* and telavancin [3], a semi-synthetic derivative of vancomycin, are already in clinical use. Although to date no clinical isolate has been found with an acquired resistance to telavancin [4], resistance to daptomycin was detected shortly after its clinical introduction [5]. The mechanism of resistance is quite diverse but involves the target site, i.e. the cytoplasmic membrane, and cell wall modifications [6].

One of the antimicrobials that permeabilizes the cytoplasmic membrane is a lipopeptide antibiotic surfactin produced by *Bacillus subtilis*. Surfactin is composed of a cyclic heptapeptide bearing two negative charges (Asp, Glu) interlinked with a β-hydroxy fatty acid comprising 12–16 carbon atoms. It is capable of inserting itself into the cytoplasmic membrane, where it interacts with its lipid moiety leading to the loss of membrane barrier properties, eventually resulting in its complete disintegration by a detergent mechanism [7–9]. Both the polar head group region and the fatty acyl chains of membrane phospholipids may modulate the surfactin-membrane interaction and its penetration into the target bilayer in vitro [10,11].

The question arises of how *B. subtilis* ensures its self-resistance to membrane permeabilization induced by surfactin at concentrations that are able to inhibit the growth of pathogenic bacteria. It could be expected that a similar strategy might be also involved as an acquired resistance in pathogens. To find the answer, we previously carried out

* Corresponding author.
E-mail address: seydlova@natur.cuni.cz (G. Seydlová).

http://dx.doi.org/10.1016/j.bbamem.2016.09.006
0005-2736/

a comparative analysis of an isogenic pair of strains – a surfactin producer and its non-producing mutant [12]. We described that in the surfactin-producing strain *B. subtilis* ATCC 21332, surfactin production results in an enhanced content of cardiolipin in the membrane, leading to a plausible electrostatic repulsive effect preventing surfactin from interacting with the membrane, and an increased rigidity of the membrane counteracting the fluidizing effect of surfactin [12]. Thus, a target site modification might be regarded to be part of the resistance mechanism in that bacterium. Now, we decided to verify the assumption of possible target site modification induced by the membrane-targeting antimicrobial surfactin. We used *B. subtilis* 168, which does not produce surfactin, and exposed it to two different surfactin concentrations during the exponential phase of growth.

B. subtilis 168 possesses all the genes necessary for non-ribosomal surfactin synthesis, however it does not produce surfactin due to a frameshift mutation in the essential gene *sfp* [13] coding for the phosphopantetheine cofactor. Nevertheless, it is highly likely that this strain bears the genetic information not only for surfactin production but naturally also for surfactin resistance. To date the only gene contributing to surfactin resistance in *B. subtilis* is *yerP* (*swrC*), encoding the homolog of a proton-dependent multidrug efflux pump belonging to the RND family. However even the *swrC*-deficient strain of *B. subtilis* 168 is able to resist high surfactin concentrations in the medium [14]. This suggests that another resistance mechanism must exist in surfactin self-resistance. As the propensity to membrane permeabilization is strongly influenced by the phospholipid composition of the entire membrane in vitro, target site modification might be taken into consideration. We aimed to determine whether *B. subtilis* 168 (i) changes its phospholipid composition (both polar heads and fatty acids of membrane phospholipids) in response to surfactin exposure, (ii) if these changes are concentration-dependent and (iii) if the adaptive modifications of the lipid bilayer might contribute to the survival of *B. subtilis* cells.

2. Materials and Methods

2.1. Growth of B. subtilis in the presence of surfactin

B. subtilis 168 (trpC2, Bacillus Genetic Stock Center) was grown aerobically in nutrient broth (Oxoid) at 30°C and the growth was monitored by measuring the optical density at 420 nm. When the culture reached the exponential phase of growth (OD ~ 0.5) it was used to inoculate agar plates (1×10^7 cells per plate) containing surfactin at a concentration of 350 and 650 μg/ml respectively, and the cultivation continued at 30°C. To follow the growth of the culture, the biomass was washed from the plate using 5 ml of physiological solution and the OD of the suspension was measured. The cell biomass for the subsequent lipid isolation and analysis was harvested from the plates during the exponential phase of growth - $\log_2$ (OD.1000) ~ 9.0 (OD_{420} ~ 0.5).

2.2. Isolation of surfactin

The surfactin-producing strain *B. subtilis* ATCC 21332 (American Type Culture Collection) was grown at 30°C in mineral salt medium containing glucose 40 g/l, KH_2PO_4 30 mM, NH_4NO_3 50 mM, Na_2HPO_4 40 mM, $MgSO_4$ 0.8 mM, $FeSO_4$ 1 mM,$CaCl_2$ 7 μM, and Na_2EDTA 4 μM for 3 days [15]. The cells were spun down, the pH of the cell-free supernatant was adjusted to pH 2.0 with HCl, and the acid precipitation was conducted overnight at 4 °C. The pelleted precipitate was extracted with methanol at room temperature; the solvent was evaporated in vacuo at 40 °C and dissolved in chloroform. The chloroform extract was filtered through glass fiber filters (GF/C, Whatman) and again evaporated in vacuo under the same conditions. The final crude extract containing surfactin was stored at -20°C.

2.3. Surfactin analysis

Surfactin concentration was determined by reverse-phase C18 HPLC using a HPLC Agilent 1200-Agilent 6460 Triple Quadrupole MS system equipped with a Zorbax Eclipse XDB-C18 column (particle size 5 μm, Agilent Technologies). The mobile phase consisted of (a) 0.1% formic acid in acetonitrile and (b) aqueous 0.1% formic acid at a ratio of a/b 80%:20% (v/v) and the mobile phase flow rate used for the analysis was 1 ml/min. The sample size was 5 μl. Five surfactin isoforms (C12–C16 surfactin and sodium adduct ions) were detected at m/z 994.6 and 1016.6, m/z 1008.6 and 1030.6, m/z 1022.6 and 1044.6, m/z 1036.6 and 1058.6, m/z 1050.6 and 1072.6, respectively. The proportions of the five surfactin isoforms were as follows: C12 0.8 ± 0.1 %, C13 7.3 ± 0.6 %, C14 46.9 ± 0.8 %, C15 41.6 ± 0.3 %, C16 3.4 ± 0.2 %. This is in agreement with commercial surfactin (Sigma-Aldrich), which served as a standard. The data were analyzed using Agilent MassHunter Workstation Data Acquisition and Agilent MassHunter Data Analyses.

2.4. Lipid extraction and analysis

Lipids were extracted from the cell biomass using a hexan-isopropanol 3:2 (v/v) mixture. After evaporation of the solvent in vacuo at 40 °C, the lipid extract was dissolved in chloroform, filtered through glass fiber filters (GF/C, Whatman) and dried again. The lipid isolate was used for fatty acid analysis or separated into phospholipid classes using TLC (silica gel 60 G plates, Merck) in chloroform-methanol-water (65:25:4, v/v/v) as the mobile phase. The spots corresponding to each phospholipid class were collected from the plate and quantified spectrophotometrically as the content of inorganic phosphate after digestion with perchloric acid [16].

2.5. Fatty acid analysis

Phospholipid fatty acids of extracted lipids were transesterified to fatty acid methyl esters by incubation in sodium methoxide at room temperature according to a previously published procedure [17]. After neutralization by the addition of methanolic HCl, the fatty acid methyl esters (FAMEs) were extracted with pentane, dried under a flow of nitrogen and dissolved in heptane before analysis using a GCMS-QP 5050A gas chromatograph (Shimadzu, Japan) with a mass spectrometer detector. A DB-5MS separation capillary column (30 m × 0.25 mm, stationary phase thickness 0.25 μm) was purchased from Agilent Technologies (USA). The linear velocity of the carrier gas was set to 30 cm s^{-1}. An AOC-20i automatic sampler (Shimadzu, Japan) was used to inject 2 μl of the samples, which were measured in split (1:20) and scan mode. Injection temperature was held at 270 °C. The measurements were carried out with the following temperature program: initial temperature 60 °C, 4 min, then 7.5 °C.min^{-1} to 250 °C, 20 min. The chromatograms were evaluated with GC Solution v. 1.21 (Shimadzu) software and mass spectra were compared with the NIST database (2011).

2.6. Steady-state fluorescence anisotropy measurements

For the fluorescence anisotropy measurements, liposomes were prepared from the isolated lipids. Lipids were dissolved in chloroform and a thin film was created under a stream of nitrogen on the walls of a glass tube. Then 50 mM Tris-HCl buffer (pH 6.6) was added and multilamellar liposomes were formed by vigorous shaking of the tube. The fluorescent probe 1,6-diphenylhexatriene (DPH, Sigma) in acetone was added at a final concentration of 1 μM (DPH/lipid molar ratio 1:400) to the liposomes (volume of the sample was 2.5 ml). The sample was then incubated in the dark at 37 °C for 30 min. The fluorescence anisotropy measurements were taken in a quartz cuvette with a Fluoromax-3 spectrofluorometer (Jobin Yvon Horiba) equipped with DataMax software and a polarization accessory. The excitation and emission wavelengths were 360 nm and 450 nm, respectively. The intrinsic

fluorescence intensity of unlabeled membranes did not exceed 2% of the experimental values. The steady-state fluorescence anisotropy is defined as the difference between intensities of vertically and horizontally polarized emissions divided by total fluorescence intensity by the equation $r_{ss} = (I_{VV} - I_{VH})/(I_{VV} + 2I_{VH})$, where I_{VV} and I_{VH} are the fluorescence intensities measured in a vertical and horizontal direction to the excitation light beam [18].

2.7. Liposome preparation and liposome leakage assay

Dioleylphosphatidylglycerol (DOPG), dioleoylphosphatidylethanolamine (DOPE) and dioleoylphosphatidic acid (DOPA) were purchased from Avanti Polar Lipids. Liposomes for the carboxyfluorescein leakage assay were prepared by mixing the appropriate amount of lipids (0.5 mg/ml) in chloroform/methanol 2:1 (v/v). The solvent was subsequently evaporated in vacuo to form a thin film on the walls of a glass tube. The hydration procedure in a buffer containing 50 mM 5(6)-carboxyfluorescein (CF), 5 mM HEPES, pH 7.4 was comprised of an incubation time of 90 min at 38 °C, interrupted by thorough vortex shaking to form multilamellar vesicles. Large unilamellar vesicles (LUVs) were prepared by repeated extrusion of the multilamellar vesicles through 100-nm polycarbonate filters (Avestin) using a Mini-Extruder apparatus (Avanti Polar Lipids). Vesicles were separated from the nonencapsulated dye by gel filtration on Sephadex G-50 using 100 mM NaCl, 0.5 mM Na_2EDTA and 5 mM HEPES, pH 7.4 as elution buffer. Fractions with the highest content of entrapped dye were put together and diluted in the same buffer to give a final phospholipid concentration of 10 μM (according to the assessed content of inorganic phosphate).

The leakage of vesicles was measured as the increase in the CF fluorescence intensity released into the milieu after the addition of surfactin to a final concentration of 50 μM (stock solution – 500 μM surfactin dissolved in 10 mM NaOH). The maximum release of CF fluorescence (F_{max}) was reached after disrupting the liposomes with 0.02% Triton X-100. Fluorescence intensity was monitored over time (excitation at 480 nm, emission at 515 nm) at 25 °C using a FluoroMax-3 (Jobin Yvon Horiba) spectrofluorometer. The following equation was used to calculate the percentage of CF leakage: $\%CF\ leakage = [(F - F_0)/(F_{max} - F_0)] \times 100$, where F is the actual fluorescence intensity and F_0 is the fluorescence intensity before the addition of the permeabilizing agent. Representative results from three individual experiments are shown.

2.8. Statistics

Student's t test was used to assess the differences between two mean values of doubling time, PL and FA levels and the half-time of liposome lysis. P values of < 0.05 were considered significant.

3. Results

3.1. Growth of B. subtilis in the presence of surfactin

First of all, we aimed at finding a surfactin concentration that would be high enough to induce a response in the bacterial cells (measured as a change in growth rate), but still would not be lethal to *B. subtilis*. From the serial dilutions of surfactin (Fig. 1) we chose two surfactin concentrations - 350 and 650 μg/ml (designated here as SF350 and SF650, respectively). *B. subtilis* was then grown in nutrient medium under optimal conditions (control) and in the presence of the two different surfactin concentrations tested (Fig. 2). Under control conditions, the doubling time of the culture was $T = 51 \pm 4$ min. When exposed to surfactin, both the cultures stopped growing for a concentration-dependent time period taking 40 min (SF350) and 180 min (SF650), respectively. After this lag period, the cells treated with 350 μg/ml of surfactin restored their growth with a shorter doubling time $T = 46 \pm 5$ min ($P < 0.05$) and the cells treated with 650 μg/ml with $T = 111 \pm 12$ min ($P < 0.0001$).

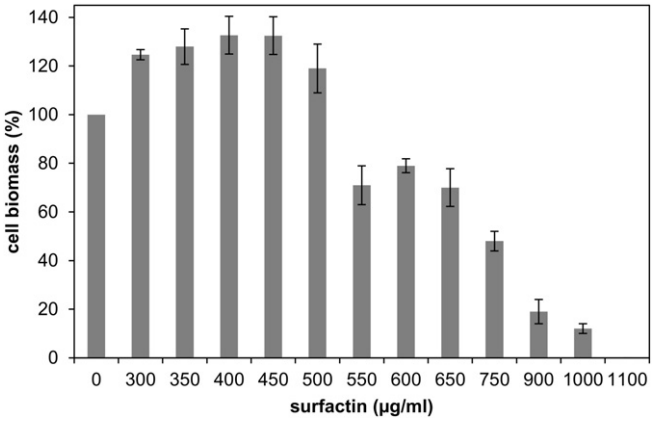

Fig. 1. Effect of surfactin on *B. subtilis* growth. *B. subtilis* (initial inoculum 10^7 cells) was grown on agar plates supplemented with surfactin at the concentrations indicated on the x axis. After overnight cultivation (14 h), the cell biomass was quantified as the optical density of the suspension washed from the plates (see part 2.1). The values are normalized to the control without surfactin.

All three cultures entered the stationary phase of growth after six generations. Thus, the presence of surfactin induced concentration-dependent alteration in the growth characteristics of the *B. subtilis* culture – the occurrence of a growth lag and a prolonged doubling time, both of which indicated a need to adapt to the presence of the antimicrobial agent.

3.2. Phospholipid composition of surfactin-treated cells

The polar heads of membrane phospholipids (PLs) are in the first line of surfactin's interaction with the membrane and can profoundly modulate surfactin penetration inside and subsequent disintegration of the cell. In order to determine whether the cells exposed to sublethal

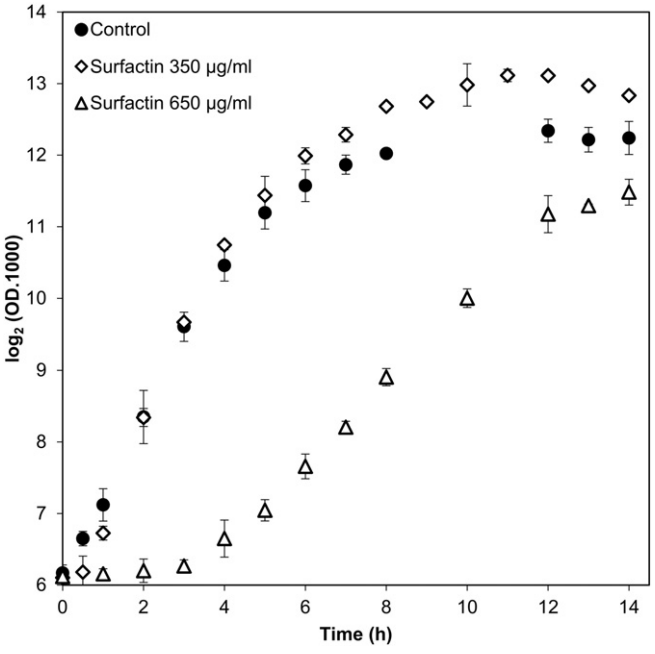

Fig. 2. Growth of *B. subtilis* in the presence of surfactin. Mid-log phase *B. subtilis* cells (initial inoculum 10^7 cells) were inoculated on agar plates containing surfactin at the concentrations indicated. The doubling time of the control cells was 51 min, surfactin-treated cells halted their growth in a concentration-dependent manner and then restored their growth with a doubling time of 46 and 110 min for 350 and 650 μg/ml of surfactin, respectively.

surfactin concentrations change their polar head group composition, we carried out a comparative analysis of the control cells and the cells exposed to the two different surfactin concentrations. The lipids were isolated from cell biomass during the exponential phase of growth (OD ~ 0.5), i.e. after 3 generations of cells growing in the presence of surfactin.

TLC analysis revealed that the presence of surfactin in the growth medium induced substantial changes in the proportion of phospholipid classes in the membrane (Fig. 3). The adaptation response differed for the two surfactin concentrations used; however, in the membrane of cells treated with either surfactin concentration we observed a decrease in the content of the major lipid component of the membrane phosphatidylglycerol (PG). Under the concentration of SF350, its content dropped from 44 % to 19 % ($P < 0.001$) and under a surfactin concentration of SF650 to 31 % ($P < 0.01$). The proportion of the second-most abundant phospholipid of the *B. subtilis* membrane, phosphatidylethanolamine (PE), did not change in response to SF350; however, it increased from 24 % to 40 % ($P < 0.01$) in the membranes of *B. subtilis* cells exposed to SF650, and thus it became the predominant lipid component of the membrane. The most striking feature of the cells treated with SF350 was the reduced level of PG accompanied with a substantial increase in the content of the common precursor of phospholipid synthesis – phosphatidic acid (PA). Its content dramatically rose from the trace levels observed in control cells up to 23 % ($P < 0.0005$). The fall in the proportion of PG was quantitatively replaced with a slightly higher cardiolipin (CL) content and increased level of PA.

3.3. Fatty acid profiles of B. subtilis cells treated with surfactin

Not only the polar heads of membrane PLs, but also their fatty acids (FAs) influence the extent of membrane permeabilization induced by surfactin. The length of the FA chains influences surfactin penetration into the membrane and, together with the FA branching pattern, has a strong impact on the fluidity of the membrane (which is also affected by surfactin). Therefore we tested how the presence of surfactin modified the FA composition of the *B. subtilis* membrane.

In contrast to the polar head groups of membrane PLs, using GC/MS almost no changes in the fatty acid composition were found in *B. subtilis* cells exposed to SF650 (Fig. 4). The typical high content (87 % in control cells) of branched-chain FAs did not change (83 %), nor did the proportion of the iso- and anteiso- branching pattern. On the other hand SF350 caused a substantial decrease in the content of branched-chain FAs to 68 % ($P < 0.05$), together with an increase in straight-chain FAs from 13 to 32 % ($P < 0.04$, dominated by the increase in 16:0 and 18:0 FAs). Thus similarly to the polar head group's profiles, we can conclude that the lower surfactin concentration has a stronger impact on the lipid composition of the membrane.

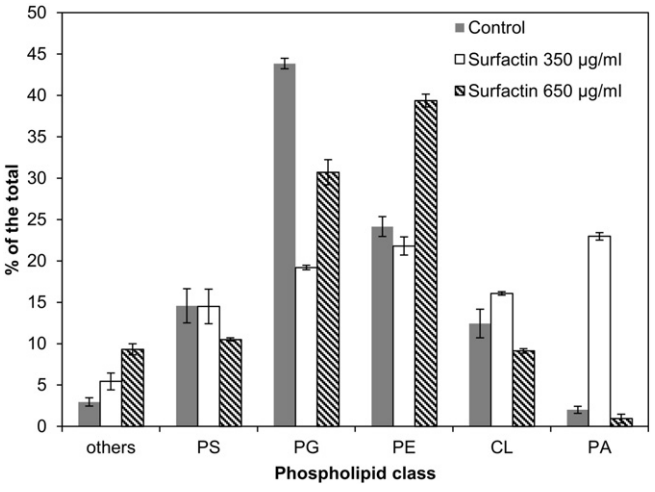

Fig. 3. Phospholipid composition of *B. subtilis* exposed to surfactin PS - phosphatidylserine, PG - phosphatidylglycerol, PE - phosphatidylethanolamine, CL - cardiolipin, PA - phosphatidic acid. Values represent means ± standard errors (n = 3).

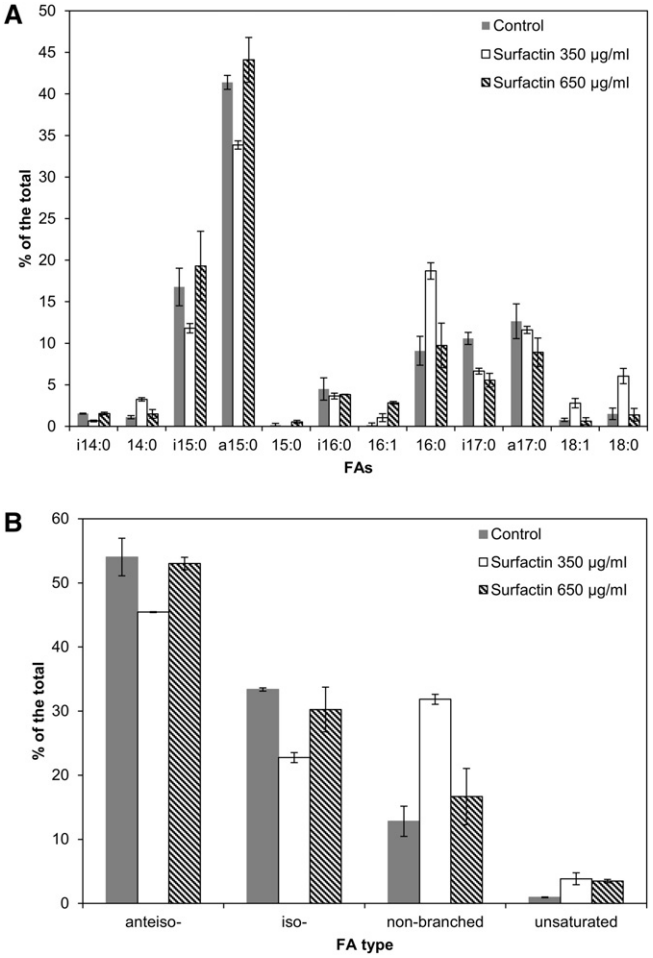

Fig. 4. Effect of surfactin on fatty acid composition of *B. subtilis* membrane. The proportions of the complete fatty acid profile are shown in (A) and the main structural types of fatty acids in (B). Values represent means ± standard errors of the means from three determinations. i- and a- stand for the respective branching pattern for iso- and anteiso-branched fatty acids, respectively.

3.4. Fluidity of membrane lipids after surfactin challenge

As the straight-chain FAs have higher melting temperatures (T_m) than the branched-chain ones, they increase the microviscosity of the membrane. Therefore, we aimed to determine how the shifts in lipid composition changed the respective fluidity of membrane lipids isolated from *B. subtilis* exposed to surfactin in the growth medium. We hypothesized that PL modifications can counteract the fluidizing effect of surfactin in the membrane. Therefore, we isolated membrane lipids from SF350, SF650 and control *B. subtilis* cells and measured their membrane fluidity using steady-state fluorescence anisotropy (r_{ss}) of the probe 1,6-diphenyl-1,3,5-hexatriene (DPH), which incorporates into the acyl chain region of the membrane, and the results are shown in Fig. 5.

Anisotropy measurements of the membrane samples at 30 °C, i.e. at a temperature equal to the cultivation temperature produced almost the same r_{ss} values for the control lipid membranes and the ones which were isolated from cells exposed to SF650. Even at lower and higher measurement temperatures, the qualitative differences were negligible between these two types of lipid membranes, which is

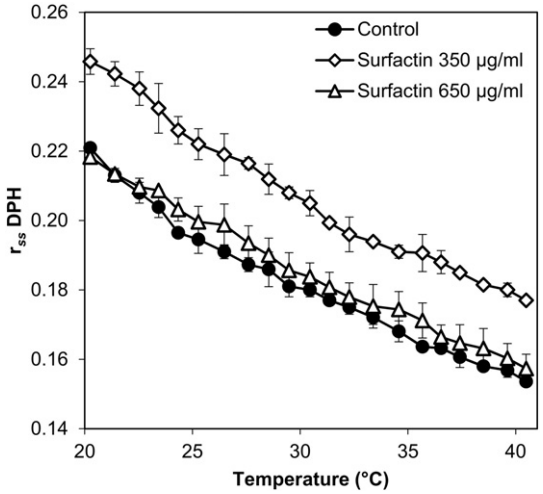

Fig. 5. Changes in DPH fluorescence anisotropy in membrane lipids. Membrane lipids were isolated from *B. subtilis* grown under control conditions or in the presence of 350 and 650 μg/ml of surfactin, respectively. Isolated lipids were used to form liposomes, labeled with DPH and the steady-state fluorescence anisotropy (r_{ss}) of DPH was measured along the temperature range indicated on the x axis. Error bars are shown when bigger than the symbols.

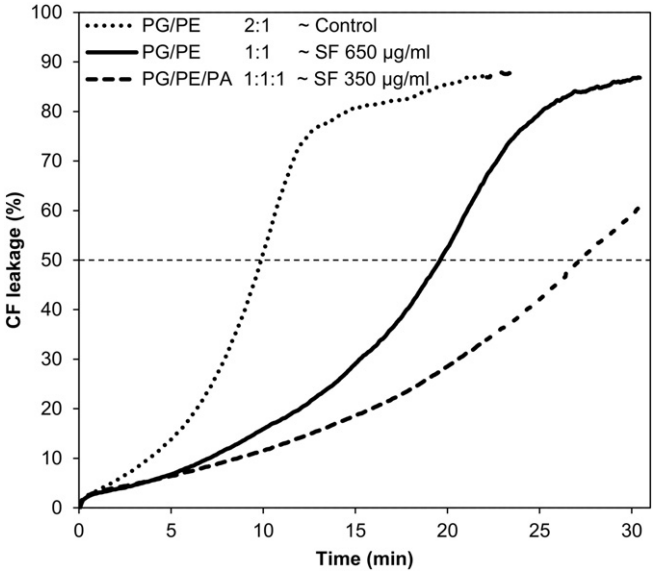

Fig. 6. Time course of surfactin-induced carboxyfluorescein release from liposomes. The lipid composition of the entire liposomes mimics the membrane phospholipid profile of control cells (PG/PE 2:1) and surfactin-adapted cells (PG/PE/PA 1:1:1 for SF350 and PG/PE 1:1 for SF650). Phospholipid concentration in the liposome suspension was 10 μM. Surfactin was added at the time point 0 s to a final concentration of 50 μM. Representative results from three independent liposome preparations are shown.

consistent with the absence of adaptive alterations in FA composition after SF650 challenge. In contrast, the r_{ss} DPH values observed for lipid membranes derived from cells treated with SF350 were substantially higher than those for control membranes throughout the whole measurement temperature range. The surfactin-adapted lipid membranes derived from SF350 cells reached the same r_{ss} value observed at 30°C for control membranes at 38°C, indicating a substantially decreased fluidity of the membrane interior.

3.5. Surfactin-induced permeabilization of vesicles resembling lipid composition of surfactin-adapted cells

Lipid analysis revealed that the polar head group composition of membrane phospholipids changed markedly in response to surfactin challenge. Importantly, under both of the tested surfactin concentrations, PG was not the predominant lipid membrane component as it was for the control cells, but the proportion of the two major membrane components PG and PE was almost equal. In addition, the level of PA increased substantially in the presence of SF350. Therefore, we next wanted to prove if these alterations in phospholipid composition can bring about an increased resistance of the bilayer towards surfactin-induced permeabilization. We prepared carboxyfluorescein (CF)-loaded liposomes composed of lipids resembling the membrane composition of *B. subtilis* control and surfactin-adapted cells (Fig. 3) and measured the release of CF from liposomes after the addition of surfactin. We used a lipid mixture with a 2:1 molar ratio of DOPG/DOPE to simulate the control cells and 1:1:1 DOPG/DOPE/DOPA and 1:1 DOPG/DOPE to simulate cells adapted to SF350 and SF650, respectively.

As documented in Fig. 6, decreasing the DOPG/DOPE ratio from the 2:1 observed in control cells to the 1:1 found in cells grown in the presence of SF650 prolonged the half-time of liposome lysis (i.e. the time needed to achieve a 50% increase in CF fluorescence intensity relatively to the maximum lysis induced by 0.02% Triton-X100) from 9.9 ± 0.6 min to 19.6 ± 0.2 min ($P < 0.001$). The inclusion of DOPA in the liposomes forming a lipid mixture of DOPG/DOPE/DOPA 1:1:1, representing the membrane of cells cultivated in the presence of SF350, extended the half-time of lysis to 27.2 ± 0.5 min ($P < 0.001$). These results indicate that the membranes consisting of equal proportions of PG/PE or PG/PE/PA resist surfactin-induced leakage better than those, where PG is the major lipid component.

4. Discussion

Target site modification is thought to be one of the feasible resistance mechanisms against membrane-penetrating antimicrobials. In this study we aimed to determine whether *B. subtilis* alters its membrane lipid composition in response to surfactin exposure. Surfactin exerts its antimicrobial effect by interacting with membrane lipids, leading to a loss of membrane barrier properties up to complete disintegration of the bilayer. Thus the target site modification realized by alterations in the proportion of membrane lipids might bring about hindered surfactin-membrane interaction, resulting in reduced leakage or possible death of the cell. Surfactin inherently acts highly cooperatively on the membrane; therefore also small changes in the concentration of surfactin in the membrane may affect its activity to a great extent. As *B. subtilis* 168 bears a point mutation in the gene essential to surfactin synthesis and thus does not produce surfactin, it provides a valuable model for studying surfactin-induced membrane adaptation when surfactin is added to the growth medium.

Surfactin-producing strains of *B. subtilis* are naturally exposed to surfactin in the stationary phase of growth, i.e. the growth phase when surfactin is synthesized. Nevertheless, we subjected exponentially growing *B. subtilis* to surfactin in order to work with a homogeneous and well defined culture of cells in good physiological condition and to yield a sufficient amount of cell biomass for membrane analysis. According to the in vitro data [19], the surfactin-to-lipid ratio in the membrane is the measure of the degree of membrane injury, so we first had to determine the optimal ratio of surfactin concentration interacting with a defined number of cells, i.e. we had to assess the number of surfactin molecules interacting with the number of phospholipid molecules in the cell membrane. On the basis of serial dilutions of surfactin against serial dilutions of *B. subtilis* cells, we selected two sublethal surfactin concentrations – 350 and 650 μg/ml, each concentration lies within a concentration range causing the stimulation (SF350) or inhibition (SF650) of *B. subtilis* biomass growth (Fig. 1). Under these conditions, *B. subtilis* physiology is substantially affected, as the culture halted its growth for a concentration-dependent time period (Fig. 2), indicating an urgent need to adapt and to possibly start to express a resistance mechanism. This mechanism must be quite effective if we consider that the minimum

bactericidal concentration (MBC) described for example for *Proteus vulgaris* is 20 μg/ml [20] or 125 μg/ml for *Listeria monocytogenes* is [21]. Under our experimental conditions the MBC for *B. subtilis* 168 was 1100 μg/ml (Fig. 1).

Both surfactin concentrations caused a growth delay. The SF650 concentration caused a cessation of growth for 3 hours and prolonged the doubling time of the renewed growth more than twice that of the control cells. Interestingly, with SF350, after the recovery from the growth arrest that lasted 40 min, the culture grew with a 10% higher growth rate than the control cells. The occurrence of a growth lag in the exponentially growing culture after exposure to surfactin signifies that the culture had to cope with the harmful effect of surfactin. With SF350 it adapted so well that the growth rate after the growth restoration was even higher than before. There could be various reasons for this slight but reproducible growth acceleration. Surfactin as a surface active compound has a strong ability to lower the surface tension of water [22] and thus can increase the solubility and availability of nutrients. Surfactin has also been described to be a signaling molecule which triggers extracellular matrix [23] and cannibalistic toxin [24] production in *B. subtilis*. Both these activities provide an advantage to the cells in the form of the protection or the release of nutrients from the killed siblings. We can hypothesize that a similar situation might also occur in our experiment. We observed a similar stimulatory phenomenon in a surfactin-producing culture of *B. subtilis* ATCC 21332 during surfactin production, when it grew faster and to higher cell biomass densities than the mutant strain which did not produce surfactin [12].

Under all conditions, cells need to maintain a native lipid membrane composition that ensures the essential low permeability to ions needed for the functional organization of the cell. As surfactin interacts with membrane phospholipids which can also modulate the degree of surfactin action on the membrane [11], we assumed that surfactin may induce changes in the proportion of membrane phospholipids. Such a target site modification involving mutations in the biosynthesis of phospholipids responsible for maintaining membrane fluidity, phospholipid content, and bilayer asymmetry was described for a daptomycin-resistant phenotype in *B. subtilis* [25] and *S. aureus* [26].

Two distinct features in the phospholipid composition were observed. The common characteristic of these changes was the drop in the PG/PE ratio in the membrane from PG/PE 1.8 to 0.9 and to 0.8 for SF350 and SF650, respectively. Apart from this, in the cells treated with SF350 the proportion of PA considerably rose to 23 %, which may signify a block in phospholipid biosynthesis as the precursor of PL synthesis accumulated and the proportions of no other membrane phospholipid increased. Even though PA is not an abundant lipid component of any organism, we propose that the accumulation of PA as well as decreasing the PG/PE ratio is intentional. PA and PE share a similar small head group size, cone shape structure and H-bonding capabilities and facilitate membrane association and the insertion of membrane proteins such as KcsA, hence increasing channel stability [27]. Both these PLs have higher melting temperatures than PG, thus decreasing the fluidity of the membrane, which may counteract the fluidizing effect induced by surfactin [28]. The cone shape of their molecules, introducing a negative curvature to the membrane, may also balance the surfactin-induced positive curvature stress [29], as was shown for PE stabilizing phosphatidylcholine liposomes against the action of surfactin [9]. Last but not least, the anionic character of PA molecule (-1.3 at pH 7) may cause the electrostatic repulsion of surfactin from the surface of the membrane and thus prevent the primary surfactin-membrane interaction. The electrostatic mechanism is also employed in the ineffectiveness of daptomycin-Ca^{2+} complex in Gram-negative pathogens, which contain low proportions of negatively charged phospholipids [30]. The accumulation of PA is also associated with vancomycin resistance in *E. coli* [31]. We consider the high content of PA, which is of central importance to bacterial physiology [32], to be the energetically cheapest way of repulsing surfactin from the membrane surface. PA is a precursor of lipid synthesis and thus is freely available in the growing cell with a rapid phospholipid turnover. A high PA content (35.6 %) was also observed in the membrane of *B. subtilis* ATCC 21332 during surfactin production. This content was slightly but significantly higher than in the surfactin non-producing mutant strain [12].

The stabilizing effect of the observed changes in the proportion of membrane phospholipids was confirmed by surfactin-induced CF leakage from liposomes resembling the lipid composition of the surfactin-adapted and control cells. Surfactin induced liposome lysis with two to three times longer half-times in bilayers resembling the composition of cells adapted to SF650 and SF350, respectively, in comparison to control membranes. This difference in susceptibility to surfactin action on the lipid bilayer may possibly explain the different growth rates observed for the two surfactin-treated cultures in the way that the cells adapted properly to the lower surfactin (SF350) concentration and thus grew faster.

The FA composition also changed greatly in response to surfactin exposure at a concentration of 350 μg/ml. The typical high content of branched-chain FAs decreased and the proportion of straight-chain FAs more than doubled. These FAs have higher melting points and thus decrease the fluidity of the membrane core. Measurement of the steady-state fluorescence anisotropy of DPH confirmed that in the surfactin-adapted membrane the high-melting FAs hinder the free rotation of the DPH probe, indicating a lowered fluidity (expressed as higher r_{ss} DPH values) of the membrane of *B. subtilis* cells exposed to SF350. These adaptive changes might reflect and counteract the disorder and increased membrane fluidity, which might be regarded as the primary direct effect of surfactin on the cytoplasmic membrane [9,28]. In contrast, almost no changes in FA composition were found in the *B. subtilis* cells exposed to SF650. The typical high content of branched-chain FAs did not change, nor did the proportion of the iso- and anteiso- branching pattern. The absence of adaptive changes correlates with the unchanged values of r_{ss} DPH in isolated lipids over the whole range of measurement temperatures.

We suggest that the surfactin non-producing strain *B. subtilis* 168 in the exponential phase of growth and the wild-type surfactin producer *B. subtilis* ATCC 21332 in the stationary phase of growth (when surfactin is synthesized) employ different strategies to cope with the antimicrobial stress both at the level of polar heads and fatty acids of membrane phospholipids. However, these strategies have something in common. The surfactin producer *B. subtilis* ATCC 21332 accumulates cardiolipin in the presence of surfactin [12]. This anionic phospholipid might confer a reduced fluidity and might shield the membrane against surfactin's action. Similarly, in *B. subtilis* 168 treated with surfactin at a concentration of 350 μg/ml, the content of PA increased substantially. This negatively charged PL may also serve to lower the fluidity of the membrane and cause a repulsive effect between the membrane surface and the negatively charged surfactin, making the membrane less prone to surfactin-induced lysis, which we confirmed with the liposome leakage assay. At the level of membrane FAs, both SF650 cells and the surfactin producer *B. subtilis* ATCC 21332 during surfactin production did not change their FA composition in response to the presence of surfactin.

In conclusion, the analysis of membrane lipids showed that *B. subtilis* 168 employs two different strategies to cope with this antimicrobial stress. These strategies differ, SF650 inducing a weaker adaptive response than SF350 at the level of membrane lipid composition. SF350 induces a response both at the level of the polar heads and the fatty acids of membrane phospholipids. The PG/PE ratio decreases and the level of PA rises in the membrane, which can be understood as a cheap but effective tool which costs no energy because merely the intermediate of PL synthesis is accumulated. However, PA might increase the overall net negative surface charge of the membrane and, together with PE decreases the fluidity of the membrane, both of which can counteract the harmful effect of surfactin on the membrane by electrostatic repulsion and combatting the fluidizing effect of surfactin, respectively. Their cone shape could compensate for the positive curvature stress induced by the already inserted surfactin

as well. Also, the FAs of membrane phospholipids participate in the lower membrane fluidity, as documented by the increase in non-branched FAs and confirmed by DPH fluorescence anisotropy measurements. In contrast, under the concentration of SF650, the only response observed at the level of lipid composition was the decrease in PG/PE ratio to almost the same value as with SF350. Nevertheless, CF leakage from liposomes resembling the assessed PL composition clearly shows that a decrease in PG/PE ratio is capable of reducing the propensity for surfactin-induced liposome leakage. The presence of PA stabilizes the membrane against surfactin action even further. In light of these observations, we suggest that target site modification at the level of membrane lipid composition might only be sufficient within a certain range of surfactin concentrations. Above this threshold, the physiological capacity of the cells might be exhausted or the cells might have to employ other tools to combat the antibiotic stress, qualitative changes in membrane proteins might be hypothesized.

Transparency document

The Transparency document associated with this article can be found, in online version.

Acknowledgements

This work was supported by grant 13-18051P from the Czech Science Foundation and by SVV project 15-01687S.

References

[1] D.A. Hopwood, How do antibiotic-producing bacteria ensure their self-resistance before antibiotic biosynthesis incapacitates them? Mol. Microbiol. 63 (2007) 937–940, http://dx.doi.org/10.1111/j.1365-2958.2006.05584.x.
[2] M.J. Rybak, The efficacy and safety of daptomycin: first in a new class of antibiotics for Gram-positive bacteria, Clin. Microbiol. Infect. 1 (2006) 24–32, http://dx.doi.org/10.1111/j.1469-0691.2006.01342.x.
[3] C.S. Lunde, S.R. Hartouni, J.W. Janc, M. Mammen, P.P. Humphrey, B.M. Benton, Telavancin disrupts the functional integrity of the bacterial membrane through targeted interaction with the cell wall precursor lipid II, Antimicrob. Agents Chemother. 53 (2009) 3375–3383, http://dx.doi.org/10.1128/AAC.01710-08.
[4] J.A. Karlowsky, K. Nichol, G.G. Zhanel, Telavancin: Mechanisms of action, in vitro activity, and mechanisms of resistance, Clin. Infect. Dis. 61 (2015) S58–S68, http://dx.doi.org/10.1093/cid/civ534.
[5] M.K. Hayden, K. Rezai, R.A. Hayes, K. Lolans, J.P. Quinn, R.A. Weinstein, Development of daptomycin resistance in vivo in methicillin-resistant *Staphylococcus aureus*, J. Clin. Microbiol. 43 (2005) 5285–5287, http://dx.doi.org/10.1128/jcm.43.10.5285-5287.2005.
[6] A.S. Bayer, T. Schneider, H.-G. Sahl, Mechanisms of daptomycin resistance in *Staphylococcus aureus*: role of the cell membrane and cell wall, Ann. N. Y. Acad. Sci. 1277 (2013) 139–158, http://dx.doi.org/10.1111/j.1749-6632.2012.06819.x.
[7] H. Heerklotz, J. Seelig, Leakage and lysis of lipid membranes induced by the lipopeptide surfactin, Eur. Biophys. J. 36 (2007) 305–314, http://dx.doi.org/10.1007/s00249-006-0091-5.
[8] J.D. Sheppard, C. Jumarie, D.G. Cooper, R. Laprade, Ionic channels induced by surfactin in planar lipid bilayer membranes, Biochim. Biophys. Acta 1064 (1991) 13–23, http://dx.doi.org/10.1016/0005-2736(91)90406-X.
[9] C. Carrillo, J.A. Teruel, F.J. Aranda, A. Ortiz, Molecular mechanism of membrane permeabilization by the peptide antibiotic surfactin, Biochim. Biophys. Acta 1611 (2003) 91–97, http://dx.doi.org/10.1016/S0005-2736(03)00029-4.
[10] S. Buchoux, J. Lai-Kee-Him, M. Garnier, P. Tsan, F. Besson, A. Brisson, E.J. Dufourc, Surfactin-triggered small vesicle formation of negatively charged membranes: A novel membrane-lysis mechanism, Biophys. J. 95 (2008) 3840–3849, http://dx.doi.org/10.1529/biophysj.107.128322.
[11] O. Bouffioux, A. Berquand, M. Eeman, M. Paquot, Y.F. Dufrene, R. Brasseur, M. Deleu, Molecular organization of surfactin-phospholipid monolayers: effect of phospholipid chain length and polar head, Biochim. Biophys. Acta 1768 (2007) 1758–1768.
[12] G. Seydlova, R. Fiser, R. Cabala, P. Kozlik, J. Svobodova, M. Patek, Surfactin production enhances the level of cardiolipin in the cytoplasmic membrane of *Bacillus subtilis*, Biochim. Biophys. Acta Biomembr. 1828 (2013) 2370–2378, http://dx.doi.org/10.1016/j.bbamem.2013.06.032.
[13] M.M. Nakano, N. Corbell, J. Besson, P. Zuber, Isolation and characterization of sfp: a gene that functions in the production of the lipopeptide biosurfactant, surfactin, in *Bacillus subtilis*, Mol. Gen. Genet. 232 (1992) 313–321, http://dx.doi.org/10.1007/BF00280011.
[14] K. Tsuge, Y. Ohata, M. Shoda, Gene yerP, involved in surfactin self-resistance in *Bacillus subtilis*, Antimicrob. Agents Chemother. 45 (2001) 3566–3573, http://dx.doi.org/10.1128/aac.45.12.3566-3573.2001.
[15] D.G. Cooper, C.R. Macdonald, S.J.B. Duff, N. Kosaric, Enhanced production of surfactin from *Bacillus subtilis* by continuous product removal and metal cation addition, Appl. Environ. Microbiol. 42 (1981) 408–412.
[16] G. Rouser, S. Fleische, A. Yamamoto, Two dimensional thin layer chromatographic separation of polar lipids and determination of phospholipids by phosphorus analysis of spots, Lipids 5 (1970) 494–496, http://dx.doi.org/10.1007/BF02531316.
[17] R.L. Glass, Alcoholysis, saponification and preparation of fatty acid methyl esters, Lipids 6 (1971) 919–925, http://dx.doi.org/10.1007/BF02531175.
[18] J.R. Lakowicz, Principles of fluorescence spectroscopy, 3rd ed. Springer Science + Business Media, LLC, New York, 2006.
[19] H. Heerklotz, J. Seelig, Detergent-like action of the antibiotic peptide surfactin on lipid membranes, Biophys. J. 81 (2001) 1547–1554, http://dx.doi.org/10.1016/S0006-3495(01)75808-0.
[20] P. Das, S. Mukherjee, R. Sen, Antimicrobial potential of a lipopeptide biosurfactant derived from a marine *Bacillus circulans*, J. Appl. Microbiol. 104 (2008) 1675–1684, http://dx.doi.org/10.1111/j.1365-2672.2007.03701.x.
[21] D.C. Sabaté, M.C. Audisio, Inhibitory activity of surfactin, produced by different *Bacillus subtilis* subsp. subtilis strains, against *Listeria monocytogenes* sensitive and bacteriocin-resistant strains, Microbiol. Res. 168 (2013) 125–129, http://dx.doi.org/10.1016/j.micres.2012.11.004.
[22] H. Razafindralambo, P. Thonart, M. Paquox, Dynamic and equilibrium surface tensions of surfactin aqueous solutions, J. Surfactant Deterg. 7 (2004) 41–46, http://dx.doi.org/10.1007/s11743-004-0286-x.
[23] D. Lopez, H. Vlamakis, R. Losick, R. Kolter, Paracrine signaling in a bacterium, Genes Dev. 23 (2009) 1631–1638, http://dx.doi.org/10.1101/gad.1813709.
[24] D. Lopez, H. Vlamakis, R. Losick, R. Kolter, Cannibalism enhances biofilm development in *Bacillus subtilis*, Mol. Microbiol. 74 (2009) 609–618, http://dx.doi.org/10.1111/j.1365-2958.2009.06882.x.
[25] A.B. Hachmann, E. Sevim, A. Gaballa, D.L. Popham, H. Antelmann, J.D. Helmann, Reduction in membrane phosphatidylglycerol content leads to daptomycin resistance in *Bacillus subtilis*, Antimicrob. Agents Chemother. 55 (2011) 4326–4337, http://dx.doi.org/10.1128/aac.01819-10.
[26] A.Y. Peleg, S. Miyakis, D.V. Ward, A.M. Earl, A. Rubio, D.R. Cameron, S. Pillai, R.C. Moellering Jr., G.M. Eliopoulos, Whole genome characterization of the mechanisms of daptomycin resistance in clinical and laboratory derived isolates of *Staphylococcus aureus*, PLoS ONE 7 (2012), e28316, http://dx.doi.org/10.1371/journal.pone.0028316.
[27] M. Raja, Do small headgroups of phosphatidylethanolamine and phosphatidic acid lead to a similar folding pattern of the K^+ channel? J. Membr. Biol. 242 (2011) 137–143, http://dx.doi.org/10.1007/s00232-011-9384-4.
[28] M. Deleu, J. Lorent, L. Lins, R. Brasseur, N. Braun, K. El Kirat, T. Nylander, Y.F. Dufrêne, M.-P. Mingeot-Leclercq, Effects of surfactin on membrane models displaying lipid phase separation, Biochim. Biophys. Acta Biomembr. 1828 (2013) 801–815, http://dx.doi.org/10.1016/j.bbamem.2012.11.007.
[29] M. Nazari, M. Kurdi, H. Heerklotz, Classifying surfactants with respect to their effect on lipid membrane order, Biophys. J. 102 (2012) 498–506, http://dx.doi.org/10.1016/j.bpj.2011.12.029.
[30] C.P. Randall, K.R. Mariner, I. Chopra, A.J. O'Neill, The target of daptomycin is absent from *Escherichia coli* and other Gram-negative pathogens, Antimicrob. Agents Chemother. 57 (2013) 637–639, http://dx.doi.org/10.1128/aac.02005-12.
[31] H.A. Sutterlin, S. Zhang, T.J. Silhavy, Accumulation of phosphatidic acid increases vancomycin resistance in *Escherichia coli*, J. Bacteriol. 196 (2014) 3214–3220, http://dx.doi.org/10.1128/jb.01876-14.
[32] J. Yao, C.O. Rock, Phosphatidic acid synthesis in bacteria, Biochim. Biophys. Acta Mol. Cell Biol. Lipids 1831 (2013) 495–502, http://dx.doi.org/10.1016/j.bbalip.2012.08.018.

scientific reports

Check for updates

OPEN

Outer membrane and phospholipid composition of the target membrane affect the antimicrobial potential of first- and second-generation lipophosphonoxins

Klára Látrová[1], Noemi Havlová[1], Renata Večeřová[2], Dominik Pinkas[1], Kateřina Bogdanová[2], Milan Kolář[2], Radovan Fišer[1], Ivo Konopásek[1], Duy Dinh Do Pham[3], Dominik Rejman[3]✉ & Gabriela Mikušová[1]✉

Lipophosphonoxins (LPPOs) are small modular synthetic antibacterial compounds that target the cytoplasmic membrane. First-generation LPPOs (LPPO I) exhibit an antimicrobial activity against Gram-positive bacteria; however they do not exhibit any activity against Gram-negatives. Second-generation LPPOs (LPPO II) also exhibit broadened activity against Gram-negatives. We investigated the reasons behind this different susceptibility of bacteria to the two generations of LPPOs using model membranes and the living model bacteria *Bacillus subtilis* and *Escherichia coli*. We show that both generations of LPPOs form oligomeric conductive pores and permeabilize the bacterial membrane of sensitive cells. LPPO activity is not affected by the value of the target membrane potential, and thus they are also active against persister cells. The insensitivity of Gram-negative bacteria to LPPO I is probably caused by the barrier function of the outer membrane with LPS. LPPO I is almost incapable of overcoming the outer membrane in living cells, and the presence of LPS in liposomes substantially reduces their activity. Further, the antimicrobial activity of LPPO is also influenced by the phospholipid composition of the target membrane. A higher proportion of phospholipids with neutral charge such as phosphatidylethanolamine or phosphatidylcholine reduces the LPPO permeabilizing potential.

The accelerating occurrence of bacterial resistance to current antibiotics poses a constant threat, because it is widely associated with the failure of antibiotic treatment. It was reported that in the USA alone, over 2 million illnesses per year are caused by multi-drug-resistant bacteria and associated annual costs for treating such infections range from $20–$35 billion[1]. This situation has prompted the search for new antimicrobial agents. In this respect, an enormous amount of effort has been focused on antimicrobial peptides (AMPs) and lipopeptides. On the one hand, AMPs offer a number of advantages such as broad-spectrum antimicrobial activities and diverse modes of action such as rapid disruption of microbial cell membranes and thus a lower risk of the development of resistance. On the other hand, the usage of AMPs is often limited to topical applications because of systemic toxicities, low solubility, low in vivo stability, limited tissue biodistribution, and high cost for large-scale manufacturing. Out of more than 3000 AMPs that have been discovered, there are several AMPs with antibacterial activity (e.g. Gramicidin, daptomycin, colistin, vancomycin, oritavancin, dalvabacin, telavancin, bacitracin, polymyxin B, teicoplanin, streptogramin, and tyrothricin) that have been approved by the US Food and Drug Administration[2,3].

[1]Department of Genetics and Microbiology, Faculty of Science, Charles University, Viničná 5, 128 00 Prague 2, Czech Republic. [2]Department of Microbiology, Faculty of Medicine and Dentistry, Palacký University Olomouc, Hněvotínská 3, 775 15 Olomouc, Czech Republic. [3]Institute of Organic Chemistry and Biochemistry, Czech Academy of Sciences v.v.i., Flemingovo nám. 2, 166 10 Prague 6, Czech Republic. ✉email: rejman@uochb.cas.cz; seydlova@natur.cuni.cz

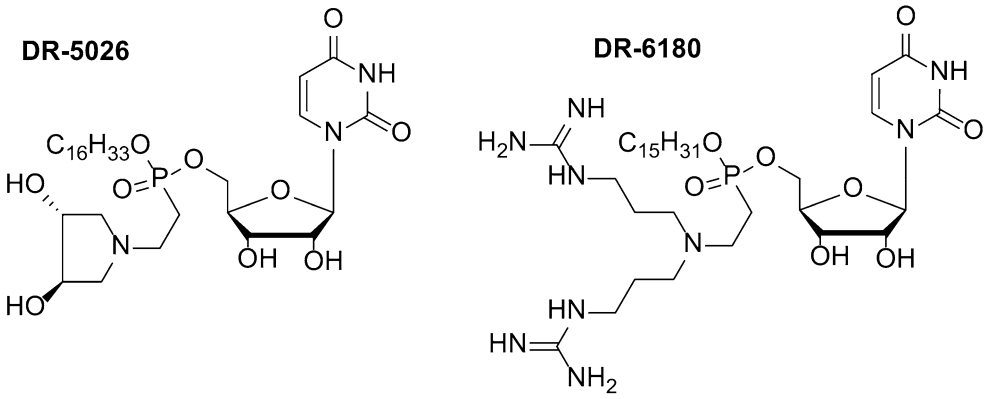

Figure 1. Selected examples of first- (DR-5026) and second-generation (DR-6180) LPPOs used in this study.

The discovery that the pharmacophore of AMPs is smaller than anticipated and knowledge of the structural features of active AMPs led to the development of small-molecular analogues of AMPs, synthetic antimicrobial peptidomimetics (SAPs), i.e. synthetic mimics of AMPs. AMPs typically adopt several structural features such as facially amphiphilic topology with hydrophilic and hydrophobic side chains segregating to opposing regions, which is essential for interaction, insertion into membrane and subsequent membrane disruption[4]. Another feature common to all AMPs is their positive charge that provides an electrostatic interaction with the negatively charged membrane surface[5]. It is generally believed that their physicochemical properties rather than primary amino acid sequence are responsible for the antimicrobial activity of AMPs.

SAPs seem to be promising because of their relative simplicity and thus easy and cost-effective production. Further, chemical synthesis also offers the use of nonproteinaceous building blocks and the possibility of obtaining SAPs in large amounts with improved properties with respect to their antimicrobial potency, selectivity, stability and biodistribution. However, the challenge of their design is to ensure selectivity while maintaining activity against bacterial pathogens. Whether the target site of an AMP (or SAP) is the cytoplasmic membrane or it has some other intracellular targets, AMP has to interact with the cell surface and reach or at least overcome the membrane. The amphipathic nature of AMPs ensures the primary interaction[6]. Positively charged hydrophilic moiety of an AMP is electrostatically attracted to the negatively charged bacterial surface components such as lipopolysaccharides (LPS), teichoic and teichouronic acids (in Gram-negative and Gram-positive bacteria, respectively) or negatively charged phospholipid headgroups. This interaction occurs less favorably in eukaryotic cells as they contain neutral lipids in the outer leaflet of their plasma membrane. The hydrophobic moiety of an AMP facilitates the interaction with the hydrophobic milieu of the membrane and inserts to it. On the other hand, increased hydrophobicity results in the loss of selectivity[7]. Thus, the general strategy is to properly balance the nature and number of appropriate cationic groups, charge distribution, hydrophobicity, and amphipathicity[8] as these characteristics determine activity in bacteria as well as selectivity[9]. The relative influence with which each of these parameters contribute to the potency and selectivity differs among different scaffolds.

The search for new antimicrobial compounds needs more studies of AMPs or SAPs which are active against Gram-negative pathogens (e.g. *Acinetobacter baumannii*, *Pseudomonas aeruginosa*, *Klebsiella pneumoniae*) that cause serious infections. Gram-negative bacteria are generally less susceptible towards antimicrobial agents because of their outer membrane, which itself acts as a permeability barrier. The presence of LPS represents a barrier to most hydrophobic as well as large hydrophilic molecules. LPS creates two potential barriers—the hydrophilic one provided by the densely packed oligosaccharide core[10], and the other hydrophobic one provided by the hydrocarbon chain region of the lipid A[11]. Thus, overcoming the LPS barrier is challenging. A considerable amount of research has been done on polymyxin B derivatives in order to overcome the limitations of its use and enhance efficacy. Some derivatives (such as polymyxin B nonapeptide) might also serve to facilitate passage of other agents across the outer membrane of Gram-negative bacteria[12,13]. Polymyxin structure (cyclic heptapeptide core linked to a linear tripeptide with an N-terminal fatty acyl moiety) and the knowledge that the lipid chain is responsible for its activity[14] has inspired research on N-lipidated peptide dimers, which are also effective antibacterial agents against Gram-negative pathogens[15], or lipidation of AMPs in general[16].

Recently, we reported[17–19] the synthesis of novel compounds termed lipophosphonoxins (LPPOs), a type of modular nonproteinaceous SAPs. LPPOs exhibit significant antibacterial activity against a wide range of bacteria, including multi-resistant strains while they do not exert any adverse effect on eukaryotic cells at bactericidal concentrations. Using living cells we have shown that LPPOs act through the permeabilization of the bacterial membrane, which finally leads in the loss of its barrier function and cell death. Using planar lipid membranes we directly proved LPPOs to be pore-forming agents. In the first generation of LPPOs (LPPO I)[17,19], the polar module is represented by a hydrophilic moiety with a small positive charge, the hydrophobic module is a linear alkyl chain (C14-16), and the auxiliary module is the nucleoside uridine (Fig. 1). LPPO I only possesses activity against Gram-positive bacteria such as methicillin-resistant *Staphylococcus aureus* or vancomycin-resistant *Enterococccus faecium*. In the LPPO II generation[18], we increased the positive charge of the polar module, while hydrophobic and auxiliary modules remained unchanged. This structural modification resulted in a broad-spectrum

LPPO	MIC (μg/ml)		HC_{50} (μg/ml)
	Bacillus subtilis	*Escherichia coli*	
I—DR-5026	3.125	> 200	25.0
II—DR-6180	0.390	0.780	20.0[a]

Table 1. Antimicrobial and hemolytic activity of selected first- and second-generation LPPOs. Antimicrobial and hemolytic activity are expressed as minimum inhibitory concentration (MIC) and the concentration causing lysis of 50% of red blood cells (HC_{50}), respectively. [a]Previously 16 μg/ml[18], volunteer blood donor changed.

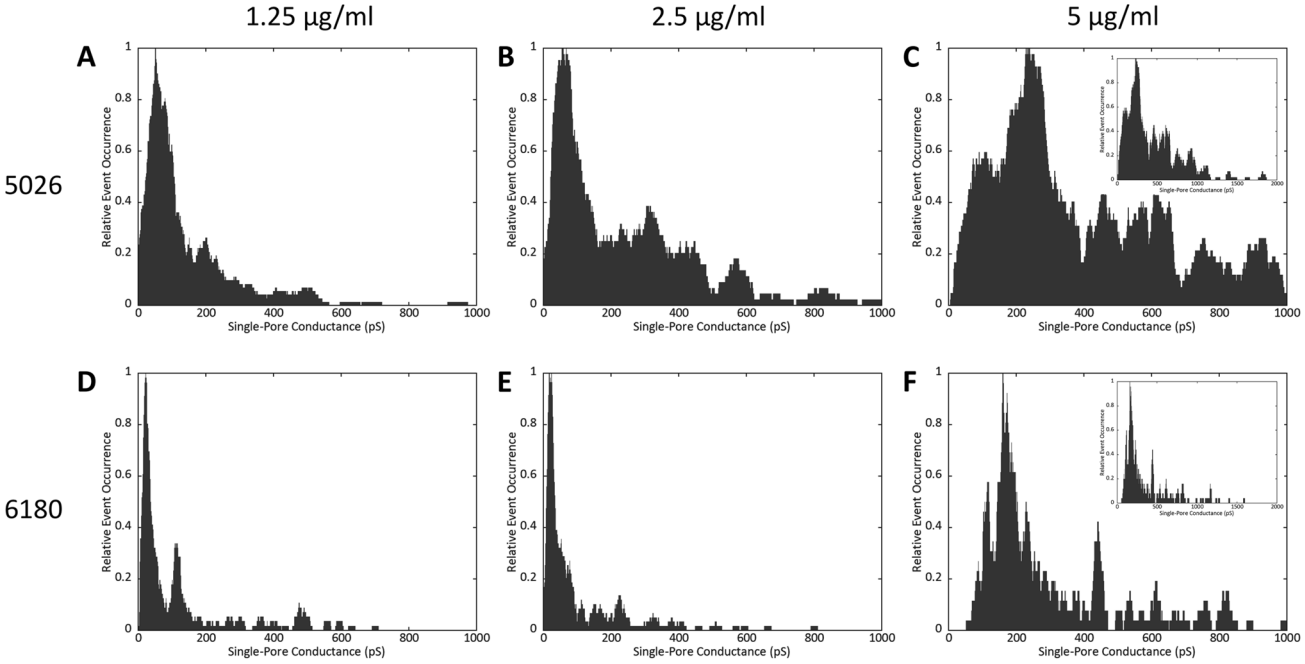

Figure 2. Concentration dependence of LPPO I and II pore formation. (**A**–**C**) LPPO I (DR-5026) single-pore openings, (**D**–**F**) LPPO II (DR-6180) single-pore openings in diphytanoylphosphatidylglycerol membranes, 1 M KCl, 10 mM Tris, pH 7.4, 50 mV. The histograms were created from pore openings using kernel density estimation (rectangular kernel with 30 pS width). The typical current recordings are shown in Supplementary Fig. S1.

antimicrobial activity against both Gram-positive and Gram-negative bacteria, including clinically significant pathogens such as *Escherichia coli*, *Pseudomonas aeruginosa* or *Salmonella enterica*.

In this work, we conducted a study in order to establish the reasons behind the different activity of LPPOs I and LPPOs II against Gram-positive and Gram-negative bacterial cells and to see why LPPOs II have higher activity against Gram-positive cells. We selected two candidate compounds from each LPPO generation and two model bacteria (Table 1)—the Gram-positive bacterium *Bacillus subtilis* and Gram-negative bacterium *Escherichia coli*. We compared LPPO I and II pore-forming activity on model membranes as well as in living cells, and we show here that both the phospholipid composition and presence of outer membrane affect LPPO antimicrobial activity.

Results

Pore formation by LPPO is concentration-dependent. Our previous studies on LPPO I and II showed that the mode of action of both LPPO generations is pore formation[17,18]. Currently, we wanted to compare the pore-forming activity of LPPO I (DR-5026) and II (DR-6180) with respect to their concentration dependence. Using conductance measurements on planar lipid membranes composed of diphytanoylphosphatidylglycerol we show (Fig. 2) that both LPPO I and II form a continuum of different pores—there appeared pores which were well resolved but there were also ones with high current noise and with fast dynamics (Supplementary Fig. S1, the raw recorded data are available online—for details see "Methods"). The distribution of LPPO I and II pore conductances was very broad and ranged from tens of pS up to nS in 1 M KCl. At 5 μg/ml (Fig. 2C,F) the most frequent pore conductance is ~ 240 and 160 pS for LPPO I and II, respectively; however, pores up to 2 nS were also seen. It is apparent that LPPO activity is substantially concentration-dependent—with DR-5026, lowering the concentration from 5 to 2.5 μg/ml (Fig. 2B,C) results in lowering the most frequent pore conductance four-fold to ~ 60 pS and the disappearance of pores larger than 1000 pS. Further lowering DR-5026 concentration to

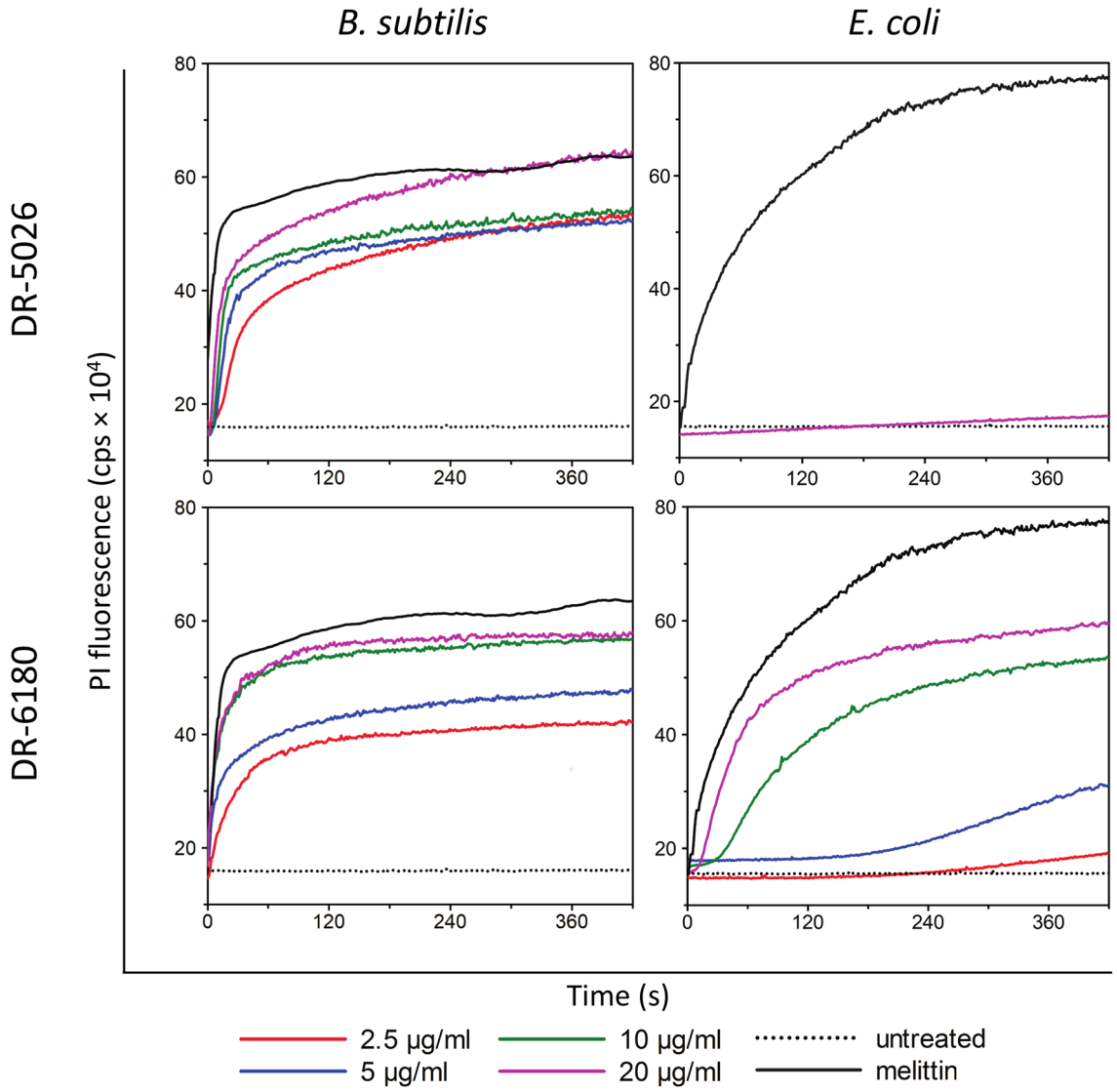

Figure 3. Permeabilization of *B. subtilis* and *E. coli* membrane induced by LPPO. Concentration dependence of LPPO I- (DR-5026) and LPPO II- (DR-6180) induced membrane permeabilization was measured as the increase in fluorescence intensity of the probe propidium iodide. The black dotted line ("untreated") shows the fluorescence of PI in the suspension of cells without LPPO addition. Melittin at a concentration of 10 µM served as a positive control. Representative kinetics from at least three independent experiments performed in duplicate are shown. With the exception of *B. subtilis* exposed to 2.5 µg/ml DR-5026 the kinetics of PI entry correlated with growth inhibition of the tested bacteria in the presence of LPPOs (Supplementary Fig. S2).

1.25 µg/ml did not change the value of the most frequent pore conductance, but led to a subsequent diminishing of pores larger than 600pS (Fig. 2A). For DR-6180, the tendencies are even more pronounced—lowering the concentration from 5 to 2.5 µg/ml resulted in lowering the most frequent conductance state eightfold to ~ 20 pS (Fig. 2E,F). Using DR-6180 at a concentration of 1.25 µg/ml (Fig. 2D) neither changed the most frequent conductance state nor the overall character of the histogram. The only exception was the appearance of a minor peak at ~ 115 pS, which is also visible at 5 µg/ml. The existence of several discrete conductance states in the histogram implies that LPPOs form oligomer channels with various stoichiometries. The constant pore conductance at lower LPPO concentrations suggests that there may be a smallest conductance state of a defined number of monomers.

LPPO I induces PI uptake in *B. subtilis* but not in *E. coli*. We measured the concentration dependence of LPPO permeabilizing activity in living *B. subtilis* and *E. coli* cells using the membrane-impermeable dye propidium iodide (PI). PI does neither penetrate the outer nor the inner membrane and only enters the cells after membrane damage. Upon entry PI binds to nucleic acids which increases its fluorescence. We tested the permeabilizing activity of the LPPOs in the concentration range of 2.5–20 µg/ml (Fig. 3). All of the LPPO concentrations used added to the *B. subtilis* suspension induced an immediate rise in PI fluorescence, suggesting that the dye entered the cells after their permeabilization. The observed effect of LPPO did not change much with respect to

the LPPO concentration used—lowering the concentration from 20 to 2.5 μg/ml only reduced the maximum PI fluorescence induced by LPPO by 30%. As expected, when using LPPO I against *E. coli*, we confirmed the data of the minimum inhibitory concentration, which exhibited inactivity against Gram-negative bacteria (Table 1). In the experiment with *E. coli*, we did not observe any rise in fluorescence intensity, even using the highest LPPO I concentration. At the same time, LPPO II permeabilized the *E. coli* inner membrane. In contrast to *B. subtilis*, the onset of the PI fluorescence intensity increase was delayed, and the overall kinetics were slower. Both of these effects were concentration-dependent—lowering the LPPO II concentration prolonged the initial delay and slowed the rise in PI fluorescence intensity. The maximum permeabilizing activity was also affected to a great extent by concentration. Concentrations of 20 and 10 μg/ml had roughly the same permeabilizing effect; however, 5 μg/ml resulted in a much more pronounced decrease in the effect.

LPPO I is capable of inducing partial dissipation of membrane potential of *E. coli*. The potency of LPPOs to permeabilize the cytoplasmic membrane apparently affects membrane potential. Thus, we further wanted to know how LPPO I and II differ in their effectivity to disrupt the membrane potential of living *B. subtilis* and *E. coli* cells. We also wanted to test whether LPPO I DR-5026, even though it is not lethal to the cells of the Gram-negative bacterium *E. coli* (according to MICs), is able to at least partially depolarize the membrane. We used membrane-bound fluorescence probe $DiSC_3(5)$, which has a high affinity for hyperpolarized membranes. After binding to the membrane, its fluorescence is quenched. The addition of a pore-forming substance leads to depolarization of the membrane, which releases the probe from the membrane and the intensity of fluorescence rises.

In line with the observed permeabilizing activity that was followed via PI, Fig. 4 shows that at any concentration used, both LPPOs are able to disrupt the membrane potential of *B. subtilis*. In this bacterium the depolarization monitored by $DiSC_3(5)$ fluorescence was, similarly to the kinetics of PI entry, again very rapid, as the maximum fluorescence was reached within 10–20 s. We did not observe any differences between the kinetics with LPPO I and II, and also almost no concentration dependency with regard to both the time-course and the maximum of fluorescence intensity. When using LPPO II against *E. coli*, we observed that the onset of the $DiSC_3(5)$ fluorescence increase appeared after a delay taking several seconds, and the overall rate of depolarization was much slower than that of *B. subtilis*. At odds with *B. subtilis*, where the time required to reach half of the fluorescence maximum was only on the order of seconds, in *E. coli* it was more than one minute when using 20 μg/ml LPPO I or LPPO II. LPPO II depolarized the *E. coli* cytoplasmic membrane in a concentration-dependent manner—increasing the LPPO II concentration from 2.5 up to 10 μg/ml led to a linear increase in the fluorescence intensity maxima. Note that there is no detectable artificial increase of intensity after mixing of LPPO and $DiSC_3(5)$ alone in the buffer (Supplementary Fig. S3). Enhancing the concentration to 20 μg/ml did not result in doubling the maximum of the 10 μg/ml concentration. Surprisingly, even when we added LPPO I to the *E. coli* suspension, we detected a slight increase in $DiSC_3(5)$ fluorescence which was concentration-dependent. Interestingly, when using the highest 20 μg/ml LPPO I concentration, the fluorescence maximum reached was comparable with 5 μg/ml of LPPO II. Thus LPPO I was able to partially disrupt the membrane potential of *E. coli*. This means that some LPPO I molecules inserted into the cytoplasmic membrane, where they formed small pores enabling the flux of ions. On the other hand, the concentration was not high enough to form bigger oligomers that allowed larger molecules such as PI to pass through (Fig. 3).

Membrane potential of the target cell does not affect the permeabilizing activity of LPPO I nor LPPO II. We next decided to test whether the permeabilizing activity of LPPO I and II is influenced by the value of membrane potential in living *B. subtilis* cells with adjusted membrane potential. We prepared three suspensions of *B. subtilis* cells in buffers differing in their KCl (K^+_{out}) concentration. We set the membrane potential using valinomycin (for details see "Materials and methods") to values of − 100, − 50 and 0 mV, and afterwards we added LPPO. We compared the kinetics of LPPO-induced PI entry into the cells treated with valinomycin with the intact (valinomycin-untreated) ones which had the physiological value of membrane potential. Figure 5A shows that the permeabilizing activity of LPPO I (DR-5026) was independent of the value of membrane potential. When using LPPO II (DR-6180, Fig. 5B) the kinetics of permeabilization of cells with adjusted membrane potential was clearly slower; however, the intensity reached the same maximum values as in the intact cells.

We further verified the finding that LPPO activity is not affected by the value of membrane potential by assessing the activity of LPPO II against a persister culture of *E. coli* (Fig. 5C). LPPO II at its MIC eradicated persisters of *E. coli* below the limit of detection (10^2 CFU/ml). At the same time, colistin reduced bacteria persister-enriched suspension below the detection limit at a concentration 5 × MIC.

LPPO I does not compromise the outer membrane of *E. coli*. We investigated the reasons why LPPO I are ineffective against Gram-negative cells of *E. coli*. We hypothesized that LPPO I are unable to disintegrate the outer membrane, which is the first hurdle that must be overcome to reach the target site—the cytoplasmic membrane. To follow the changes in the integrity of the outer membrane, we used the probe NPN, the fluorescence of which increases when the outer membrane is compromised. The data in Fig. 6 (and Supplementary Fig. S5) clearly show that LPPO II DR-6180 is capable of compromising the integrity of the outer membrane. The effect reaches its maximum at a concentration of 5 μg/ml. Using this DR-6180 concentration led to a level of disintegration of the outer membrane that was 26% of that induced by polymyxin B. Increasing the concentration up to 10 and 20 μg/ml did not enhance the efficiency of outer membrane permeabilization. In contrast, LPPO I DR-5026 was almost incapable of compromising the integrity of the outer membrane—irrespective of the concentration used, the efficiency of outer membrane permeabilization compared to that of polymyxin B was at most 4%.

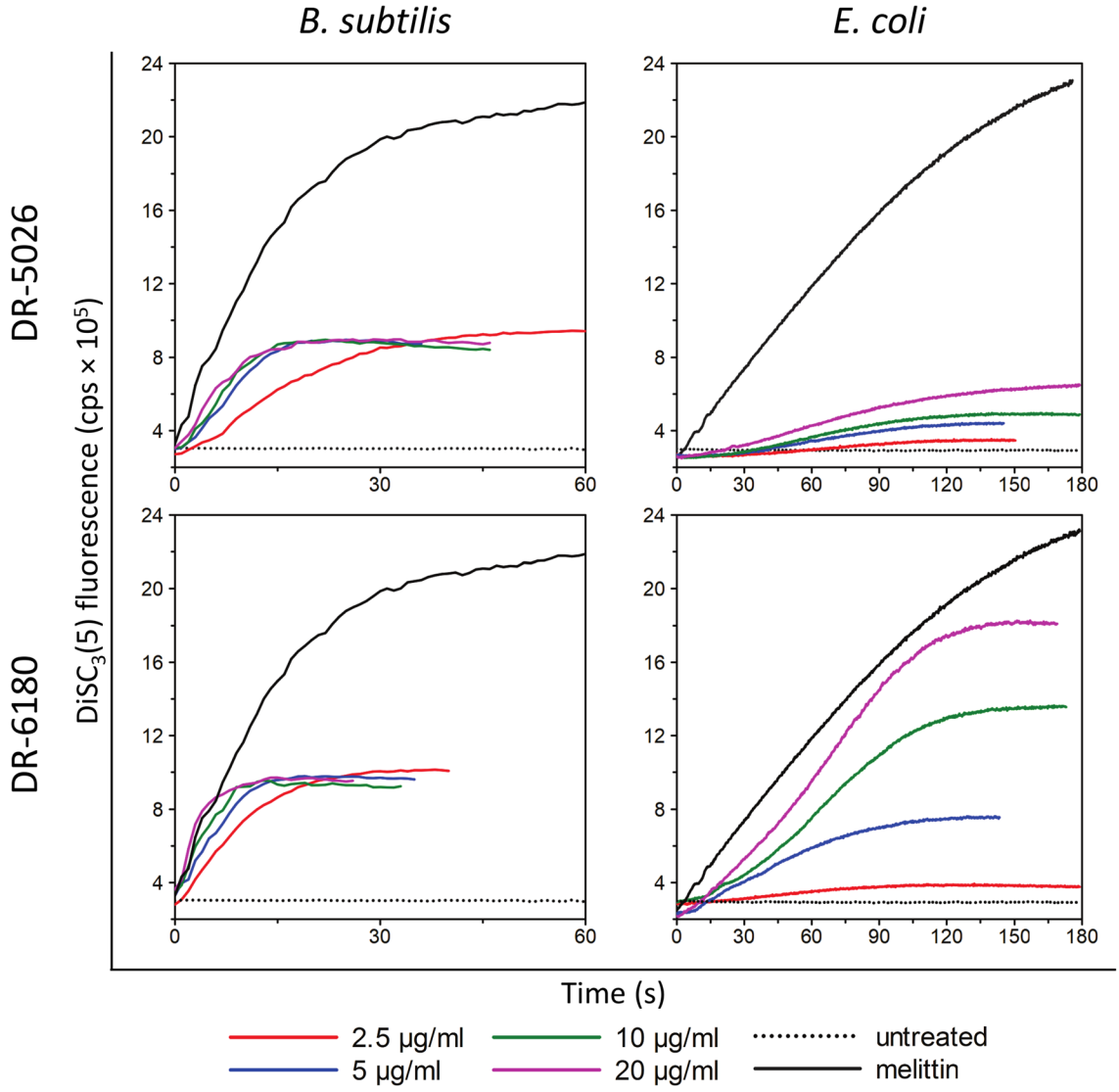

Figure 4. Dissipation of membrane potential of *B. subtilis* and *E. coli* induced by LPPO. Concentration dependence of LPPO I- (DR-5026) and LPPO II- (DR-6180) induced membrane permeabilization was measured as the increase in fluorescence intensity of the probe $DiSC_3(5)$, which corresponds to the disruption of physiological membrane potential. The black dotted line ("untreated") shows fluorescence of $DiSC_3(5)$ in the suspension of cells without LPPO addition. Melittin at a concentration of 10 µM served as a positive control. Representative kinetics from at least three independent experiments performed in duplicate are shown.

Phospholipid composition of the target membrane affects LPPO activity. We next tested another hypothesis, that besides the presence of the outer membrane, the phospholipid composition of the target inner membrane also affects LPPO activity. Whereas in *E. coli* phosphatidylethanolamine represents the major phospholipid of the inner membrane[20], in case of *B. subtilis* it is phosphatidylglycerol[21]. We prepared carboxyfluorescein-loaded liposomes composed of phospholipid mixtures in a 2:1 (w/w) ratio which resembled the proportion of the two major phospholipids in the *B. subtilis* and *E. coli* cytoplasmic membrane. The mixtures contained phosphatidylglycerol/phosphatidylethanolamine (PG/PE) or phosphatidylethanolamine/phosphatidylglycerol (PE/PG) in order to represent *B. subtilis* and *E. coli* phospholipid composition of the inner membrane, respectively. The third membrane system was composed of neutral phosphatidylcholine/phosphatidylethanolamine (PC/PE) and represented characteristic phospholipids from the outer leaflet of the eukaryotic plasma membrane.

The data in Fig. 7A–C show that LPPO I DR-5026 disrupted the PE/PG liposomes more slowly than the PG/PE ones. The leakage half-time (the time required after the addition of LPPO necessary to reach 50% of the maximum) was three times as long when using 20 µg/ml in PE/PG liposomes than in PG/PE ones. The DR-5026-induced lysis exhibited a dose-dependent behavior for all the phospholipid compositions tested. Of note, the kinetics up to 5 µg/ml were hyperbolic-like, and at a concentration of 10 and 20 µg/ml the curves exhibit a sigmoidal character. From Fig. 8A, which plots the concentration dependence of maximum LPPO-induced

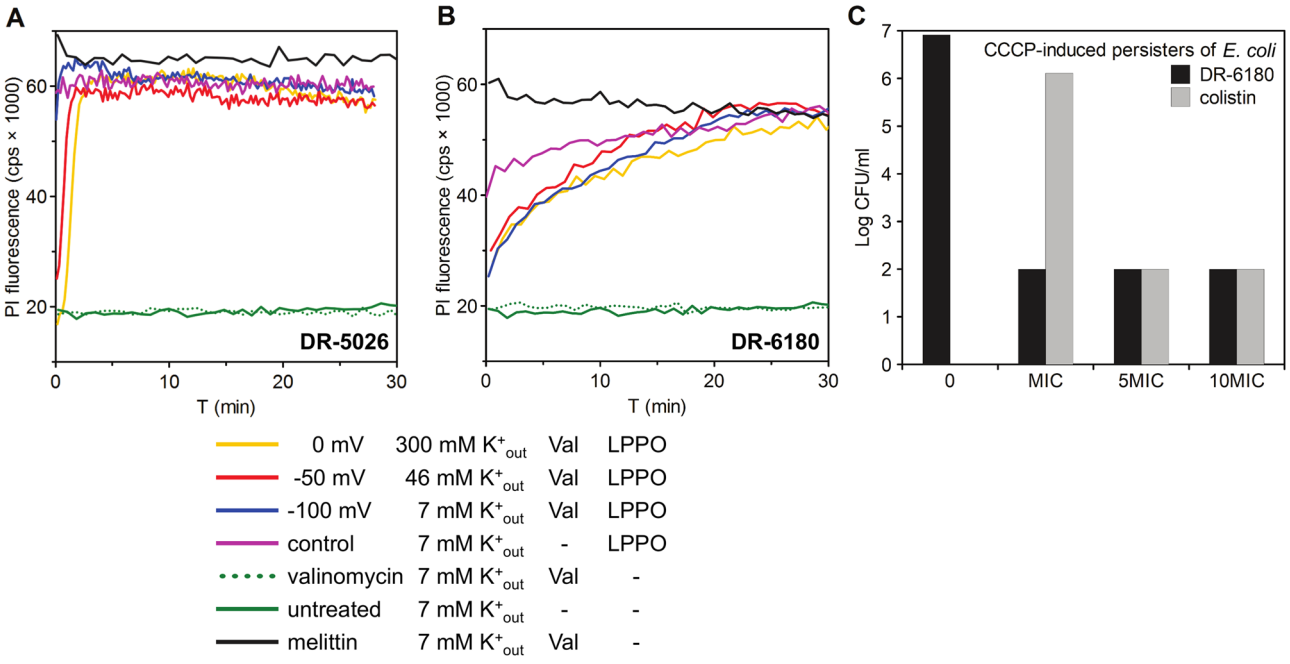

Figure 5. Effect of membrane potential of target cells on LPPO-induced permeabilization. (**A**,**B**) Membrane permeabilization induced by (**A**) LPPO I (DR-5026) and (**B**) LPPO II (DR-6180) at the concentration of 5 µg/ml was measured in *B. subtilis* via the entry of propidium iodide. The cells were resuspended in buffers with different K^+_{out} concentrations (indicated in the graph legend) and the membrane potential was adjusted to the desired value of ΔΨ (in millivolts) by the addition of 4 µM valinomycin (for details, see "Materials and methods"). Untreated and valinomycin (Val) control kinetics for a buffer with a 7 mM K^+_{out} concentration are shown. Representative results from three independent experiments performed in duplicate are shown. None of the values of adjusted membrane potential affected the activity of the positive control of melittin (10 µM). For clarity, only the kinetics for ΔΨ − 100 mV (7 mM K^+_{out} buffer with 4 µM valinomycin) are presented. (**C**) Activity of LPPO II DR-6180 and colistin against CCCP-induced persisters of *E. coli*. Antimicrobial activity was evaluated by CFU/ml counting after three hours of incubation of persisters with the tested compound at concentrations corresponding to MIC (minimal inhibitory concentration), 5 × MIC and 10 × MIC. The value of 10^2 CFU/ml was used as the detection limit.

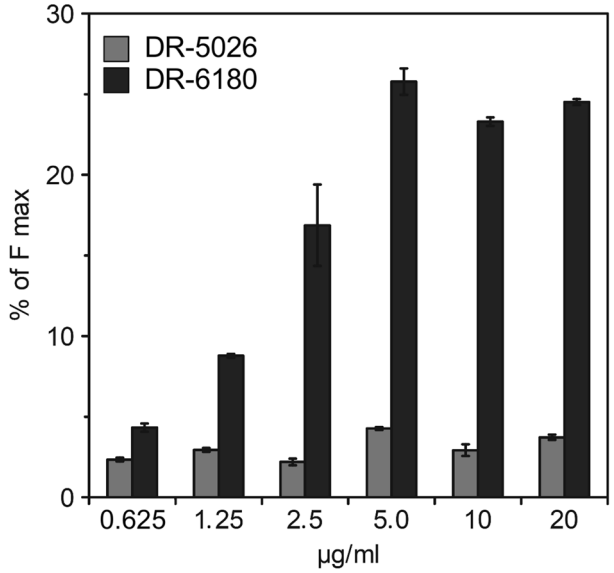

Figure 6. *Escherichia coli* outer membrane permeability induced by LPPO. The integrity of the outer membrane was assessed by measuring the increase in fluorescence intensity due to NPN uptake by cells with a compromised outer membrane induced by LPPO. The data represent the percentage of fluorescence intensity from the entire kinetics plot after reaching the plateau relative to the maximum induced by the addition of 100 µM polymyxin B.

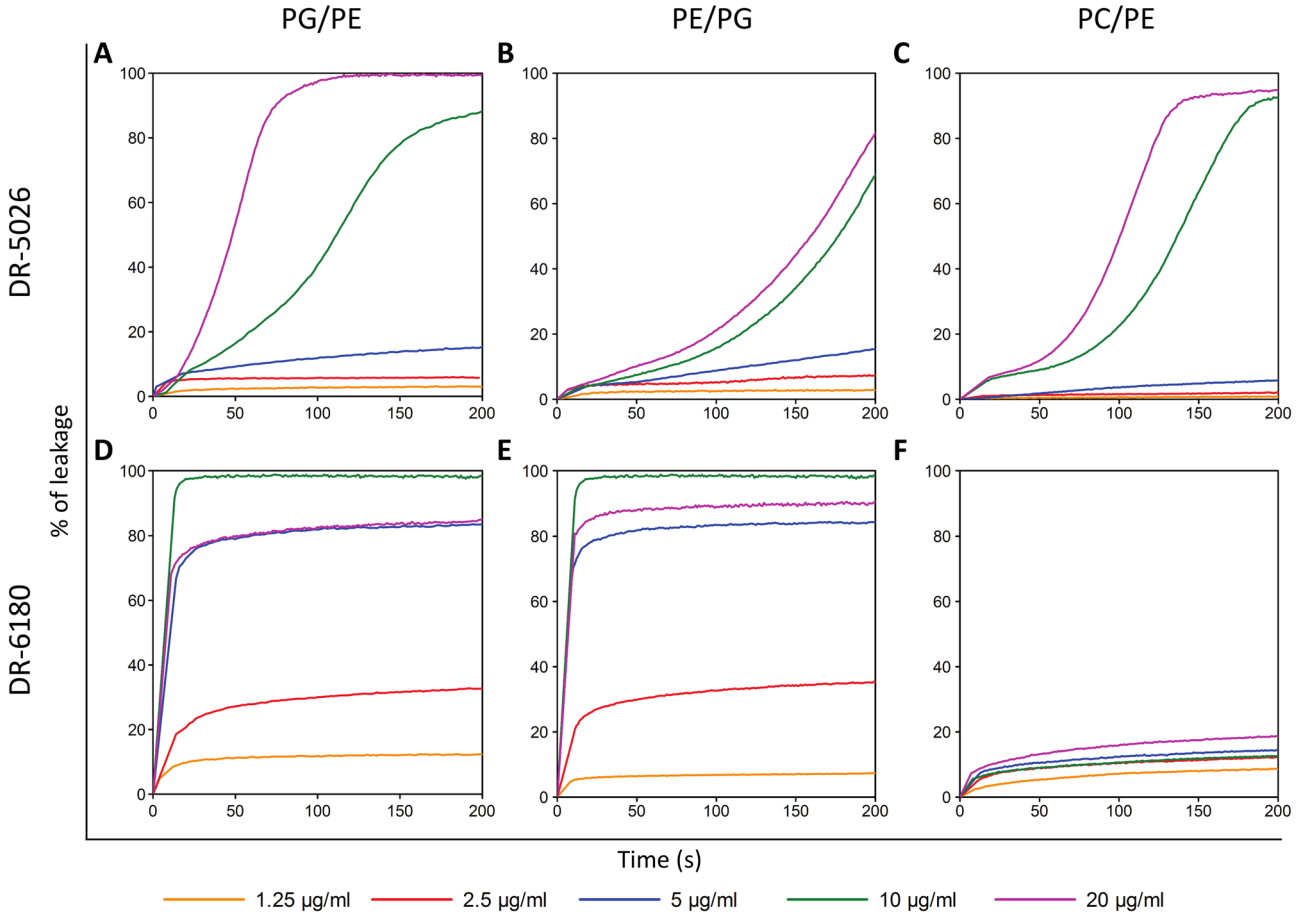

Figure 7. LPPO-induced leakage of carboxyfluorescein from liposomes. The curves show concentration dependence of LPPO I- (DR-5026, **A**–**C**) and LPPO II- (DR-6180, **D**–**F**) induced leakage from liposomes over time. The liposomes were composed of dioleyl-phospholipids in a 2:1 (w/w) ratio—PG/PE, PE/PG and PC/PE. The LPPO/phospholipid ratios were as follows: DR-5026—0.18/1, 0.36/1, 0.72/1, 1.43/1 and 2.86/1; DR-6180—0.14/1, 0.29/1, 0.58/1, 1.15/1 and 2.30/1. 100% leakage was achieved using 0.1% Triton X-100. Representative kinetics from at least three independent liposome preparations are shown.

lysis as a function of liposome composition shown in Fig. 7, it is apparent that the inflection point corresponds to an even lower concentration than 10 μg/ml. This indicates the presence of two different modes of membrane permeabilization at lower and higher LPPO I concentration ranges. The effectivity of membrane permeabilization expressed as the initial rate of lysis (% s^{-1}, Fig. 8C,D) and the maximum in the plateau is highest in PG/PE membranes. Leakage from the PE/PG and PC/PE liposomes was substantially slower and reached lower maximum values.

When using LPPO II DR-6180 (Fig. 7D–F), we observed higher permeabilizing activity in both PG/PE and PE/PG liposomes compared to DR-5026—the fluorescence intensity rose more steeply, and a concentration of just 10 μg/ml caused complete lysis. Surprisingly, the concentration of 20 μg/ml had a comparable effect to that of 5 μg/ml. In contrast to LPPO I DR-5026, the initial rates of lysis were much higher in both PG/PE and PE/PG liposomes (Fig. 8D) and the dose–response curves in Fig. 8B exhibited hyperbolic-like behavior. The overall extent of liposome lysis was the same for both bacteria-like liposomes; however, the DR-6180 activity changed substantially in the completely neutral membrane of PC/PE liposomes. Almost irrespective of the concentration used (Figs. 7F, 8B), the LPPO II-induced lysis was at most 20%.

The presence of lipopolysaccharide decreases the effectiveness of LPPO-induced permeabilization. Finally, we investigated whether the presence of lipopolysaccharide (LPS) could influence LPPO permeabilizing activity in the membrane. We used the same PG/PE and PE/PG liposomes as in the previous experiment (Fig. 7) and incubated those with LPS prior to LPPO addition. In Fig. 9 we can see that LPS apparently hinders LPPO action. With LPPO II (Fig. 9C,D) at a concentration of 5 μg/ml, the degree of liposome leakage was markedly reduced—the effect was even more pronounced in the PG/PE (Fig. 9C) membrane than in PE/PG one (Fig. 9D). The presence of LPS decreased the maximum degree of PG/PE liposome lysis 2.5-fold. This effect however disappeared when the LPPO II concentration was increased to 10 μg/ml. In contrast, with LPPO I (Fig. 9A,B), we observed a decreased permeabilization efficiency of liposome suspension containing LPS using both concentrations of LPPO. In PG/PE liposomes (Fig. 9A) this effect exhibited a greater concentration

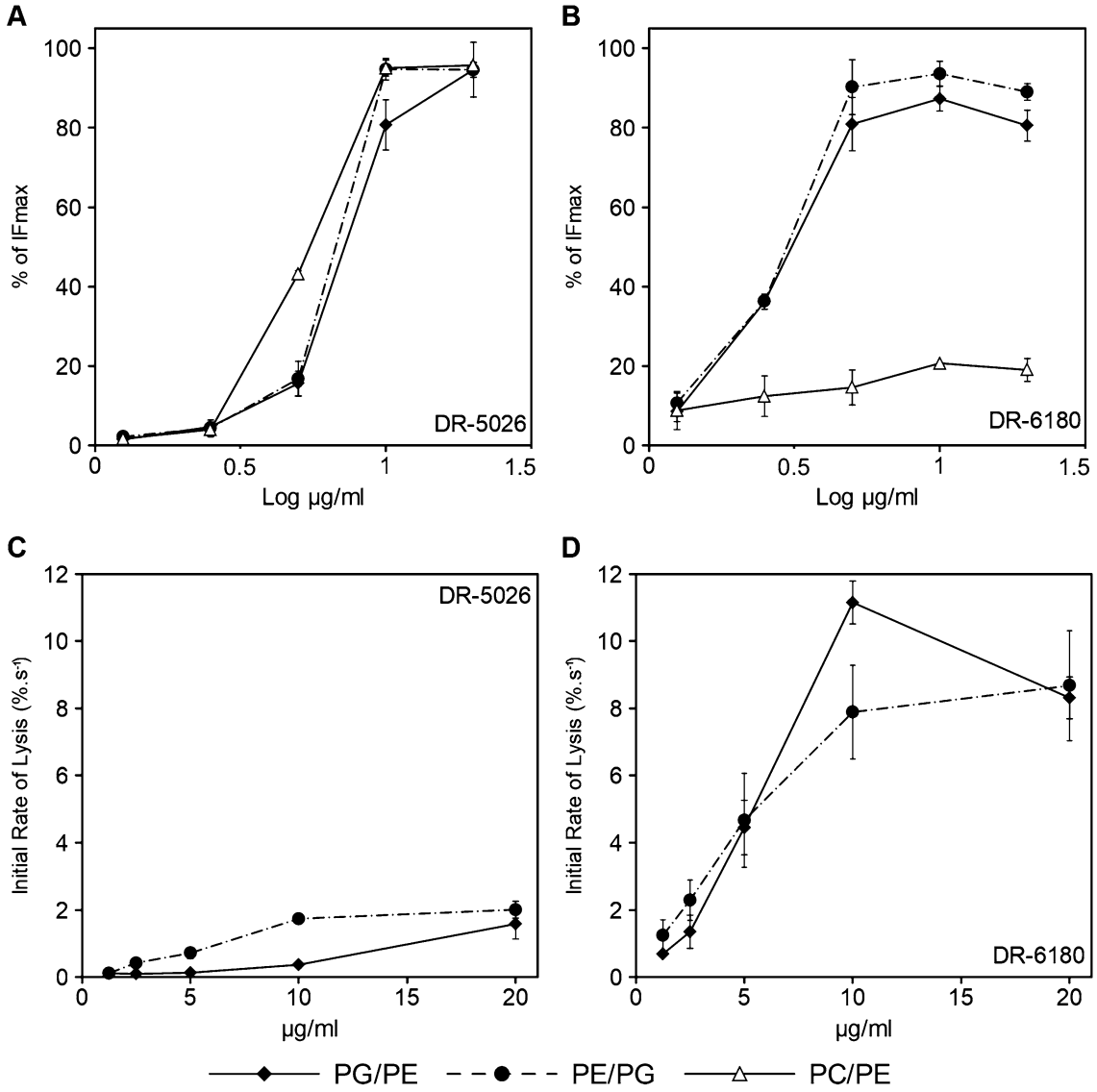

Figure 8. Concentration dependence of maximum LPPO-induced lysis and initial rate of lysis as a function of liposome membrane composition. (**A**,**B**) The data were taken from Fig. 7 and are plotted as the maximum reached in the plateau after exposure to a given LPPO concentration. (**C**,**D**) Dependence of the initial rate of lysis on LPPO concentration in liposomes differing in their lipid compositions. Average values from at least three liposome preparations and a standard deviation are shown.

dependency than in PE/PG ones (Fig. 9B). In PG/PE liposomes, the presence of LPS lowered the maximum degree of lysis (not shown) 12-fold and 2.5-fold when using 5 and 10 µg/ml of LPPO I, respectively. With PE/PG liposomes, the maximum degree of lysis dropped threefold and fivefold when using 5 and 10 µg/ml of LPPO I, respectively. The results of these experiments are thus in line with the data obtained using living cells.

***Escherichia coli* with compromised outer membrane is susceptible to LPPO I action.** All the above experiments showed that the membrane lipid composition, namely the presence of higher proportions of neutral lipids, and the presence of outer membrane are responsible for the ineffectiveness of LPPO I in *E. coli*. Thus we finally decided to employ *E. coli* imp4213 with a compromised outer membrane to assess its sensitivity to the action of LPPO. This strain bears an in-frame deletion of the imp gene encoding the essential outer membrane protein LptD, which is involved in LPS assembly[22,23]. This produces permeability defects of the outer membrane of the mutant *E. coli* strain. The values of the minimum inhibitory concentration clearly showed (Table 2) that in contrast to *E. coli* CCM 3954, which has an intact outer membrane, the strain imp4213 is highly sensitive to the action of LPPO I DR-5026, as its MIC dropped from > 256 to 8 µg/ml when compared with *E. coli* CCM 3954. With respect to LPPO I activity in the Gram-negative bacterium, this result confirmed the substantial role of the outer membrane as a physical barrier that complements the effect of LPS.

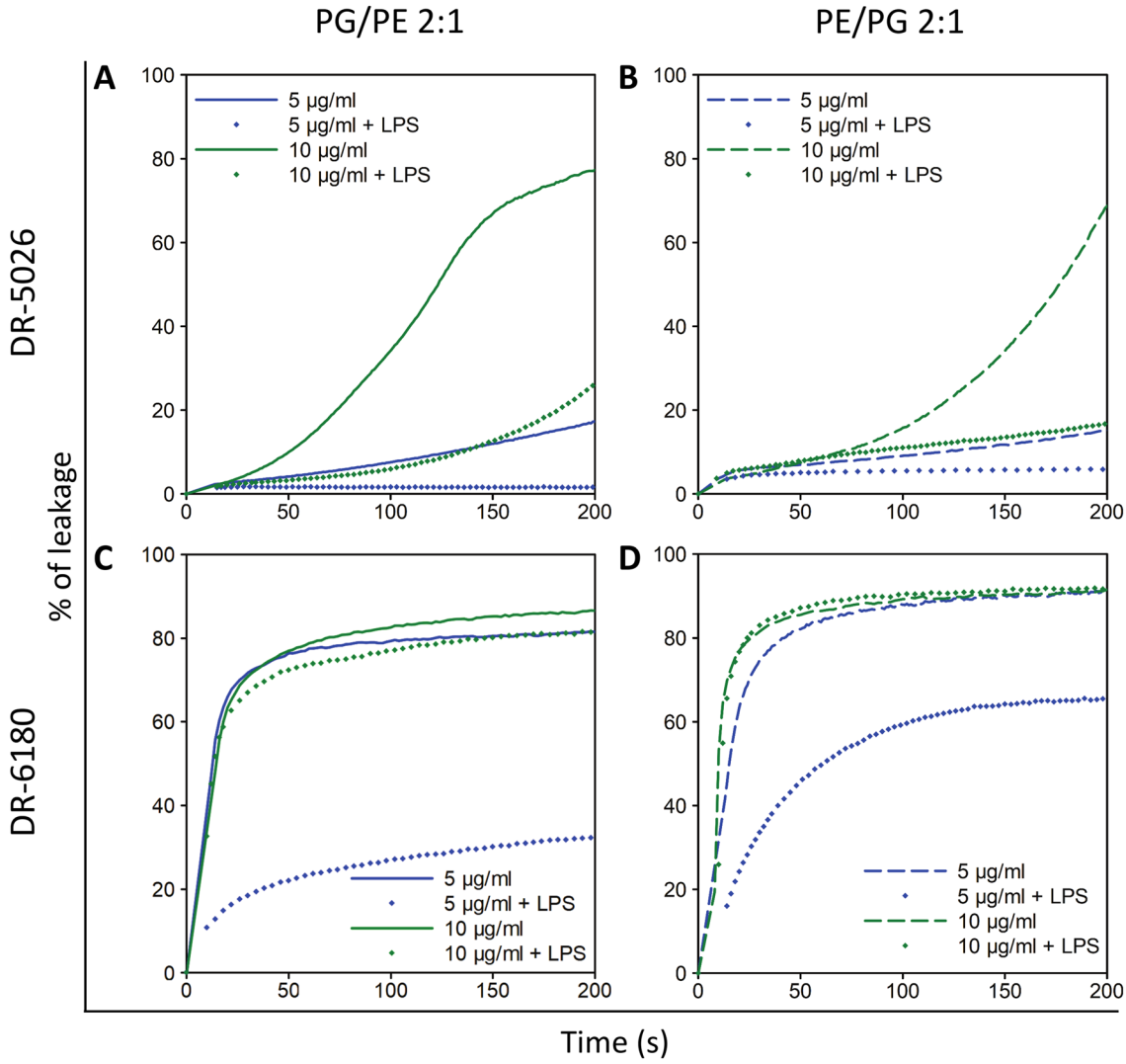

Figure 9. Effect of LPS on LPPO-induced leakage from liposomes. Carboxyfluorescein-loaded liposomes composed of dioleyl-phosphatidylglycerol (solid line) and diolelyl-phosphatidylethanolamine (dashed line) in ratios of 2:1 and 1:2 (w/w), respectively, which is the same as in Fig. 7A,B,D,E. Liposomes were preincubated with LPS (for details, see "Materials and methods") and then exposed to LPPO I DR-5026 (**A**,**B**) and LPPO II DR-6180 (**C**,**D**) at the indicated concentrations. The resulting leakage curves (diamonds) are compared with those using liposomes without LPS treatment. The phospholipid concentration in liposome suspension was 10 µM. Representative kinetics from three independent liposome preparations are shown.

	MIC µg/ml	
	DR-5026	DR-6180
E. coli CCM3954	> 256	2
E. coli imp4213	8	1

Table 2. Minimum inhibitory concentrations of LPPO I (DR-5026) and II (DR-6180).

Discussion

LPPOs are modular antimicrobials with promising potential for future use as alternatives to current antibiotics. They kill bacteria by disrupting their cytoplasmic membrane via pore formation[17,18]. First-generation LPPOs were found to be effective against Gram-positive bacteria. However, they do not exhibit any activity against Gram-negative bacteria. The modification of the imino-sugar module of the LPPO molecule and the increase in the number of positive charges gave rise to second-generation LPPOs which exhibit activity against both Gram-positive and Gram-negative bacteria. In this study, we aimed at elucidating the nature of the different effectiveness of LPPO I and LPPO II against Gram-positive and -negative bacteria. We studied the effect of LPPOs over a wide

concentration range, using both in vitro approaches and in vivo studies with model bacteria. We mostly had to use LPPO concentrations well above their MICs, because lower concentrations only resulted in a weak effect. The possible reason for this was that it was necessary to adjust the LPPO concentration to the higher number of cells in our assays (~ 10^7 cells/ml compared to MIC—~ 10^6 cells/ml), resulting in a larger membrane area.

Both generations of LPPOs share the same mode of action—pore formation. The distribution of pore conductances is very broad, ranging from a few pS up to nS in 1 M KCl. In this respect, the pore-forming activity is comparable to other small pore-forming antimicrobials such as daptomycin, which forms pores in model membranes (according to recent papers[24–26]), or surfactin[27]. In some pores the unpredictable dynamics may point to the fact that certain LPPO complexes do not adopt exact pore stoichiometry or it can change rapidly in time. Possibly membrane phospholipids take part in the pore formation. With our instrumentation we cannot be sure about the instant conductance of the events with the fast current fluctuations but the average conductance should be close to the correct value. However, for pores with very short opening dwell time the recorded conductance might be lower than the real one. Nevertheless, the most frequent pore conductances do not differ much between the two LPPOs tested. Also, the concentration dependency shows the same pattern for both LPPOs—a twofold decrease in LPPO concentration leads to a several-fold decrease in the most frequent conductance states and a disappearance of the large conductance states with a pore conductance of several hundred pS. When we further lowered the LPPO concentration, the most frequent pore conductance states did not change. This suggests that LPPO pores are probably oligomeric with a varying number of monomers depending on LPPO concentration, and that a minimal conductance unit exists which most likely has a conductance of 20 pS.

Based on the known MICs for the model Gram-positive bacterium *B. subtilis* and the Gram-negative bacterium *E. coli* (Table 1), we tested the permeabilizing activity in living cells using the dyes PI and $DiSC_3(5)$. While an increase in PI generally signifies inner membrane permeabilization, the rise in $DiSC_3(5)$ fluorescence indicates membrane depolarization, i.e. that the membrane is permeable for small ions such as H^+, K^+ or Na^+. The PI assay showed (Fig. 3) that the permeabilizing activity is concentration-dependent (although very weakly in *B. subtilis*). In line with very high MIC values for *E. coli*, this experiment proved that LPPO I DR-5026 is ineffective against *E. coli* cells. Of note, using LPPO II DR-6180, we observed different shapes of the kinetics traces for *B. subtilis* and *E. coli*. While the kinetics of PI entry into *B. subtilis* were steep and hyperbolic, kinetics with *E. coli* were slow and multiphasic, suggesting that several modes of membrane permeabilization occurred. We speculated that this might be caused by the different phospholipid composition of the cytoplasmic membrane (discussed further in the text) and different structure of the cell envelope. The presence of the outer membrane represents a barrier which the LPPO molecules must first overcome to reach their target and thus the permeabilizing process is delayed. In *E. coli* it took several minutes to reach the plateau, whereas in *B. subtilis* it was only several tens of seconds. We might speculate that at first LPPO II acts on *E. coli* at lower concentrations, forming smaller oligomers in the cytoplasmic membrane, and then when the molecules accumulate in the periplasmic space, the formation of the larger oligomers predominates and thus the rate of permeabilization increases.

The experiment with the probe $DiSC_3(5)$ confirmed that both LPPO I and II are capable of depolarizing the cytoplasmic membrane of the tested bacteria. With regard to LPPO type and model organism, the $DiSC_3(5)$ kinetics (Fig. 4) shared the same difference in their shape and time-course as the PI ones. Surprisingly, we also observed a slight depolarization of the cytoplasmic membrane of *E. coli* treated with LPPO I (DR-5026); however, the maximum effect induced by a concentration of 20 µg/ml was comparable to that of 5 µg/ml of LPPO II DR-6180. This means that, even in *E. coli*, some DR-5026 molecules must have entered the cytoplasmic membrane and formed small pores which allowed the passage of small ions. Nevertheless, these pores were not large enough to enable the passage of the probe PI, which has a molecular weight of 668 Da. However, such a small depolarization is not able to induce a sufficient effect on cellular metabolism to be observable as a decrease in MIC value.

Based on the results from PI and $DiSC_3(5)$ kinetics, we put forward several plausible reasons for the different susceptibility of *B. subtilis* and *E. coli* to LPPO I and II. We hypothesized that it may be caused by (i) the different structure of their cell envelopes, i.e. the presence of the outer membrane in *E. coli*, and/or by (ii) different lipid composition of the target cytoplasmic membrane. Generally, the activity of membrane-active antimicrobials depends on target membrane characteristics such as membrane lipid composition[20,28] and membrane potential[29,30]. The mode of action of some antimicrobial peptides includes targeting specific lipids[31] of the bacterial inner membrane. Therefore, modified lipid composition or decreased value of membrane potential may lead to a lowered antibiotic activity[24] or even to antimicrobial resistance[32]. As for the membrane potential, in our experiments we did not observe any marked impact of the value of the target membrane potential on the activity of LPPO I or LPPO II (Fig. 5A,B). This is a highly desirable feature of an antimicrobial compound, as it means that persistent cells, which have a lower membrane potential[30], are also susceptible to their antimicrobial effect, which we confirmed in the experiment shown in Fig. 5C.

To test the hypothesis that LPPO I molecules cannot traverse through the outer membrane, we performed an NPN assay (Fig. 6), which showed that LPPO I (DR-5026) only negligibly compromises the integrity of the outer membrane of living *E. coli* cells across the whole concentration range of 0.625–20 µg/ml. On top of that, leakage from liposomes with a composition that mimics the inner membrane phospholipid composition of Gram-positive, Gram-negative bacteria and the plasma membrane of eukaryotic cells showed that a different phospholipid composition substantially influences the permeabilizing potential of the tested LPPOs (Figs. 7, 8). The permeabilizing activity of LPPO II (DR-6180) was the same in liposomes with a different PG and PE ratio; however, it was substantially reduced in "eukaryotic" PC/PE liposomes (Fig. 8B) which is in line with the almost same MIC for *B. subtilis* and *E. coli* and LPPO II's low hemolytic activity[18]. When using LPPO I DR-5026, we observed that the rate of leakage was generally lower than for DR-6180, with the exception of PC/PE liposomes, where higher DR-5026 concentrations also resulted in a massive leakage. This observation is at odds with the fact that DR-5026 had no detectable activity on normal primary cell viability and toxicity at the MIC concentrations[19].

We suggest that in living cells other lipids, sterols or non-lipid compounds of membrane may also affect LPPO activity. We also need to take into account the different LPPO/lipid ratio in cells and liposomes.

Importantly, the overall activity of DR-5026 decreased in liposomes mimicking the Gram-negative bacterial inner membrane. This suggests that the higher proportion of negatively charged PG in the Gram-positive-like membrane plays a key role in the interaction and/or pore formation by LPPO. Our results indicate that the affinity of LPPO II DR-6180 for PG is higher compared to LPPO I DR-5026. This might be due to the coulombic effect between the positive charges of LPPO and the negative charge of PG. Both DR-5026 and DR-6180 bear a positive charge (born by the tertiary amine and the nucleobase) which is attracted to the negative charge of PG. In addition, DR-6180 has two highly positive guanidinium groups which may result in higher electrostatic interaction between DR-6180 and PG compared to DR-5026. Thus the absence of PG in PC/PE liposomes may result in inefficacy of LPPO II in these types of bilayers.

LPS, which is part of the outer membrane of Gram-negative bacteria, hinders the activity of antimicrobial compounds[33] by creating a barrier that is relatively impermeable to hydrophobic compounds[34]. This phenomenon was also confirmed in our leakage experiment with liposomes pre-incubated with LPS prior to the addition of LPPO (Fig. 9). The reduced activity was the most pronounced in PE/PG liposomes treated with DR-5026, or in other words the activity of DR-5026 was hindered the most substantially in these liposomes. We presume that in these LPS-liposomes two effects are combined—the presence of a lower proportion of negatively charged PG and the barrier function of LPS. The substantially reduced magnitude of DR-5026-induced leakage in LPS-PE/PG liposomes corroborated the results of the NPN assay in living *E. coli* cells, which showed that DR-5026 is unable to compromise the outer membrane. Finally, the role of the outer membrane in LPPO I ineffectiveness was further confirmed by the MIC value of DR-5026 against an *E. coli* imp4213 strain[22] with compromised integrity of the outer membrane (due to a mutation in LPS assembly). Of note, the data showed that this strain was susceptible to LPPO I (Table 2).

The protective function of LPS is realized both by its hydrophilic densely packed oligosaccharide core with very low fluidity and by the hydrophobic hydrocarbon chain region[34]. The negatively charged phosphate groups on LPS are thought to be responsible for the interaction and binding of cationic AMPs[35], which is a prerequisite for their subsequent insertion into the membrane. A recent study on the small AMP crabrolin showed that an increase in positive charges parallels an increased binding to LPS[36]. Hence, we propose that the substantially higher positive charge of LPPO II leads to a stronger electrostatic interaction with the negatively charged membrane. This interaction increases the probability that the hydrophobic part of LPPO II is anchored to the membrane, which results in higher antimicrobial activity against Gram-negative bacteria. The role of the number of positive charges on LPS binding and the antibacterial potential has been thoroughly studied using polymyxin B derivatives. Reduction in the number of positive charges of polymyxin B derivatives NAB7061 or NAB741 results in loss of any antibacterial activity; however, these derivatives potentiates activity of other antibiotics by reducing their MICs against Gram-negative pathogens[12].

We might also speculate that not only the charge but also the fluidity of the outer membrane affects LPPO action as the mutant *E. coli* imp4213 strain which has reduced membrane stiffness[37] become susceptible to LPPO I. In this mutant strain the presence of defective LPS molecules inhibits the insertion of many outer membrane proteins, which place is substituted with phospholipids. This results in a much higher permeability than the normal LPS/phospholipid bilayer[38]. All in all, although LPS is highly negatively charged and considered as the first target for cationic antimicrobial peptides, it can also serve as a barrier to prevent the insertion of AMPs into the inner phospholipid membrane due to its tight packing which hinders AMPs to traverse into the cytoplasmic membrane[33,39]. In conclusion, the inability of first-generation LPPO to exhibit antimicrobial activity against Gram-negative bacteria is due to several factors. We propose that the inability to overcome the outer membrane of Gram-negative bacteria might be the first factor explaining the inefficiency of LPPO I against Gram-negatives. LPPO I molecules probably interact with LPS and are incapable of disrupting the outer membrane, which in turn reduces their permeabilizing effect in the cytoplasmic membrane. After all, some of the LPPO I molecules finally reach their target, where they form pores through which small ions are able to pass, and the membrane is partially depolarized. However, the formation of larger pores that would lead to complete depolarization and cell death is probably limited by the absence of enough monomers. Moreover, the phospholipid composition of the target cytoplasmic membrane also reduces the efficiency of pore formation—the higher proportion of neutral lipids in *E. coli* leads to reduced membrane permeabilization. These effects add up, and might be the basis for LPPO I ineffectiveness in Gram-negative bacteria. The findings should be taken into account when designing new antimicrobial compounds.

Methods

Planar lipid bilayer experiments. A Teflon chamber was divided into two compartments connected by a circular aperture of approx. 0.5 mm in diameter. Planar lipid bilayers (black lipid membranes) were formed by painting a solution of 3% (w/v) 1,2-diphytanoyl-sn-glycero-3-phospho-(1′-rac-glycerol) (Avanti Polar Lipids) in *n*-decane-butanol (9:1, v/v) across the hole. Both compartments contained 1 ml of 1 M KCl, 10 mM Tris, pH 7.4. The temperature was kept at 25 °C. LPPO was added to the *cis* side of the membrane at a concentration of 5, 2.5 or 1.25 µg/ml, respectively. The membrane current was measured with Ag/AgCl electrodes with a constant applied voltage of 50 mV. The current signal was amplified with an LCA-200-100GV amplifier (Femto) and digitized with a KPCI-3108 card (Keithley). The signal was processed with QuB software[40]. In order to prevent the bin edge effect the histograms of single-pore conductance were created using kernel density estimation (rectangular kernel with a 30 pS width). For a more detailed explanation of kernel density estimation please see the Supplementary information. Raw experimental data from these conductivity measurements are available at Zenodo repository (http://dx.doi.org/10.5281/zenodo.4694562).

ΔΨ (mV)	$[K^+]_{in}$ (mM)	$[K^+]_{out}$ (mM)
0	300	300
− 50	300	46
− 100	300	7

Table 3. Demanded ΔΨ equilibrium potentials and corresponding calculated $[K^+]$.

Membrane permeabilization assay. The assay was performed as described previously[41]. Bacterial cells of *Bacillus subtilis* (168, *trp*$^+$, BaSysBio[42]) and *Escherichia coli* CCM 3954 were grown aerobically in LB medium at 37 °C to the mid log phase (OD_{450nm} ~ 0.5). The cells were harvested (8000*g*, 25 °C, 10 min), washed, and resuspended (final OD_{450nm} ~ 0.2) in a buffer containing 10 mM HEPES (pH 7.2), 0.5% glucose and 10 µM propidium iodide (PI, Invitrogen). This cell suspension was readily used for the assay without further incubation. LPPOs were added to 2 ml of bacterial suspension in a 10 × 10-mm quartz cuvette and propidium iodide (PI) uptake into cells (indicating membrane permeabilization) was monitored as the increase in fluorescence intensity (excitation at 515 nm, emission at 620 nm with bandpass 5 and 5 nm, respectively) at 25 °C using a FluoroMax-3 spectrofluorometer (Jobin Yvon, Horriba). We used optical filters to suppress light scattered by the cells (Omega Optical filters 3RD500-530 and 3RD570LP in excitation and emission paths, respectively). The bacterial suspension was continuously stirred with a magnetic stirrer during the measurements. As a positive control for cell permeabilization, 10 µM melittin (Sigma) was added to the cuvette, whereas the addition of the buffer alone served as a negative control. The presented data are the recorded intensities without background subtraction. LPPOs interaction with PI in solution resulted in maximum 5% change in fluorescence intensity (Supplementary Fig. S3).

To adjust the desired value of electrical membrane potential ΔΨ on bacterial cells, we used a common method utilizing the selective K^+ ionophore valinomycin and a known K^+ gradient across the membrane[43,44]. The Nernst equation was used to calculate the K^+ concentration in the buffer (K^+_{out}) from the desired ΔΨ value, a mean intracellular K^+ concentration (K^+_{in}) of 300 mM[45] was used. The calculated (K^+_{out}) values were used to prepare buffers with different KCl concentrations (Table 3) and containing 10 mM HEPES (pH 7.2), 0.5% glucose. To compensate for the different ionic strengths of the buffers, NaCl was added to reach a final electrolyte concentration of 300 mM. After the addition of 4 µM valinomycin (Sigma) to the bacteria, the electrical current across their membrane was induced by selective K^+ transport, which sets up a diffusion potential (Supplementary Fig. S4) within a few minutes. The assay was carried out in a 96-well plate using a MicroMax 384 Microwell-Plate Reader, each well contained 200 µl of the cell suspension. The increase in PI fluorescence intensity was measured at 25 °C using a FluoroMax-3 spectrofluorometer (Jobin Yvon, Horriba) using the same settings as described above (with the exception of bandpasses, which were both 15 nm in this case). Due to the delay in the preparation of samples on the well plate, the first points of the presented kinetics are missing. Before the addition of a tested compound, the initial intensities were comparable in all data sets.

Membrane potential measurement. For observing the changes in membrane potential in *B. subtilis* and *E. coli*, we used the voltage-sensitive dye $DiSC_3(5)$ (1 µM, 1% DMSO, Sigma), which accumulates in hyperpolarized membranes, where its fluorescence is quenched. The probe released from the depolarized membranes exerts increased fluorescence intensity[44]. Bacteria were grown aerobically in LB medium at 37 °C to the mid log phase (OD_{450nm} ~ 0.5). The cells were harvested (8000*g*, 25 °C, 10 min), washed, and resuspended in a buffer containing 10 mM HEPES (pH 7.2), 0.5% glucose and 1 µM $DiSC_3(5)$ (Sigma)ml to final OD_{450nm} ~ 0.2 (corresponding to ~ 2×10^7 cells/ml). The incubation took 90 min in the dark and the cell suspension was continuously stirred. These labeling conditions ensured stable fluorescence signal. LPPOs were added to 2 ml of this suspension in a 10 × 10-mm quartz cuvette, and the increase in $DiSC_3(5)$ fluorescence intensity was measured at 25 °C using a FluoroMax-3 spectrofluorometer (Jobin Yvon, Horriba). Excitation and emission wavelengths were set to 600 nm and 670 nm, respectively (both bandpasses of 4 nm). Optical filters (Omega Optical filters RPB590-610 and RPE650LP in the excitation and emission paths, respectively) were used to suppress light scattered by the cells. As a positive control for membrane depolarization, 10 µM melittin (Sigma) was added to the cuvette, whereas addition of the buffer alone served as a negative control. LPPOs interaction with $DiSC_3(5)$ in solution resulted in ~ 10% change in fluorescence intensity (Supplementary Fig. S3). The presented data are the recorded intensities without background subtraction.

Persister killing assay. The experiment was performed as described by Grassi et al.[46] using *E. coli* CCM 3954. Carbonyl cyanide *m*-chlorphenylhydrazone (CCCP, Sigma-Aldrich, United States) was diluted in DMSO (stock solution 40 mg/ml) and stored at − 20 °C. Minimum inhibitory concentrations of DR-6180 and colistin (Sigma-Aldrich, United States) were determined (as described above in Determination of MIC values) and concentrations corresponding to MIC and 5xMIC were used in the experiment.

The bacterial suspension was cultivated overnight in MH broth at 35 ± 1 °C with shaking. 1 ml of suspension was transferred into a microtube and incubated for 3 h at 35 ± 1 °C with 10 µl of CCCP (200 µg/ml). After the treatment, the bacteria were washed twice in saline solution (0.9% w/v NaCl) at 1700×*g* for 10 min and resuspended in saline at a final density of 5×10^8 CFU/ml.

To evaluate the activity of LPPO II DR-6180 and colistin against CCCP-induced persisters, CCCP-treated and untreated bacteria were diluted in PBS (phosphate-buffered saline) supplemented with 1% MH broth to a

final density of 10^6 CFU/ml. After 3 h of incubation with gentle shaking at 35 ± 1 °C, samples were exponentially diluted and inoculated on MH agar. After additional incubation for 24 h at 35 ± 1 °C, the bacterial cells were counted to determine CFU/ml.

Outer membrane integrity assays. The enhanced permeability of the outer membrane induced by LPPO was determined as the increase in fluorescence of the probe 1-*N*-phenylnapthylamine (NPN, Sigma-Aldrich). When the outer membrane of the cells is compromised, NPN can access the periplasmic space and bind the phospholipids, which increases its fluorescence[47,48]. Bacterial cells of *E. coli* CCM 3954 were grown to the mid-log phase (OD_{450nm} ~ 0.5), harvested (8000*g*, 25 °C, 10 min), washed, and resuspended (final OD_{450nm} ~ 0.2) in a buffer containing 10 mM HEPES (pH 7.2), 0.5% glucose and 10 µM NPN. This cell suspension was readily used for the assay without further incubation. LPPOs were added to 2 ml of bacterial suspension in a 10 × 10-mm quartz cuvette, and the increase in fluorescence intensity of NPN was monitored over time (excitation at 350 nm, emission at 420 nm with bandpass 5 and 5 nm, respectively) at 25 °C using a FluoroMax-3 spectrofluorometer (Jobin Yvon, Horriba). The representative kinetics of NPN uptake are shown in Supplementary Fig. S5. The bacterial suspension was continuously stirred with a magnetic stirrer during the measurements. The data are presented as the percentage of NPN uptake in the presence of LPPO relative to the maximum induced by 100 µM polymyxin B (IF_{max}, Sigma-Aldrich) – % NPN uptake = $(IF_{LPPO} - IF_0)/(IF_{max} - IF_0) \times 100$, where IF_{LPPO} is the fluorescence intensity in the plateau phase after the addition of LPPO, and IF_0 is the fluorescence of *E. coli* cells in the buffer before the addition of LPPO. LPPOs interaction with NPN in solution resulted in ~ 5–15% change in fluorescence intensity (Supplementary Fig. S3).

Liposome preparation. Liposomes were prepared using the method that we described previously[21]. 1,2-dioleoyl-sn-glycero-3-phospho-(1′-rac-glycerol) (DOPG), 1,2-dioleoyl-sn-glycero-3-phosphoethanolamine (DOPE) and 1,2-dioleoyl-sn-glycero-3-phosphocholine (DOPC) were purchased from Avanti Polar Lipids. Liposomes to be used in the carboxyfluorescein leakage assay were prepared by mixing the appropriate amounts of lipids (1 mg/ml) in chloroform. The solvent was evaporated in vacuo, obtaining a thin film on the walls of a glass tube. The hydration procedure in a buffer containing 50 mM 5(6)-Carboxyfluorescein (CF), 5 mM HEPES pH 7.4 lasted for 90 min at 40 °C, being interrupted by thorough vortex shaking to form multilamellar vesicles. Large unilamellar vesicles (LUVs) were prepared by repeated extrusion of the multilamellar vesicles through 100 nm polycarbonate filters (Whatman) using an extruder (Avanti Polar Lipids). Liposomes were separated from nonencapsulated dye by gel filtration on Sephadex G-50 using 100 mM NaCl, 0.5 mM Na_2EDTA and 5 mM HEPES, pH 7.4 as elution buffer. The liposome suspension was diluted in the same buffer to give a final phospholipid concentration of 10 µM (according to the assessed content of inorganic phosphate).

Liposome leakage assay. The leakage of liposome contents was evaluated by the increase in fluorescence intensity due to CF release into the milieu[21] after adding LPPO solution to the final concentration indicated in the respective graph legends. The concentrations used in this assay are not comparable to the concentrations used in the cells since it is unclear how much of the compound would reach the inner membrane and how much is retained in the outer membrane and/or cell wall. Thus the compound/lipid ratios in cell cultures cannot be reasonably estimated.

To test the effect of the presence of lipopolysaccharide (LPS) on LPPO-induced liposome leakage, liposome suspension (10 µM inorganic phosphate concentration) was incubated with 20 µg/ml of lipopolysaccharide (LPS from *E. coli* O111:B4, Sigma-Aldrich) for 10 min prior to LPPO addition, thus the lipid-LPS ratio was 2:5 (w/w)[49]. The maximum increase in CF fluorescence (F_{max}) was induced by lysing the vesicles with 0.1% (v/v) Triton X-100. Fluorescence intensity was monitored over time (excitation at 480 nm, emission at 515 nm) at 25 °C using a FluoroMax-3 spectrofluorometer (Jobin Yvon, Horriba). The following equation was used to calculate the percent of CF leakage: %CF leakage = $[(F - F_0)/(F_{max} - F_0)] \times 100$, where F is the actual fluorescence intensity and F_0 is the fluorescence intensity before the addition of the tested compound. Representative results from at least three individual experiments are shown.

Determination of MIC values. The antimicrobial activity of the tested compounds against *E. coli* imp4213, in which the mutation in the imp gene causes a higher permeability of the outer membrane[23], was assessed using the microdilution method to determine the minimum inhibitory concentration (MIC)[50]. Disposable microtitration plates were used for the tests. The compounds were diluted in MH broth (Himedia) to yield a concentration range between 256 and 1 µg/ml. The plates were inoculated with a standard amount of the tested microbe—the inoculum density in each well was equal to 10^6 CFU/ml. The MIC was read after 24 h of incubation at 35 °C as the minimum inhibitory concentration of the tested substance that inhibited the growth of the bacterial strains.

Code availability

A custom made Perl script used to generate histograms of single-pore conductance presented in Fig. 2 is provided in Supplementary information.

Received: 18 January 2021; Accepted: 27 April 2021
Published online: 17 May 2021

References

1. Scott, W. R. & Tew, N. G. Mimics of host defense proteins; strategies for translation to therapeutic applications. *Curr. Top. Med. Chem.* **17**, 576–589 (2017).

2. Lei, J. *et al.* The antimicrobial peptides and their potential clinical applications. *Am. J. Transl. Res.* **11**, 3919–3931 (2019).
3. Chen, C. H. & Lu, T. K. Development and challenges of antimicrobial peptides for therapeutic applications. *Antibiotics* **9**, 24 (2020).
4. Giuliani, A. *et al.* Antimicrobial peptides: Natural templates for synthetic membrane-active compounds. *Cell. Mol. Life Sci.* **65**, 2450–2460 (2008).
5. Matsuzaki, K. Control of cell selectivity of antimicrobial peptides. *Biochim. Biophys. Acta Biomembr.* **1788**, 1687–1692 (2009).
6. Oh, D. *et al.* Antibacterial activities of amphiphilic cyclic cell-penetrating peptides against multidrug-resistant pathogens. *Mol. Pharm.* **11**, 3528–3536 (2014).
7. Kustanovich, I., Shalev, D. E., Mikhlin, M., Gaidukov, L. & Mor, A. Structural requirements for potent versus selective cytotoxicity for antimicrobial dermaseptin S4 derivatives. *J. Biol. Chem.* **277**, 16941–16951 (2002).
8. Boto, A., De La Lastra, J. M. P. & González, C. C. The road from host-defense peptides to a new generation of antimicrobial drugs. *Molecules* **23**, 311 (2018).
9. Thaker, H. D., Cankaya, A., Scott, R. W. & Tew, G. N. Role of amphiphilicity in the design of synthetic mimics of antimicrobial peptides with gram-negative activity. *ACS Med. Chem. Lett.* **4**, 481–485 (2013).
10. Snyder, S., Kim, D. & McIntosh, T. J. Lipopolysaccharide bilayer structure: Effect of chemotype, core mutations, divalent cations, and temperature. *Biochemistry* **38**, 10758–10767 (1999).
11. Bertani, B. & Ruiz, N. Function and biogenesis of lipopolysaccharides. *EcoSal Plus.* **8**, 1–33 (2018).
12. Vaara, M. Polymyxin derivatives that sensitize gram-negative bacteria to other antibiotics. *Molecules* **24**, 249 (2019).
13. Brown, P. & Dawson, M. J. Development of new polymyxin derivatives for multi-drug resistant Gram-negative infections. *J. Antibiot.* **70**, 386–394 (2017).
14. Vaara, M. & Vaara, T. Sensitization of Gram-negative bacteria to antibiotics and complement by a nontoxic oligopeptide. *Nature* **303**, 526–528 (1983).
15. Koh, J. J. *et al.* N-Lipidated peptide dimers: Effective antibacterial agents against gram-negative pathogens through lipopolysaccharide permeabilization. *J. Med. Chem.* **58**, 6533–6548 (2015).
16. Rounds, T. & Straus, S. K. Lipidation of antimicrobial peptides as a design strategy for future alternatives to antibiotics. *Int. J. Mol. Sci.* **21**, 9692 (2020).
17. Panova, N. *et al.* Insights into the mechanism of action of bactericidal lipophosphonoxins. *PLoS ONE* **10**, e0145918 (2015).
18. Seydlová, G. *et al.* Lipophosphonoxins II: Design, synthesis, and properties of novel broad spectrum antibacterial agents. *J. Med. Chem.* **60**, 6098–6118 (2017).
19. Rejman, D. *et al.* Lipophosphonoxins: New modular molecular structures with significant antibacterial properties. *J. Med. Chem.* **54**, 7884–7898 (2011).
20. Epand, R. M. & Epand, R. F. Bacterial membrane lipids in the action of antimicrobial agents. *J. Pept. Sci.* **17**, 298–305 (2011).
21. Uttlová, P. *et al.* Bacillus subtilis alters the proportion of major membrane phospholipids in response to surfactin exposure. *Biochim. Biophys. Acta Biomembr.* **1858**, 2965–2971 (2016).
22. Caetano, T., Krawczyk, J. M., Mösker, E., Süssmuth, R. D. & Mendo, S. Lichenicidin biosynthesis in *Escherichia coli*: licFGEHI immunity genes are not essential for lantibiotic production or self-protection. *Appl. Environ. Microbiol.* **77**, 5023–5026 (2011).
23. Braun, M. & Silhavy, T. J. Imp/OstA is required for cell envelope biogenesis in *Escherichia coli*. *Mol. Microbiol.* **45**, 1289–1302 (2002).
24. Seydlová, G., Sokol, A., Lišková, P., Konopásek, I. & Fišer, R. Daptomycin pore formation and stoichiometry depend on membrane potential of target membrane. *Antimicrob. Agents Chemother.* **63**, e01589–18 (2019).
25. Gray, D. A. & Wenzel, M. More than a pore: A current perspective on the in vivo mode of action of the lipopeptide antibiotic daptomycin. *Antibiotics* **9**, 17 (2020).
26. Zuttion, F. *et al.* High-speed atomic force microscopy highlights new molecular mechanism of daptomycin action. *Nat. Commun.* **11**, 1–16 (2020).
27. Pinkas, D. *et al.* Bacillus subtilis cardiolipin protects its own membrane against surfactin-induced permeabilization. *Biochim. Biophys. Acta Biomembr.* **1862**, 183405 (2020).
28. Song, C., de Groot, B. L. & Sansom, M. S. P. Lipid bilayer composition influences the activity of the antimicrobial peptide dermcidin channel. *Biophys. J.* **116**, 1658–1666 (2019).
29. Damper, P. D. & Epstein, W. Role of the membrane potential in bacterial resistance to aminoglycoside antibiotics. *Antimicrob. Agents Chemother.* **20**, 803–808 (1981).
30. Benarroch, J. M. & Asally, M. The microbiologist's guide to membrane potential dynamics. *Trends Microbiol.* **28**, 304–314 (2020).
31. Johnston, C. W. *et al.* Assembly and clustering of natural antibiotics guides target identification. *Nat. Chem. Biol.* **12**, 233–239 (2016).
32. Hachmann, A. B. *et al.* Reduction in membrane phosphatidylglycerol content leads to daptomycin resistance in *Bacillus subtilis*. *Antimicrob. Agents Chemother.* **55**, 4326–4337 (2011).
33. Papo, N. & Shai, Y. A molecular mechanism for lipopolysaccharide protection of gram-negative bacteria from antimicrobial peptides. *J. Biol. Chem.* **280**, 10378–10387 (2005).
34. Snyder, D. S. & McIntosh, T. J. The lipopolysaccharide barrier: Correlation of antibiotic susceptibility with antibiotic permeability and fluorescent probe binding kinetics. *Biochemistry* **39**, 11777–11787 (2000).
35. Rosenfeld, Y., Sahl, H. G. & Shai, Y. Parameters involved in antimicrobial and endotoxin detoxification activities of antimicrobial peptides. *Biochemistry* **47**, 6468–6478 (2008).
36. Cantini, F. *et al.* Effect of positive charges in the structural interaction of crabrolin isoforms with lipopolysaccharide. *J. Pept. Sci.* **26**, e3271 (2020).
37. Rojas, E. R. *et al.* The outer membrane is an essential load-bearing element in Gram-negative bacteria. *Nature* **559**, 617–621 (2018).
38. Nikaido, H. Restoring permeability barrier function to outer membrane. *Chem. Biol.* **12**, 507–509 (2005).
39. Allende, D. & McIntosh, T. J. Lipopolysaccharides in bacterial membranes act like cholesterol in eukaryotic plasma membranes in providing protection against melittin-induced bilayer lysis. *Biochemistry* **42**, 1101–1108 (2003).
40. Nicolai, C. & Sachs, F. Solving ion channel kinetics with the QuB software. *Biophys. Rev. Lett.* **8**, 191–211 (2013).
41. Seydlová, G. *et al.* Lipophosphonoxins II: Design, synthesis, and properties of novel broad spectrum antibacterial agents. *J. Med. Chem.* **60**, 6098–6118 (2017).
42. Nicolas, P. *et al.* Condition-dependent transcriptome reveals high-level regulatory architecture in *Bacillus subtilis*. *Science (80-).* **335**, 1103–1106 (2012).
43. Klapperstück, T., Glanz, D., Klapperstück, M. & Wohlrab, J. Methodological aspects of measuring absolute values of membrane potential in human cells by flow cytometry. *Cytom. Part A* **75A**, 593–608 (2009).
44. te Winkel, J. D., Gray, D. A., Seistrup, K. H., Hamoen, L. W. & Strahl, H. Analysis of antimicrobial-triggered membrane depolarization using voltage sensitive dyes. *Front. Cell Dev. Biol.* **4**, 29 (2016).
45. Whatmore, A. M., Chudek, J. A. & Reed, R. H. The effects of osmotic upshock on the intracellular solute pools of *Bacillus subtilis*. *J. Gen. Microbiol.* **136**, 2527–2535 (1990).
46. Grassi, L. *et al.* Generation of persister cells of *Pseudomonas aeruginosa* and *Staphylococcus aureus* by chemical treatment and evaluation of their susceptibility to membrane-targeting agents. *Front. Microbiol.* **8**, 1917 (2017).
47. Helander, I. M. & Mattila-Sandholm, T. Fluorometric assessment of Gram-negative bacterial permeabilization. *J. Appl. Microbiol.* **88**, 213–219 (2000).

48. Nikaido, H. Molecular basis of bacterial outer membrane permeability revisited. *Microbiol. Mol. Biol. Rev.* **67**, 593–656 (2003).
49. Singh, S., Kasetty, G., Schmidtchen, A. & Malmsten, M. Membrane and lipopolysaccharide interactions of C-terminal peptides from S1 peptidases. *Biochim. Biophys. Acta Biomembr.* **1818**, 2244–2251 (2012).
50. European Committee for Antimicrobial Susceptibility Testing (EUCAST) of the European Society of Clinical Microbiology and Infectious Diseases (ESCMID). Determination of minimum inhibitory concentrations (MICs) of antibacterial agents by broth dilution. *Clin. Microbiol. Infect.* **9**, ix–xv (2003).

Acknowledgements

This work was supported by the Grant GAUK 1360218 from Charles University (to K.L.), SVV project 260568 (to K.L. and D.P.), funds from the Institute of Organic Chemistry and Biochemistry, Czech Academy of Science, v.v.i. to D.R., and Czech ministry of health Grant No. 17-29680A to D.R.

Author contributions

G.M., D.R., R.F. and M.K. conceived and designed the experiments. D.D.D.P. and D.R. provided material (LPPO). K.L., N.H., R.F. R.V. and K.B. performed the experiments. G.M., D.R., R.F. and D.P. analyzed the data. I.K. critically reviewed the manuscript and provided expert opinions. G.M., D.R. and R.F. wrote the manuscript text.

Competing interests

The authors declare no competing interests.

Additional information

Supplementary Information The online version contains supplementary material available at https://doi.org/10.1038/s41598-021-89883-0.

Correspondence and requests for materials should be addressed to D.R. or G.M.

Reprints and permissions information is available at www.nature.com/reprints.

Publisher's note Springer Nature remains neutral with regard to jurisdictional claims in published maps and institutional affiliations.

Terms and Conditions

Springer Nature journal content, brought to you courtesy of Springer Nature Customer Service Center GmbH (“Springer Nature”).
Springer Nature supports a reasonable amount of sharing of research papers by authors, subscribers and authorised users (“Users”), for small-scale personal, non-commercial use provided that all copyright, trade and service marks and other proprietary notices are maintained. By accessing, sharing, receiving or otherwise using the Springer Nature journal content you agree to these terms of use (“Terms”). For these purposes, Springer Nature considers academic use (by researchers and students) to be non-commercial.
These Terms are supplementary and will apply in addition to any applicable website terms and conditions, a relevant site licence or a personal subscription. These Terms will prevail over any conflict or ambiguity with regards to the relevant terms, a site licence or a personal subscription (to the extent of the conflict or ambiguity only). For Creative Commons-licensed articles, the terms of the Creative Commons license used will apply.
We collect and use personal data to provide access to the Springer Nature journal content. We may also use these personal data internally within ResearchGate and Springer Nature and as agreed share it, in an anonymised way, for purposes of tracking, analysis and reporting. We will not otherwise disclose your personal data outside the ResearchGate or the Springer Nature group of companies unless we have your permission as detailed in the Privacy Policy.
While Users may use the Springer Nature journal content for small scale, personal non-commercial use, it is important to note that Users may not:

1. use such content for the purpose of providing other users with access on a regular or large scale basis or as a means to circumvent access control;
2. use such content where to do so would be considered a criminal or statutory offence in any jurisdiction, or gives rise to civil liability, or is otherwise unlawful;
3. falsely or misleadingly imply or suggest endorsement, approval , sponsorship, or association unless explicitly agreed to by Springer Nature in writing;
4. use bots or other automated methods to access the content or redirect messages
5. override any security feature or exclusionary protocol; or
6. share the content in order to create substitute for Springer Nature products or services or a systematic database of Springer Nature journal content.

In line with the restriction against commercial use, Springer Nature does not permit the creation of a product or service that creates revenue, royalties, rent or income from our content or its inclusion as part of a paid for service or for other commercial gain. Springer Nature journal content cannot be used for inter-library loans and librarians may not upload Springer Nature journal content on a large scale into their, or any other, institutional repository.
These terms of use are reviewed regularly and may be amended at any time. Springer Nature is not obligated to publish any information or content on this website and may remove it or features or functionality at our sole discretion, at any time with or without notice. Springer Nature may revoke this licence to you at any time and remove access to any copies of the Springer Nature journal content which have been saved.
To the fullest extent permitted by law, Springer Nature makes no warranties, representations or guarantees to Users, either express or implied with respect to the Springer nature journal content and all parties disclaim and waive any implied warranties or warranties imposed by law, including merchantability or fitness for any particular purpose.
Please note that these rights do not automatically extend to content, data or other material published by Springer Nature that may be licensed from third parties.
If you would like to use or distribute our Springer Nature journal content to a wider audience or on a regular basis or in any other manner not expressly permitted by these Terms, please contact Springer Nature at

onlineservice@springernature.com